Spoofing and disguise variations in face recognition

Neslihan Kose

ParisTech
INSTITUT DES SCIENCES ET TECHNOLOGIES
PARIS INSTITUTE OF TECHNOLOGY

TELECOM ParisTech

2014-ENST-0020

EDITE - ED 130

Doctorat ParisTech

T H È S E

pour obtenir le grade de docteur délivré par

TELECOM ParisTech

Spécialité « Signal et Images »

présentée et soutenue publiquement par

Neslihan KÖSE

le 14 Avril 2014

Spoofing and Disguise Variations in Face Recognition

Directeur de thèse : **Jean-Luc DUGELAY**

Jury

M. Marc ANTONINI, Directeur de Recherche, Laboratoire I3S 2000, CNRS	Rapporteur
M. Abdenour HADID, Professeur, Université d'Oulu	Rapporteur
M. Mohamed DAOUDI, Professeur, Telecom Lille 1	Examinateur
Mme. Özgül SALOR DURNA, Assoc. Professeur, Université de Gazi	Examinateur
M. Kieron MESSER, Doctorant, Digital Barriers	Examinateur

TELECOM ParisTech
école de l'Institut Télécom - membre de ParisTech

THÈSE

Spoofing and Disguise Variations in Face Recognition

Neslihan Köse

A doctoral dissertation submitted to:

TELECOM ParisTech

in partial fulfillment of the requirements for the degree of:

DOCTOR OF PHILOSOPHY

Major subject: Biometrics, Image Processing

Approved by the following examining committee:

Supervisor:	Prof. Jean-Luc Dugelay
President of the jury:	Prof. Mohamed Daoudi
Reviewer:	Prof. Marc Antonini
Reviewer:	Prof. Abdenour Hadid
Examiner:	Assoc. Prof. Özgül Salor Durna
Examiner:	Dr. Kieron Messer

Abstract

Human recognition has become an important topic as the need and investments for security applications grow continuously. Biometrics enable reliable and efficient identity management systems by using physical and behavioral characteristics of the subjects that are permanent, universal and easy to access. This is why, the topic of biometrics attracts higher attention today.

Numerous biometric systems exist which utilize various human characteristics. Among all biometrics traits, face recognition is advantageous in terms of accessibility and reliability. It allows identification at relatively high distances for unaware subjects that do not have to cooperate.

In this dissertation, two challenges in face recognition are analyzed. The first one is face spoofing. Initially, spoofing in face recognition is explained together with the countermeasure techniques that are proposed for the protection of face recognition systems against spoofing attacks. The second challenge explored in this thesis is disguise variations. In the second part of the thesis, the impact of disguise variations on face recognition is analyzed and the proposed techniques that are robust to these variations are explained.

In a spoofing attempt, a person tries to masquerade as another person and thereby, tries to gain access to a recognition system. Since face data can be acquired easily in a contactless manner, spoofing is a real threat for face recognition systems.

In this dissertation, initially, a countermeasure technique is proposed for the detection of photograph attacks, which was our preliminary study that helps to gain insight into the topic of face spoofing.

Then 3D mask attacks to face recognition systems are investigated. Compared to 2D spoofing attacks such as photograph and video, 3D mask attacks to face recognition systems is a considerably new subject. In this thesis, we evaluate how vulnerable the existing 3D and 2D face recognition systems are to spoofing mask attacks. The results of this study show that existing recognition systems are not robust against mask attacks and hence countermeasures have to be developed to mitigate their impact.

Next, we analyze several characteristics of masks and real samples such as texture, reflectance and smoothness, and propose four countermeasure techniques for the detection of 3D mask attacks. All these countermeasures provide significant detection accuracies alone. However we observed that fusion of these countermeasures further improves the results.

The second challenge in face recognition explored in this thesis is disguise variations. In the next part of this thesis, the disguise variations which are due to facial alterations, facial makeup and facial accessories (occlusions) are explored.

Modifications on the facial surface can be achieved in countless different ways such as applying plastic surgery, prosthetic makeup and latex appliances. In our study regarding facial alterations, a simulated nose alteration database was prepared using FRGC v1.0, then the impact of nose alteration was evaluated on both 2D and 3D face recognition.

Next, we propose a block based face recognition approach, which mitigates the impact of facial alterations on face recognition. Although this technique is applied for nose alterations in our study, it can be applied for any types of surgical operations on face.

Facial makeup is another type of disguise variations. In order to analyze the impact of facial makeup on face recognition, we prepared a facial cosmetics database, which includes many samples annotated as non-makeup, slight makeup and heavy makeup. The impact of makeup on face recognition was analyzed in detail and we observed that especially makeup for eye region takes an important role in face recognition.

Finally, in order to establish the connections between the Kinect sensor and face recognition, we present the first publicly available face database based on the Kinect sensor for face recognition. The database consists of different data modalities and multiple facial variations. We conduct benchmark evaluations on the proposed database using standard face recognition methods. The performance gain is demonstrated by integrating the depth data with the RGB data via score-level fusion. We also compare the Kinect images with the traditional high quality 3D scans (of the FRGC database), which demonstrates the imperative needs of the proposed database for face recognition.

Acknowledgments

First of all, I would like to present my special thanks to my supervisor Prof. Jean-Luc Dugelay for his guidance, understanding and support throughout the development of this thesis. Next, I would like to thank all of my colleagues for their friendship and collaboration.

I am also grateful to the members of the examining committee of this dissertation for their precious time and for their constructive comments.

My warmest thanks are to my family in Turkey who supported and motivated me with their never ending sacrifice, support, understanding and love throughout this demanding study. I always feel very lucky to have such a wonderful family.

Finally, I would like to express my deepest gratitude to my dear husband Aykut for his love, support and understanding. He has always been with me. I am thankful to him for sharing this entire amazing journey with me.

Contents

List of Figures

List of Tables

List of Publications

Book Chapter

- Kose Neslihan, Dugelay Jean-Luc, Vatsa Mayank, Singh Richa, "Recognizing Face Images With Disguise Variations", Face Recognition in Adverse Conditions, IGI Press; 2014.
- Velardo Carmelo, Dugelay Jean-Luc, Daniel Lionel, Dantcheva Antitza, Erdogmus Nesli, Kose Neslihan, Min Rui, Zhao Xuran, "Introduction to Biometry", Multimedia Image and Video Processing, CRC Press; 2012; ISBN:978-1439830864.

Journal

- Kose Neslihan, Dugelay Jean-Luc, "Mask Spoofing in Face Recognition and Countermeasures", submitted to Image and Vision Computing Journal - Elsevier, under second round review.
- Min Rui, Kose Neslihan, Dugelay Jean-Luc, "KinectFaceDB: a Kinect Face Database for Face Recognition", accepted for IEEE Transactions on Systems, Man, and Cybernetics: Systems.
- Dugelay Jean-Luc, Erdogmus Nesli, Kose Neslihan, "3D face recognition: Where we are", IEEE COMSOC MMTC E-Letter, vol. 6, no 11, pp. 14-16, November 2011.

Conference

- Kose Neslihan, Dugelay Jean-Luc, "Shape and Texture Based Countermeasure to Protect Face Recognition Systems Against Mask Attacks", IEEE Computer Society Workshop on Biometrics, CVPR Workshop on Biometrics 2013, June 23-28 2013, Portland, USA.
- Kose Neslihan, Dugelay Jean-Luc, "Reflectance Analysis Based Countermeasure Technique to Detect Face Mask Attacks", IEEE International Conference on Digital Signal Processing, DSP 2013, July 1-3 2013, Santorini, Greece.
- Kose Neslihan, Dugelay Jean-Luc, "Countermeasure for the Protection of Face Recognition Systems Against Mask Attacks", IEEE International Conference on Automatic Face and Gesture Recognition, FG 2013, April 22-26 2013, Shanghai, China. (Received **Best Student Paper Honorable Mention Award**)
- Kose Neslihan, Dugelay Jean-Luc, "On The Vulnerability of Face Recognition Systems to Spoofing Mask Attacks", IEEE International Conference on Acoustics, Speech, and Signal Processing, ICASSP 2013, May 26-31 2013, Vancouver, Canada.

- Eckert Marie-Lena, Kose Neslihan, Dugelay Jean-Luc, "Facial Cosmetics Database and Impact Analysis on Automatic Face Recognition", IEEE International Workshop on Multimedia Signal Processing, MMSP 2013, Sep 30 - Oct 2 2013, Sardinia, Italy.

- Kose Neslihan, Erdogmus Nesli, Dugelay Jean-Luc, "Block Based Face Recognition Approach Robust to Nose Alterations", IEEE International Conference on Biometrics: Theory, Applications and Systems, BTAS 2012, Sep 23-27 2012, Washington DC.

- Erdogmus Nesli, Kose Neslihan, Dugelay Jean-Luc, "Impact Analysis of Nose Alterations on 2D and 3D Face Recognition", IEEE International Workshop on Multimedia Signal Processing, MMSP 2012, Sep 17-19 2012, Canada.

- Kose Neslihan, Dugelay Jean-Luc, "Classification of Captured and Recaptured Images to Detect Photograph Spoofing", International Conference on Informatics, Electronics & Vision, ICIEV 2012, May 18-19 2012, Dhaka, Bangladesh.

Chapter 1

Introduction

1.1 Motivation

Biometrics aim to measure and analyze biological data such as fingerprints, eye retinas, irises, DNA, facial patterns, voice patterns and hand measurements, for authentication purposes.

Due to the increasing need and investments for security applications, authentication by biometric verification is becoming increasingly common in corporate and public security systems. The reason is that biometrics enable reliable and efficient identity management systems by using physical and behavioral characteristics of the subjects that are permanent, universal and easy to access.

For a long time, passwords have been utilized for user authentication. However, since users are required to remember more, longer, and changing passwords, the need for more convenient and secure solution to user authentication increases. The motivation to improve the security systems based on single or multiple biometric traits rather than passwords comes from this fact.

Each biometric has their own advantages and disadvantages. For example, fingerprint is the most wide-spread biometric from a commercial point of view [3], however it requires strong user collaboration. Similarly, iris recognition is very accurate, however it highly depends on the image quality and also requires active participation of the subjects.

Face recognition is advantageous in terms of both accessibility and reliability. It allows identification at relatively high distances for unaware subjects that do not have to cooperate.

Despite the fact that face recognition has been investigated extensively, it still suffers from variations due to various factors in real-world scenarios such as illumination, pose, expression, occlusion and age. Since the three-dimensional (3D) face evades pose and illumination problems, 3D face recognition became very popular.

In this thesis, two challenges in face recognition are analyzed, which are spoofing and disguise variations. Although these challenges affect the performances of both 2D and 3D face recognition systems significantly, the studies on these topics are limited.

In a spoofing attempt, a person tries to masquerade as another person and thereby, tries to gain access to a recognition system. Since face data can be acquired easily in a contactless manner, spoofing is a real threat for face recognition systems. Due to the limited number of studies on this topic, today spoofing (including anti-spoofing) is a very popular topic for researchers in face recognition domain.

The most common spoofing attacks to face recognition systems are achieved by using photographs and videos due to their convenience and low cost. It has been shown that face recognition systems are vulnerable to photograph and video attacks. Aim is to develop non-intrusive countermeasures without extra devices and human involvement which can be integrated into existing face recognition systems to protect them against spoofing attacks.

Compared to 2D spoofing attacks such as photograph and video, 3D mask attacks to face recognition systems is a considerably new subject. The main reason for the delay in mask spoofing studies is due to the unavailability of public mask databases. The preparation of a mask attacks database is much more difficult and expensive than the preparation of photograph or video attacks databases. Initially, to prepare a high quality mask, a 3D scanner is necessary to obtain the 3D model of the target person, which are generally high-cost devices. The procedure continues with manufacturing of the masks which is also an expensive procedure.

In this dissertation, the main motivation is to develop countermeasure techniques in order to protect face recognition systems against spoofing attacks. For this purpose, we investigated both 2D and 3D face spoofing.

We first analyzed 2D spoofing attacks, which can be performed by using photographs or videos. We proposed a new countermeasure technique in [72] for the detection of photograph attacks. This study was our preliminary study that helps to gain insight into the topic of face spoofing.

After our analysis on 2D attacks, we investigated 3D mask attacks. There are still only a few number of studies regarding 3D mask spoofing in face recognition. Initially, we show how vulnerable the existing 3D and 2D face recognition systems are to spoofing mask attacks. The results of this study show that existing recognition systems are not robust against mask attacks and countermeasures have to be developed to mitigate the impact of these attacks.

Next, we analyzed several characteristics of masks and real face samples such as texture, reflectance and smoothness, and developed several countermeasure techniques. We also integrated the countermeasure providing the best performance to the selected 3D face recognition system in order to show the performance improvement with the countermeasure.

Disguise accessories can be used to alter the appearance of an individual, to impersonate another person, or to hide one's identity. Although face recognition with disguise variations is a major challenge, the research studies on this topic are limited. The motivation to analyze disguise variations in face recognition comes from this fact. In this dissertation, variations due to facial alterations, facial makeup and facial accessories are investigated.

Since plastic surgery becomes more advanced and affordable, it introduces new challenges for face recognition systems. There is no publicly available 3D plastic surgery database. Therefore, in order to analyze the impact of facial alterations on both 2D and 3D face recognition, we prepared a 2D+3D simulated nose alteration database, in which nose of each sample is replaced with another randomly chosen one. In our study, we demonstrated the decrease in recognition performances for both modalities, especially for 3D, in the existance of nose alterations. This is why, next, we proposed a block based face recognition approach, which mitigates the impact of facial alterations on face recognition.

Facial makeup changes the perceived appearance of a face and therefore have an impact on face recognition. Since makeup does not change 3D shape characteristics of a face, it has mainly an impact on 2D face recognition. In order to evaluate their impact in detail, we present a facial cosmetics database, which includes many samples annotated as non-makeup, slight makeup and heavy makeup.

Finally, in order to establish the connections between the Kinect sensor and face recognition, we present a Kinect face database, which is the first publicly available face database collected by Kinect sensor. Although being very cheap compared to the high-quality scanners, significant recognition performances can be achieved with the use of Kinect sensor. Benchmark evaluations were conducted on the proposed database for several variations including occlusions, expression and illumination.

1.2 Original Contributions

The original contributions of this thesis can be summarized in eight classes: the impact analysis of mask spoofing on existing face recognition systems, several countermeasures to detect mask and photograph attacks, a simulated nose alteration database, an approach robust to facial alterations, an extensive facial cosmetics database, an extensive Kinect Face Database, and several benchmark evaluations to show the performances of techniques using Kinect data.

Spoofing is a real threat for existing face recognition systems. Up to now, several countermeasures have been developed in order to protect face recognition systems against spoofing attacks. However, these countermeasures have been developed

mainly against photograph and video attacks.

One of the main contributions of this study is that 3D mask spoofing in face recognition is analyzed in detail. To the best of our knowledge, the impact of 3D mask attacks on both 2D and 3D face recognition systems was first analyzed in our study [74].

Then, we analyzed several characteristics of masks and real samples and developed countermeasures based on texture, reflectance and smoothness characteristics. In our study [73], it was the first time 3D data was utilized to detect 3D mask attacks. Each of these proposed countermeasures is novel and also is still one of the few studies which exists in the literature for the detection of 3D mask attacks. All the countermeasures proposed against mask attacks in this dissertation provide significant detection accuracies alone, however we also observed that almost perfect detection accuracy can be reached by the fusion of these countermeasures.

Disguise variations is another major challenge in face recognition. Although several challenges in face recognition have been explored extensively, there are still limited studies on variations due to facial alterations, facial makeup and occlusions.

For facial alteration analysis, since there is no publicly available 3D plastic surgery database, in order to simulate facial alterations, we prepared a 2D+3D nose alterations database, which enables to analyze the impact of facial alterations on both 2D and 3D face recognition.

Next, a block based face recognition approach is proposed in this study, which can be applied for any facial surgical operations, to increase the recognition performances.

For facial makeup analysis, a publicly available facial cosmetics database is presented and the impact of facial makeup on face recognition is demonstrated and analyzed in detail.

Finally, the first publicly available Kinect Face Database is presented. Benchmark evaluations are conducted and the performance gain is demonstrated by integrating the depth data with the RGB data via score-level fusion. We also compare the Kinect images with the traditional high quality 3D scans (of the FRGC database) in the context of face biometrics, which demonstrates the imperative needs of the proposed database for face recognition.

1.3 Outline

The outline of the dissertation is as follows:

- In Chapter 2, we provide an introduction to face spoofing and disguise varia-

tions, reviewing the state-of-the-art for the relevant work.

- In Chapter 3, our countermeasure technique, which is utilized to protect face recognition systems against photograph attacks, is presented.
- In Chapter 4, the impact of mask spoofing on both 2D and 3D face recognition is evaluated.
- In Chapter 5, our countermeasure techniques, which are utilized to protect face recognition systems against 3D mask attacks, are presented.
- In Chapter 6, the impact of facial alterations (particularly nose alteration) on both 2D and 3D face recognition is analyzed.
- In Chapter 7, a block based face recognition approach, which is robust to facial alterations, is proposed.
- In Chapter 8, we initially present a facial cosmetics database. Then we analyze the impact of facial cosmetics on face recognition.
- In Chapter 9, a Kinect Face Database, which includes different modalities and several variations, is presented. We conduct benchmark evaluations using standard face recognition methods, and demonstrate the performance gain by integrating the depth data with the RGB data via score-level fusion.
- In Chapter 10, the conclusions and future perspectives are provided.

Chapter 2

Face Spoofing and Disguise Variations

2.1 Introduction

Human recognition has become an important topic as the need and investments for security applications grow continuously. Biometrics enable reliable and efficient identity management systems by using physical and behavioral characteristics of the subjects that are permanent, universal and easy to access. This is why, the topic of biometrics attracts higher attention today.

In this section, we initially explain how a biometrics system works and then we give a brief information on face recognition.

2.1.1 Biometrics

Biometric systems usually consist of the following components:

- Sensor module: This module acquires biometric data (e.g. face image).
- Feature extraction module: This module is used to extract features of a biometric trait (e.g. fingerprint minutiae).
- Matching module: The matching module compares the acquired biometric features with the stored biometric templates and then match (similarity) scores are generated.
- Decision-making module: The users identity is either identified or a claimed identity is accepted or rejected based on the scores.

There are two modes in biometric systems, which are enrollment mode and authentication mode. Furthermore, authentication is achieved either in verification mode or identification mode.

- Enrollment mode: Subjects present one or more biometric data samples. The biometric templates are generated from these samples. These templates constitute the gallery set. Enrollment is generally performed in a well-controlled environment.

- Authentication mode: Biometric data of user is acquired and used by the system either for verification or identification purposes. The biometric data captured for recognition is a probe sample. In verification mode, the probe sample is matched with the claimed template for validation, and it either accepts or rejects the identity claim. Verification is one-to-one matching. On the other hand, in identification mode, all biometric references in the gallery are examined and the one with the best match-score denotes the class of the input. Identification is one-to-many matching.

In verification mode, if the match score is above some threshold, the identity claim is accepted. Otherwise, it is rejected. There are four outcomes of this setting which are:

1. True accept: The person is genuine and the claim is verified.
2. True reject: The person is impostor and the claim is not verified.
3. False accept: The person is impostor and the claim is verified.
4. False reject: The person is genuine and the claim is not verified.

In order to show the verification performances of recognition systems, generally Receiver Operating Characteristic (ROC) curve is utilized, which represents the probability of true acceptance versus probability of false acceptance. In this thesis, we report the verification performances not only using ROC curves. In some cases, we also show verification performances using Detection Error Trade-Off (DET) curve, which is a variant of ROC curve. The primary difference is that y-axis is the false rejection rate instead of true acceptance rate in DET curve. Finally, in this study, we also use the term Equal Error Rates (EER) to show verification performances. EER is the value where False Acceptance Rate (FAR) and False Rejection Rate (FRR) are equal.

In identification, rank phenomenon is introduced. In this thesis, the rank-1 identification is utilized to show the identification performances. In rank-1 identification, a probe is identified as the first ID in the list of subjects sorted in decreasing order of computed similarity scores.

2.1.2 Face Recognition

Face recognition [144] is the least intrusive biometric technique from the acquisition point of view. It has been applied to a wide range of commercial and law enforcement applications. In comparison to other popular biometric characteristics (such as fingerprint [60] and iris [35]), face recognition (for either identification or verification) requires less user cooperation and thus can be integrated in many advanced conditions (notably in video surveillance).

In face recognition systems, first face is detected and segmented from the background. Next, several landmarks are annotated, which are used in normalization of the face. Then feature extraction is applied and authentication is done either in verification or identification mode.

Although literature works (salient contributions such as Eigenface [12], Fisherface [12] and Local Binary Patterns (LBP) [4]) reports highly accurate results on well controlled datasets, the introduction of new face databases (for example, The Facial Recognition Technology (FERET) [108], Face Recognition Vendor Test (FRVT) [14] and Face Recognition Grand Challenge (FRGC) [107] by National Institute of Standards and Technology (NIST)) challenges the standard techniques by providing different variations (expressions, illuminations, poses etc.), large number of subjects, as well as new data modalities (2D, 3D, video etc.). As a consequence, the proposition of those databases greatly stimulates the development of more robust and reliable face recognition methods.

Recent surveys [3, 18] have suggested that face recognition exploiting 3D shape cues (either in the format of 3D curvature description or 2.5D depth feature) demonstrates the superiority over typical intensity image based methods. For instance, 3D shape information is invariant to illumination variations. It supplies complementary information with respect to 2D textures and viewpoint variations are readily addressed by rigid surface registrations [13, 24]. However, because most of the literature works report their results on the face database with high quality 3D data (e.g. 3D faces in FRGC, which are obtained by a digital laser scanner [122], with depth resolution of 0.1 mm within the typical sensing range), there is an unbalanced matching between the 2D and 3D data in terms of both efficiency and accuracy. With respect to efficiency, the acquisition of a high resolution RGB image normally takes $< 0.05s$, whereas the laser scanning of a face depth map consumes $9s$ in average [107] (and hence with high user cooperation, which is conflicting with the non-cooperative property of face recognition). Regarding accuracy, the measurement of an object with 10 cm depth along the z axis needs 10 $bits$ representation, whereas all intensity information are represented by 8 $bits$. Due to the above imbalance, it is not perfectly fair to compare 2D and 3D face recognition using such data, and it impedes the use of 3D and multi-modal (2D+3D) face recognition in practical scenarios.

Fortunately, the Kinect sensor reduces above problems by providing both 2D and 3D information simultaneously at interactive rates, where the practical 3D and 2D+3D face recognition systems are feasible for real-time and online processing [95]. Even though the overall sensing quality of the Kinect is known better than the sensors using stereo vision or ToF, it is still much inferior than the laser scanning quality which is usually considered in 3D face recognition researches.

As 3D sensing technologies advance and the acquisition devices become more accurate and less expensive, the utilization of 3D face recognition and range data

together with color data broadens.

In this thesis, the aim is not to propose new face recognition techniques. On contrary, we analyze how the performances of 2D and 3D face recognition systems are affected by spoofing attacks and disguise variations and then we propose countermeasure techniques to mitigate their impact on face recognition.

Security reflects how vulnerable the biometric system is to attacks like spoofing or tampering biometric data. Despite the fact that face recognition has been investigated extensively, spoofing is a major challenge for face recognition systems. In this chapter, first, we briefly describe what face spoofing is. A survey of the literature on spoofing in face recognition including the impact analysis and countermeasures is presented.

Disguise variations is another major challenge in face recognition. This is why, in the second part, we describe disguise variations and then a survey of the literature on disguise variations in face recognition including the impact analysis and countermeasures is presented.

2.2 Spoofing in Face Recognition

In a spoofing attempt, a person tries to masquerade as another person and thereby, tries to gain access to a recognition system. Since face data can be acquired easily in a contactless manner, spoofing is a real threat for face recognition systems.

There are several types of spoofing attacks such as photograph, video or mask attacks. Due to its 3D face shape characteristics, the detection of 3D mask attacks appears to be more challenging compared to the detection of 2D attacks such as photograph and video attacks. In this section, spoofing in face recognition is analyzed in two groups as *2D spoofing attacks and countermeasures* and *3D spoofing attacks and countermeasures*.

2.2.1 2D Spoofing Attacks and Countermeasures

The most common spoofing attacks to face recognition systems are achieved by using photographs and videos due to their convenience and low cost. It has been shown that face recognition systems are vulnerable to photograph and video attacks. For instance, in the study of Määtta et al. [87], it is stated that the Windows XP and Vista laptops of Lenovo, Asus and Toshiba can be spoofed easily. These laptops authenticate users by scanning their faces. According to [87], at Black Hat 2009 conference, the Security and Vulnerability Research Team of the University of Hanoi demonstrated how to easily spoof the systems "Lenovo's Veriface III", "Asus' SmartLogon V1.0.0005", and "Toshiba's Face Recognition 2.0.2.32" using fake facial images of the user. In [87], it is also claimed that this vulnerability is now listed

in the National Vulnerability Database of the National Institute of Standards and Technology (NIST) in the US. This simple example demonstrates that countermeasure techniques have to be developed to enhance the security and robustness of face biometric systems. Figure 2.1 shows an example for photograph spoofing.

Figure 2.1: An example photograph attack for spoofing purposes. Figure is taken from [64].

The subject of spoofing has started to gain more popularity in the recent years, however the studies on face anti-spoofing methods are still very limited. Therefore, anti-spoofing is a popular topic for researchers. Aim is to develop non-intrusive countermeasures without extra devices and human involvement which can be integrated into existing face recognition systems.

Various approaches have been developed to detect photograph spoofing. The existing techniques mainly concentrate on liveness detection and motion analysis in case analysis are not restricted to a single image. There are also several countermeasure techniques based on texture analysis, which can be applied on single images.

Motion analysis approaches rely on the fact that even there is motion, depth map is plane for photos; whereas it varies in case of live faces. In the literature, there are several countermeasures based on motion analysis [9, 26, 70, 71, 89]. In [9], under the assumption that the test region is a 2D plane, the authors obtain a reference field from the actual optical flow field data. Then the degree of differences between the two fields is used to distinguish between a 3D face and a 2D photograph. In [89], a set of facial points are located automatically and their geometric invariants are used to detect attacks. In [26], they use 3D depth information of a human head to detect the presence of an actual person as opposed to an image of that person. Kollreider et al. [70] evaluate the trajectories of selected part of the face from the sequence of images using a simplified optical flow analysis followed by a heuristic

classifier. In the other study of Kollreider et al. [71], they fuse these scores with liveness properties such as eye-blinks or mouth movements.

Countermeasures based on liveness detection examine movements such as eye-blinking [105] or lip movements [25]. However, since liveness is detected by recognizing spontaneous eye-blinks or lip movements, again analysis require several images among time.

There are also several texture analysis based countermeasure techniques, which can be applied on single images. For instance, spoofing can be detected by analyzing the frequency spectrum of a live face [82, 131]. In [82], it is assumed that the high frequency components of photos are less than those of live face images. However, this method gives good results when photo images have low definition and small size as stated in [131]. In [8], images are examined to find printing artifacts. In the studies of Määtta et al. [87, 88], micro-texture details and texture and local shape details of real faces and face prints are analyzed, respectively, and very satisfactory performances are reported for the detection of face print attacks using the publicly available NUAA Database [33].

In the study of Chakka et al. [22], the results of a competition on countermeasures to 2D facial spoofing attacks are reported. This study provides a comparative study of different techniques using the same protocols and data. For the competition, they used the publicly available PRINT-ATTACK biometric (face) database [34]. The database consists of 200 videos of real accesses and 200 videos of attack attempts of 50 different identities. The motivation behind this competition is to compare the performance of different state-of-the-art algorithms on the same database using a unique evaluation method. Six different teams from universities around the world have participated in the contest. Two teams, IDIAP and UOULU proposed texture analysis based countermeasures and obtained zero percent Equal Error Rate (EER) on development set and zero percent Half Total Error Rate (HTER) on test set. This leads to the conclusion that, the attack videos in PRINT-ATTACK database mainly consist of detectable texture patterns. Most of the algorithms involved in this competition are able to clearly separate spoof attempts from real accesses. The results suggest the investigation of more complex attacks.

2.2.2 3D Spoofing Attacks and Countermeasures

Compared to 2D spoofing attacks such as photograph and video, 3D mask attacks to face recognition systems is a considerably new subject. The main reason for the delay in mask spoofing studies is due to the unavailability of public mask databases. The preparation of a mask attacks database is much more difficult and expensive than the preparation of photograph or video attacks databases. Initially, to prepare a high quality mask, a 3D scanner is necessary to obtain the 3D model of the target person, which are generally high-cost devices. The procedure continues with manu-

facturing of the masks which is also an expensive procedure.

When 3D masks are introduced as attacks, some of the countermeasures proposed for the detection of 2D spoofing attacks are no more applicable. The study of Kollreider et al. [71] shows that a face recognition system relying on eye blinking and lip movements can be defeated by using photographic masks wrapped over face with eyes and mouth regions cut out. Also, since motion based countermeasures depend on different movements of 2D and 3D surfaces, they are not applicable when masks are used instead of photos or videos. It appears that the detection of 3D mask attacks is more challenging compared to the detection of 2D facial attacks.

If a 3D mask is not able to spoof a recognition system, it is not a successful attack, and there is no need to develop a countermeasure against it. Therefore, initially the spoofing performances of the masks have to be analyzed. Unfortunately, there are only two studies in the literature which evaluates the spoofing performances of 3D mask attacks. In our study [74], we analyzed how well the spoofing performances of the masks used in our studies are. To the best of our knowledge, the spoofing performances of mask attacks on both 2D and 3D face recognition were first analyzed in our study [74] using the mask database which was prepared within the context of the European Union (EU) research project TABULA RASA [111]. The mask database used in our study [74] includes both 2D and 3D data hence we were able to evaluate the impact of mask attacks on both 2D and 3D face recognition. Since this database consists of very high-quality masks, they have almost perfect spoofing performances especially in 3D. After our study which examines spoofing performances of 3D mask attacks [74], very recently a new study is published by Erdogmus et al. [41], which presents the 3D Mask Attack Database (3DMAD). 3DMAD was recorded with a low-cost depth camera (Microsoft Kinect sensor). In [41], they also analyzed the spoofing performances of 3D mask attacks using 3DMAD database however only for 2D face recognition, which is the main limitation of the study. The reported results in [41] demonstrate that facial masks can pose a serious threat to 2D face recognition systems.

The spoofing performances of 3D mask attacks are very dependent to the technique used for manufacturing of masks. The masks in 3DMAD are prepared by the company "Thats My Face" [132] which provides colored masks (Figure 2.2). Masks are manufactured by utilizing one frontal and one profile picture of the target person. The advantage of this service over the others is the possibility of creating a 3D mask only by providing these two facial images instead of providing the 3D model. However, since these masks are not prepared based on the 3D models of the target faces, they do not show exact 3D face shape characteristic of their target faces. This is why, spoofing performances of these masks are expected to be lower, especially in 3D, compared to spoofing performances of the high-quality masks which are manufactured by utilizing the exact 3D models of their target faces.

In face spoofing analysis, it is very important to evaluate the spoofing performances of mask attacks before proposing countermeasures against them. The reason is that there is no need to develop a countermeasure against a mask attack which is not able to spoof a recognition system.

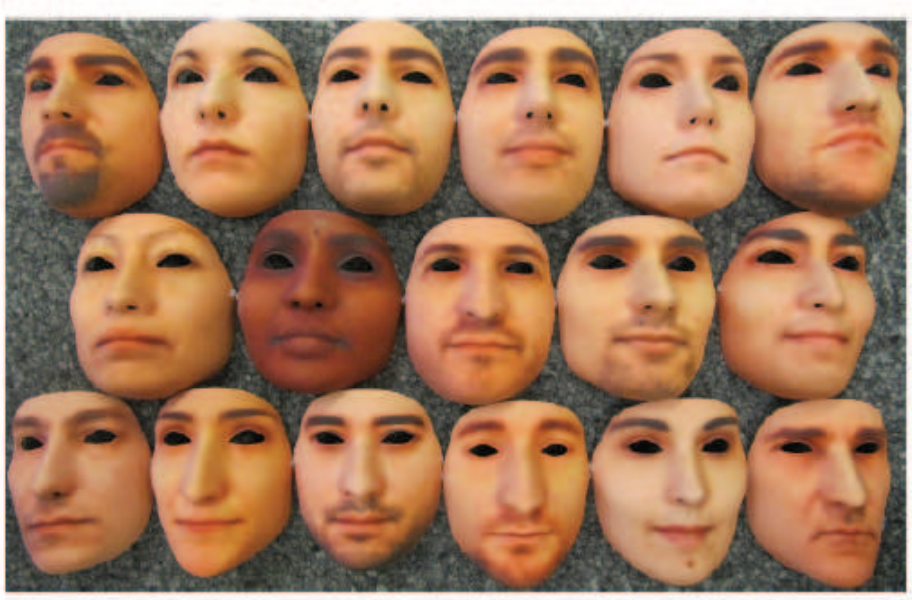

Figure 2.2: Masks obtained from ThatsMyFace.com. The picture is taken from [41].

Since 3D mask attacks to FR systems is a considerably new subject, the studies regarding countermeasure techniques for the protection of face recogniton systems against mask attacks are also very limited. To our knowledge, in the literature, there are three countermeasure studies against 3D mask attacks [41, 66, 142] excluding our studies. The two studies [66, 142] are based on reflectance analysis. They utilize 2D data (texture images) in their approach to detect 3D mask attacks. Kim et al. [66] exploit the reflectance disparity based on albedo between real faces and mask materials (silicon, latex or skinjell). The feature vector, which is used in their approach for mask detection, consists of radiance measurements of the forehead region under 850 and 685 nm illuminations. They report 97.78% accuracy for mask detection. In [66], the experiments are done directly on the mask materials not on the real facial masks. Thus, it is not possible to report spoofing performances of the masks used. The measurements are done at exactly 30 cm and on the forehead region for mask detection. The requirement for an exact distance and occlusion possibility in the forehead during the measurements are the limitations of this method. In [142], multi-spectral reflectance analysis is proposed. After measuring the albedo curves of facial skin and mask materials with varying distances, two discriminative wavelengths (850 and 1450 nm) are selected. Finally, a Support Vector Machine (SVM) [23] classifier is used to discriminate between real and fake samples. Experi-

ments are conducted on a database of 20 masks from different materials (4 plastic, 6 silica gel, 4 paper pulp, 4 plaster and 2 sponge). The results show that this method can achieve 89.18% accuracy. The superiorities of [142] compared to [66] are the elimination of range limitation and the usage of real facial masks. However, spoofing performances of the masks are still not reported. In the very recent study [41], an analysis on LBP-based countermeasures using color and depth images obtained from Kinect is explained. In [41], HTER values are found to be 0.95% and 1.27% for color and range images, respectively, by applying LDA classification of block-based extracted uniform LBP features. The limitation of [41] is that the spoofing performances of mask attacks are only analyzed in 2D face recognition. Hence it is not possible to learn the spoofing performances of the masks used (shown in Figure 2.2) in 3D face recognition from their study.

In order to contribute this compelling research problem and fill the missing portions of the existing studies, we have proposed several countermeasure techniques against 3D mask attacks in [73], [76], [75] and [77], which will be explained in Chapter 5.

2.3 Disguise Variations in Face Recognition

In recent face recognition studies, under normal changes in constrained environment, the performance of existing face recognition systems is greatly enhanced. However, in most real world applications, there can be several problems such as using images of low quality or non-cooperative users or temporal variations and dissimilarities in facial characteristics that are created using disguise accessories.

In the second part of this thesis, we focus on recognizing face images with disguise variations. Although face recognition with disguise variations is a major challenge, the research studies on this topic are limited. In this section, several disguise variations are described and a survey of the literature on disguise variations and robust techniques against these variations are presented. We investigated mainly three types of disguise variations which are variations due to facial alterations, facial makeup and finally occlusions (facial accessories).

2.3.1 Facial Alterations and Countermeasures

Plastic surgery is considered to be a relatively new challenge in face recognition when compared to pose, expression or illumination variations. With the increasing number of people resorting to plastic surgery for correction of feature defects, cosmetic reasons or even law evasion, it becomes of interest for the biometric community to investigate and prevent the impact of facial alterations on recognition performances. Yet, very few studies exist which address this problem.

To the best of our knowledge, the impact of facial alterations, specifically due to plastic surgeries, on face recognition was first analyzed in [126] where the effect of

plastic surgery is evaluated on six recognition algorithms. The database used consisted of 506 subjects with 2 images: before and after the plastic surgeries. Later, this work was extended in [127] by augmenting the database up to 900 subjects and additionally including a different non-surgery database for performance comparison. Figure 2.3 shows an example from the plastic surgery database explained in [127]. The results showed that the evaluated appearance, feature and texture-based algorithms were unable to effectively mitigate the decline caused by plastic surgery procedures.

Figure 2.3: Example for (a) lip augmentation, (b) Otoplasty or ear surgery, (c) liposubmental chin implant and liposuction of chin/neck, and (d) face resurfacing. The pictures are taken from [127].

Three shortcomings of these studies [126, 127] can be identified as follows:

- Due to the fact that a single image is provided before the plastic surgery procedure, a non-surgery vs. non-surgery recognition experiment had to be conducted on a separate database with different subjects. Unfortunately, for face recognition algorithms, the accuracy can vary widely depending on the difficulty of the database. Hence, an authentic comparison is not possible.
- In the plastic surgery database, the before and after images differ not only as a result of the procedure, but also due to expressions, makeup and facial hair

variations. This leads to an additional decrease in the performances which clouds the true measurement of the plastic surgery effect.

- Since this is an image database, the analyses are restricted to 2D. However, 3D face recognition gains a rising popularity as it offers superiority over to its 2D counterpart by being intrinsically robust against illumination and pose variations. For this reason, the impact of the facial alterations on 3D algorithms should also be investigated.

In our study [40], these limitations are eliminated by creating a synthetic database using FRGC v1.0 [107] for which nose regions are randomly exchanged between subjects. In this way, a 2D+3D database is obtained for nose alterations and since the conditions and the subjects are identical for the original and the simulated databases, measuring the exact impact of the applied changes is possible. This study will be explained in Chapter 6 in detail.

Since there is only one publicly available plastic surgery database, similar to the lack of studies on impact analysis of facial alterations, the studies which propose robust techniques to facial alterations are also very limited.

In [15], an evolutionary granular approach is proposed for matching a post-surgery face image with a pre-surgery face image and 15% improvement in identification performance is reported. Furthermore, two new methods, FARO and FACE, based on fractals and a localized version of correlation index, respectively, are implemented in [90] which claims that the performance of these two algorithms compare favorably against standard face recognition methods such as PCA and LDA in case of plastic surgery changes. Singh et al. adopted the near set theory to classify facial images that have previously undergone some feature modifications in [125]. Finally, in [78], we proposed a block-based face recognition approach, which mitigates the impacts of facial alterations on face recognition. The details of this approach are explained in Chapter 7. It provides significant recognition performances both in 2D and 3D face recognition in the existance of facial alterations using the simulated nose alteration database presented in our previous study [40].

2.3.2 Facial Makeup and Countermeasures

Facial cosmetics are a common part of the daily life in many cultures since Ancient Egypt [7] and change the perception of a face. The impact of facial cosmetics on the perception of a face is shown in Figure 2.4.

Research on the impact of facial cosmetics is limited, mainly because of the lack of public database which contains multiple images with and without facial cosmetics for a significant number of women. In [119], the authors develop a system which detects the most suitable makeup for a given human face. Unfortunately, they cannot provide public access to the database which they used for their study. Some

databases (e.g. [114], [42]) provide images with facial cosmetics but there are no corresponding images without facial cosmetics hence these databases are inappropriate for the evaluation of face recognition.

Figure 2.4: Reference Image and Makeup Serie Images.

One rare investigation of the facial cosmetics challenge in face recognition can be found in [29]. The authors state that facial cosmetics have an impact on the performances of face recognition systems. They mention about the need for a better understanding of the altering effects of facial cosmetics and the development of robust algorithms. Since the database used in their study is not publicly available, the obtained results are not reproducible. Also, the amount of applied facial cosmetics and the cosmetics' application area are not evaluated in detail.

In our study [37], we contribute to studies related to facial cosmetics by providing a suitable database as well as an objective classification of facial cosmetics. The database contains multiple images with and without facial cosmetics for each person and provides detailed information about the application area and amount of applied cosmetics for each image. In this study, preliminary tests concerning the impact of facial cosmetics on face recognition are conducted and we observed that especially makeup for eye region takes an important role in face recognition. The details of this study is explained in Chapter 8.

2.3.3 Facial Accessories (Occlusions) and Countermeasures

Recognition of faces with disguise is a major challenge and has been recently addressed by several researchers [5, 113, 124, 128]. Figure 2.5 shows an example for facial accessories (occlusions) from the AR Face Database [91].

In the book chapter of Singh et al. [129], some studies on disguise variations are explained. According to this chapter, Ramanathan et al. [113] studied facial similarity for several variations including disguise by forming two eigenspaces from two halves of the face, one using the left half and other using the right half. From the test image, optimally illuminated half face is chosen and is projected into the eigenspace. This algorithm has been tested on the AR face database [91] and the National Geographic database [113] which consists of variations in smile, glasses, and illumination. Silva and Rosa [124] uses Eigen-eyes to handle several challenges

Figure 2.5: Example of images for occlusion from the AR Face Database [91].

of face recognition including disguise. Using the Yale face database [48], the algorithm was able to achieve an accuracy of around 87.5%. The advantage of the algorithm is that alterations in facial features excluding the eye region do not affect the accuracy. Pamudurthy et al. [104] proposed a face recognition algorithm which uses dynamic features obtained from skin correlation and the features are matched using nearest neighbor classifier. On a database of 10 individuals, authors reported that this approach gives accurate results. Alexander and Smith [5] used PCA based algorithm with Mahalanobis angle as the distance metric. The results show an accuracy of 45.8% on the AR database.

The limitation of these algorithms is that the performance degrades when important regions such as the eye and mouth are covered. Moreover, in [128], it is stated that the AR and Yale databases do not contain many images with disguise and therefore are not ideal for validating algorithms under comprehensive disguise scenarios. In [128], the impact of disguise variations is evaluated on several face recognition techniques using one database.

Since the existing databases do not contain many images with disguise, we present the first publicly available face database based on the Kinect sensor for face recognition, which is explained in Chapter 9. The database consists of different data modalities and multiple facial variations. The proposed database consists of 936 shots of well-aligned 2D, 2.5D and 3D face data and 104 video sequences from 52 individuals taken by the Kinect sensor. It contains 9 different facial variations within 2 different sessions. We carefully selected 9 types of facial variations in both sessions: neutral face, smiling, mouth open, strong illumination, occlusion by sunglasses, occlusion by hand, occlusion by paper, right face profile and left face profile. We conduct benchmark evaluations on the proposed database using a number of baseline face recognition methods. Specifically, we report the results (of identification/verification) of Eigenface [12], LBP [4], SIFT [85], and LGBP [140] for the 2D and 2.5D

based face recognition, and conduct both the rigid method (i.e., ICP) [93] and the non-rigid method (i.e., TPS) [39] for 3D based face recognition. Score-level fusion of the RGB and depth data is also conducted, which demonstrates significantly improved results. The proposed KinectFaceDB are compared with a widely used high quality 3D face database (i.e., the FRGC database), in order to show the effects of 3D data quality in the context of face biometrics.

In 2D and 2.5D face recognition, we observed that the partial occlusions (i.e., sunglasses, hand on face, and paper on face) are very challenging to all tested methods, especially in the verification mode. Nevertheless, LGBP based method is more robust to partial occlusions in comparison to the other methods, and gives the best overall performances. This result conforms to the findings in [140], where the authors suggested that the multi-resolution/multi-orientation based Gabor decomposition and the local patch based representation of LGBP can enhance the robustness in presence of partial occlusions.

In the same study, we also observed that the TPS based method generates better recognition results in most cases than the ICP based method. This is because the non-linear alignment acted by TPS can partially handle the facial expression problem to some extent (which conforms to the results in [39]). Nevertheless, none of these methods can handle the partial occlusion problem. For faces occluded by hand and paper, the large surface distortions completely mislead the face registration.

Experimental results suggest that the performances of existing algorithms are not sufficient enough against disguise variations. Thus, face recognition with disguise variations is still a major challenge and more robust techniques against occlusions have to be developed to mitigate its impact on face recognition.

2.4 Conclusions

In this chapter, we started with a short introduction to general biometrics and face recognition. Next, we presented an in-depth description for the current state of the topic "spoofing in face recognition", which is analyzed in two parts as 2D face spoofing and 3D face spoofing. Then, we explored the state-of-the-art for "disguise variations in face recognition". Since in this thesis the variations due to facial alterations, facial makeup and facial accessories (occlusions) are analyzed, we presented an in-depth description for the current state of these variations.

Chapter 3

Countermeasure Technique Against Photograph Attacks

In this chapter, a new face anti-spoofing approach, which is based on analysis of contrast and texture characteristics of captured and recaptured images, is proposed to detect photograph spoofing. Since photo image is a recaptured image, it may show quite different contrast and texture characteristics when compared to a real face image. Rotation invariant local binary pattern variance (LBPV) method is selected to be used in this study for feature extraction. The approach is tested on the publicly available NUAA photo-impostor database, which is constructed under illumination and place change. The results show that the approach is competitive with other existing methods tested on the same database. The technique is robust to illumination change, non-intrusive and simple.

3.1 Introduction

There are several types of spoofing attacks such as photograph, video or mask attacks. Due to 3D face shape characteristics of masks, the 3D face shape analysis, which is very beneficial for the detection of photograph and video attacks, is no more applicable in the existance of 3D mask attacks. Before examining 3D mask spoofing and countermeasures, which are explained in the next chapters, we first analyzed photograph attacks in our study [72]. This preliminary study helped us to gain an insight on the topic of face spoofing and countermeasures.

Various approaches have been developed to detect photograph spoofing. A good survey of approaches against photograph spoof can be found in Section 2.2.1. The existing techniques mainly concentrate on liveness detection and motion analysis in case analysis are not restricted to a single image. There are also several countermeasure techniques based on texture analysis, which can be applied on single images.

In this chapter, an approach, which is based on contrast and texture analysis of captured and recaptured images, is proposed to detect photograph spoofing. Each face anti-spoofing technique differs from each other in terms of the need for data quality, additional hardware, and user collaboration. In our approach, a rotation invariant Local Binary Patterns Variance (LBPV) [52] based method is used to detect photograph spoofing. This method relies on a single image. Only a generic webcam

is used, hence there is no need for extra hardware and user collaboration.

This chapter is organized as follows: Section 3.2 gives the specifications of the selected NUAA photograph database [131]. Section 3.3 describes the proposed approach. Section 3.4 explains the experiments and analysis. Conclusions are provided in Section 3.5.

3.2 The Photograph Database

The NUAA photo database [131], which is one of the few publicly available photo databases, is selected for this study. It is constructed by using a generic webcam. Figure 3.1 shows the live and photograph images in different sessions. Place and illumination condition of each session is different. Test and train sets are constructed from different sessions. The database involves 15 subjects. In each session, the images of both live subjects and their photos are captured with frame rate 20 fps. 500 images are collected for each subject. Images are all frontal with neutral expression. There are no apparent movements like eye-blink and head movements. Therefore, captured and recaptured images have more similarities, which makes the spoofing detection more challenging.

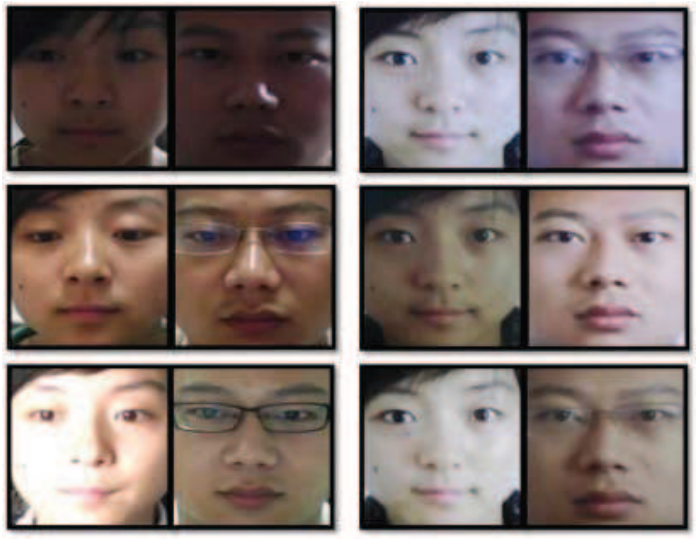

Figure 3.1: Each column contains samples from session 1, session 2 and session 3. In each row, the left pair is from a live human and the right from a photo. It contains various changes (e.g., sex, illumination, with/without glasses). Figure is taken from [131].

A high definition photo of each subject is taken using a Canon camera for the NUAA photo database. Photographs are developed in two ways. First way is to print them on a photographic paper with the common size of $6.8cm \times 10.2cm$ (small)

and $8.9cm \times 12.7cm$ (bigger). Second way is to print them on a 70g A4 paper using a usual color HP printer. To make an exact comparison with the existing methods in [131], the same database is selected, and experiments are done with the same train-test set partitioning.

Table 3.1 gives statistics of the number of images involved in the NUAA database for each train and test sets. Since each set contains images from different sessions, there is no overlapping between test and train set images. In the NUAA database [33], 6 subjects out of 9 subjects do not appear in the train set for live human case, and 6 subjects out of 15 subjects do not appear in the train set for photo case. This shows that in our study, the subject appeared in the test set may not be appeared in the train set, which makes the detection of photograph spoofing more challenging.

Table 3.1: Number of Images in the NUAA Database for Train and Test Sets

	Session 1	**Session 2**	**Session 3**	**Total**
Train Set				
Client	889	854	0	1743
Impostor	855	893	0	1748
Test Set				
Client	0	0	3362	3362
Impostor	0	0	5761	5761

3.3 The Proposed Approach

In this study, the problem is simply a classification problem with two classes. First class is the real image class, which are in fact captured images, and second class is the class of photograph images of real faces. Since the image of a photo is an image of a real face which passes through the camera system twice and the printing system once, it is in fact a recaptured image, which has lower image quality compared to a real face image taken under same imaging conditions.

The proposed countermeasure relies on different contrast and texture characteristics of captured images and recaptured images to detect photograph spoofing. In the proposed approach, initially a Difference of Gaussian (DoG) filter is used to obtain a special frequency band which gives considerable information to discriminate between real and photo images. Then, features are extracted from DoG filtered image by applying LBPV method.

3.3.1 Pre-Processing

Recaptured image has less sharpness (lower image quality) when compared to a captured image; therefore recaptured image contains less high frequency components [82, 131]. This fact can be observed by analyzing the 2D Fourier spectra of a

real face and a photo face image.

DoG filtering is used to remove noise while preserving the high frequency components, which are especially image edges. In this approach, instead of analyzing all high frequency bands, the high-middle band frequency spectrum is analyzed. For the DoG filter, a quite narrow Gaussian ($\sigma_0 = 0.5$) is formed without introducing noise. To filter out misleading low spatial frequency information, $\sigma_1 = 2$ is selected for the outer Gaussian. This pre-processing technique helps to remove misleading information and noise; hence we can focus on the part of the spectrum which provides fundamental information to discriminate between captured and recaptured images.

The positive effect of applying DoG filtering as the pre-processing step in the proposed approach is also verified in Section 3.4.

3.3.2 Feature Extraction

LBP [102] is one of the most popular texture analysis approaches, which characterizes the spatial structure of the local image texture. Texture can be characterized by a spatial structure (e.g. LBP), which varies with rotation, and the contrast (e.g variance of local image texture), which does not vary with rotation [52]. LBPV is a simplified and efficient joint LBP and contrast distribution method [52]. The contrast and pattern of a texture are complementary features. LBPV adds additional contrast measures to the pattern histogram. LBPV calculation is based completely on LBP calculation. $LBP_{P,R}$ is calculated as follows:

$$LBP_{P,R} = \sum_{p=0}^{P-1} s(g_p - g_c)2^p \tag{3.1}$$

$$s(x) = \begin{cases} 1, & x \geq 0 \\ 0, & x < 0 \end{cases} \tag{3.2}$$

$LBP_{P,R}$ is computed such that for a given central pixel in an image, a pattern number is computed by comparing its value with those of its neighbours. In Equation (3.1), g_c is the gray value of the central pixel, g_p is the value of its neighbours, P is the number of neighbours around a circle of radius R.

To obtain LBP histogram of an $X \times Y$ image, the LBP pattern of each pixel (i, j) is used in calculation.

$$H(k) = \sum_{i=2}^{X-1} \sum_{j=2}^{Y-1} f(LBP_{P,R}(i,j), k), \quad k = [0 \;\; K-1] \tag{3.3}$$

$$f(x,y) = \begin{cases} 1, & x = y \\ 0, & else \end{cases} \tag{3.4}$$

In Equation (3.3), K is the maximal LBP pattern value. In this histogram, each LBP pattern has weighting factor of 1. LBPV algorithm is used to add contrast information to this histogram. Variance is computed for the P sampling points around a circle of radius R using Equations (3.5) and (3.6).

$$Var_{P,R} = \frac{1}{P}\sum_{p=0}^{P-1}(g_p - u)^2 \tag{3.5}$$

$$u = \frac{1}{P}\sum_{p=0}^{P-1} g_p \tag{3.6}$$

The LBPV computes the variance from a local region and accumulates it into the LBP bin as the weighting factors [52]. LBPV histogram is calculated using Equations (3.7) and (3.8).

$$LBPV_{P,R}(k) = \sum_{i=2}^{X-1}\sum_{j=2}^{Y-1} w(LBP_{P,R}(i,j),k), \qquad k = [0 \;\; K-1] \tag{3.7}$$

$$w(LBP_{P,R}(i,j),k) = \begin{cases} var_{P,R}(i,j), & LBP_{P,R}(i,j) = k \\ 0, & else \end{cases} \tag{3.8}$$

The start and the end values for i and j in Equations 3.3 and 3.7 depend on the selected R value. In these equations we assumed that R is selected as 1. Since it is not possible to compute LBP at the borders, the start value for i and j is 2, and the end values for i and$j$ are $X-1$ and $Y-1$, respectively. The representations of two different selections for P and R values are shown in Figure 3.2. The study in [52] states that when P and R values are increased, even better results are obtained; however with a cost of increasing computational complexity. In the proposed approach, P and R values are selected as $P = 8$, $R = 1$.

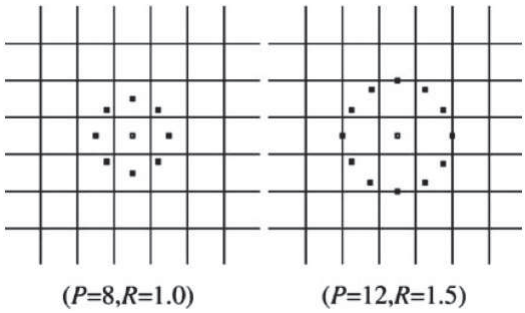

Figure 3.2: Circular representations of selections ($P = 8$, $R = 1$) and ($P = 12$, $R = 1.5$). Figure is taken from [52].

Instead of using all LBPV patterns, uniform patterns can be used as features. Uniform patterns are verified to be the fundamental patterns of local image texture.

A local binary pattern is called uniform if the binary pattern contains at most two bitwise transitions from 0 to 1 or vice versa when the bit pattern is traversed circularly. The notation is $LBP^{u2}_{P,R}$. $u2$ stands for using only uniform patterns and labeling all remaining patterns with a single label.

$$U(LBP_{P,R}) = |s(g_{p-1} - g_c)| - |s(g_0 - g_c)| + \sum_{p=1}^{P-1} |s(g_p - g_c)| - |s(g_{p-1} - g_c)| \quad (3.9)$$

In Equation (3.9), U value is the number of spatial transitions (bitwise 0/1 changes) in the pattern. The patterns which satisfy $U \leq 2$ are selected as uniform patterns. Instead of using all patterns, sufficient information can be obtained using only uniform patterns. The number of uniform patterns is $P \times (P-1) + 2$.

In our case, since P is equal to 8, the uniform LBP, $LBP^{u2}_{P,R}$, results in a 59-bin histogram feature vector (58 out of 256 patterns are uniform and all the non-uniform patterns are labeled with a single label). This means that K value in Equation (3.7) is equal to 59 for $LBP^{u2}_{P,R}$; whereas it is equal to 256 when all LBPV patterns are used. In [102], it is claimed that in their experiments, uniform patterns account for a bit less than 90% of all patterns when using the (8,1) neighborhood and for around 70% in the (16,2) neighborhood case.

In Section 3.4, the performances are evaluated using "all LBPV patterns" and using "only uniform patterns of LBPV ($LBPV^{u2}_{P,R}$)", separately, in order to observe the slight performance decrease when only uniform patterns are used.

Figure 3.3: Different photo-attacks are shown from column (1) to column (5): (1) move the photo horizontally, vertically, back and front; (2) rotate the photo in depth along the vertical axis; (3) the same as (2) but along the horizontal axis; (4) bend the photo inward and outward along the vertical axis; (5) the same as (4) but along the horizontal axis. Figure is taken from [131].

In the proposed approach, an algorithm which is robust against rotation is preferred to detect recaptured images. The reason is that it is quite possible to make movements while holding photos. They can even be bent to make them visually closer

to a 3D face or to move horizontally or vertically to act like a live face. Figure 3.3 shows illustration of some types of photo-attacks.

There are both local and global rotation invariant algorithms in texture classification. In the proposed approach, a hybrid method, which is based on globally rotation invariant matching with locally variant LBPV texture features [52], is used to extract features for classification. Thereby, both global spatial information and local texture information are preserved in classification.

In our study, the global matching is implemented using exhaustive search scheme [52] to find the minimal distance in all candidate orientations, which is a simple method. The LBPV histogram is reorganized and represented by a rotation variant histogram H^{rv}, and a rotation invariant histogram H^{ri}. Then for two texture images, the matching distance is calculated as shown in Equation (3.10).

$$\begin{cases} D_{ES}(H_S, H_M) = D_{ri}(H_S^{ri}, H_M^{ri}) + D_{min}(H_S^{rv}, H_M^{rv}) \\ D_{ri}(H_S^{ri}, H_M^{ri}) = D(H_S^{ri}, H_M^{ri}) \\ D_{min}(H_S^{rv}, H_M^{rv}) = min(D(H_S^{rv}, \overline{H_M^{rv}(j)})), \quad j = 0, 1, \ldots, 7 \\ \overline{H_M^{rv}(j)} = [h^M_{mod(0-j,8)}, h^M_{mod(1-j,8)}, \ldots, h^M_{mod(7-j,8)}] \end{cases} \tag{3.10}$$

In Equation (3.10), $D(X, Y)$ represents chi-square distance defined in Equation (3.11). H_S is the test sample image and H_M is the model image histograms. $\overline{H^{rv}(j)}$ is the new matrix which is obtained by shifting j columns of original H^{rv} matrix. From Equation (3.10), it is clear that distance between two histograms is composed of two parts. $D_{ri}(H_S^{ri}, H_M^{ri})$ is derived from rotation invariant part and the other one $D_{min}(H_S^{rv}, H_M^{rv})$ is obtained by searching minimal distance within rotation variant part. Matching by exhaustive search is explained in [52, 69] in more details.

In the proposed approach, chi-square distance is selected to be used as the dissimilarity metric. Chi-square distance between sample and model histograms is computed as:

$$D(S, M) = \sum_{i=1}^{N} \frac{(S_i - M_i)^2}{S_i + M_i} \tag{3.11}$$

where N is the number of bins, and S_i and M_i are the values of the sample and model histograms at the n^{th} bin, respectively.

For each test image, matching by exhaustive search (Equation 3.10) is applied using chi-square distance metric (Equation 3.11), and distances from each test sample to all samples (x_i) in the client and impostor model sets are computed. Then, quadratic means of distances are computed for client and impostor model sets, consecutively, using Equation (3.12). In Equation (3.12), N is the number of images in the model set and x_i is the distance between test sample and model sample.

$$QM = \sqrt{\frac{1}{N}\sum_{i=1}^{N}(x_i^2)} \tag{3.12}$$

Finally, each test image is classified in the nearest class by comparing the two quadratic mean values, which are obtained for client and impostor sets.

3.4 Experiments and Analysis

To test the effectiveness of the proposed approach, two types of experiments are done. The first experiment includes exact comparison results between the proposed approach and the methods published in [131]. The second experiment is done to show the effect of DoG filtering in the proposed approach.

3.4.1 Test 1: Results under Illumination Change

For this test, the proposed countermeasure is applied using all LBPV patterns and using only the uniform patterns, seperately, for comparison purposes. The results of the approach using all LBPV patterns are given in Table 3.2 and the results of the approach using only the uniform LBPV patterns are given in Table 3.3.

Table 3.2: Proposed Approach Results Using All LBPV Patterns

Test Set	**Total # of Images**	**# of Wrong Detection**	**FRR (%)**	**FAR (%)**	**Total Error (%)**
Client	3362	308	9.16%		11.97%
Impostor	5761	784		13.61%	

Table 3.3: Proposed Approach Results Using only Uniform LBPV Patterns

Test Set	**Total # of Images**	**# of Wrong Detection**	**FRR (%)**	**FAR (%)**	**Total Error (%)**
Client	3362	399	11.87%		13.05%
Impostor	5761	792		13.75%	

The total error using all LBPV patterns is computed as 11.97% in Table 3.2; on the other hand, when only uniform patterns are used, it is computed as 13.05% in Table 3.3. This fact shows that instead of using all LBPV patterns, if only uniform LBPV patterns are used, the result is 8.28% worse. Out of 9123 test images, 99 more images are detected as true in case all LBPV patterns are used in classification.

Figure 3.4 shows the comparison of classification accuracies (%) computed by applying three classification techniques to five types of input features explained in [131].

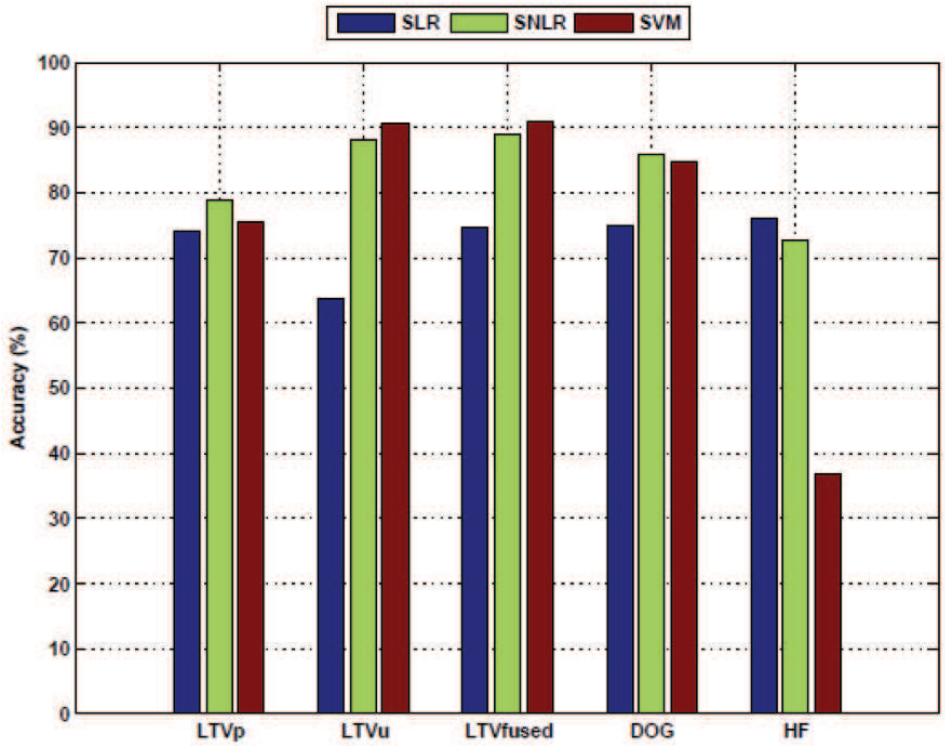

Figure 3.4: Comparison of detection rates using SLR, SNLR, SVM as classifiers and LTVp, LTVu, LTVfused, DoG and HF as input features. This figure is taken from [131].

The database proposed by Tan et al. [131] is used in this chapter to make an exact comparison with the other existing methods in [131]. Sparse Linear Logistic Regression (SLR) [83], Sparse Nonlinear Logistic Regression (SNLR) and Support Vector Machine (SVM) [23] classifiers are selected to be used as classifiers; illuminance component of image estimated with Logarithmic Total Variation (LTVu), reflectance component of image estimated with Logarithmic Total Variation (LTVp), DoG filtered image (DoG), and high frequency component of image (HF) are selected to be used as input features in the study of Tan et al. [131]. The illuminance and reflectance components of images are also fused (LTVfused) and used as another input feature in [131], which gives the best results as shown in Figure 3.4. According to the results in Figure 3.4, it is clear that the proposed approach is quite competitive with the existing techniques, even better when compared to most of the results shown in this figure.

The remarks extracted from Figure 3.4 are; initially, the proposed approach gives better results compared to the results obtained by applying SLR classifier to all input feature types. It is also clear that SLR, SNLR and SVM classifiers give worse results compared to our result (88.03%) in case DoG, HF, and LTVp are used as

input features. Best results are obtained for the cases where LTVu and LTVfused are used as input features and SNLR and SVM are used as classifiers as shown in Figure 3.4. However, the result of the proposed approach (88.03%) is also competitive with these results. Our approach even has some advantages compared to the techniques providing the best results in this figure. For example, for the techniques based on LTVu and LTVfused features, the image has to be decomposed into illuminance and reflectance components; whereas in the proposed approach, the method is applied directly on the image. Furthermore, classification method is very simple in our approach. Therefore, we can say that the proposed method can be considered to provide sufficient detection accuracy of 88.03% with the advantages of less computational complexity, robustness to illumination and rotation changes.

The texture and contrast analysis based countermeasure technique explained in this study was published in [72]. After our analysis on NUAA database, several studies have been published for the detection of photograph spoofing using the same database. Up to now, the best detection accuracies for face prints have been reported by Määtta et al. in their studies [87, 88]. Both of these studies provide almost perfect spoofing detection rates using the NUAA database.

3.4.2 Test 2: Effect of DoG Filtering in the Proposed Approach

In Test 1, approximately 88% success is achieved under illumination change for recaptured face image detection. For Test 1, as pre-processing step, DoG filter is used to extract the regions from which considerable spoofing information can be obtained.

In this test, the aim is to show the effect of DoG filtering in the proposed approach. Table 3.4 shows the results of the approach, which is applied both with and without DoG filtering.

The effect of DoG filtering can easily be observed from Table 3.4. With DoG filtering, there is a significant improvement compared to the case where DoG filtering is not applied as the pre-processing step. The effect of DoG filtering is due to the fact that DoG filtering helps to remove misleading information and noise, and thereby it provides a frequency spectrum which gives significant information for the detection of recaptured images.

Table 3.4: Proposed Approach Results with DoG Filtering and without DoG Filtering as Pre-Processing Step

Proposed Approach	**Total # of Images**	**Total # of Wrong Detection**	**Error (%)**
with DoG Filtering	9123	1092	**11.97%**
without DoG Filtering	9123	2140	**23.46%**

3.5 Conclusion

In this chapter, a recaptured image detection method, which is based on the analysis of different contrast and texture characteristics of captured and recaptured images, is proposed.

The proposed approach gives quite satisfactory results when compared to the results reported in [131], which use the same NUAA database in their experiments. The approach is simple and there is no need for user collaboration, which are its advantages.

There have been several studies on countermeasure techniques for the detection of photograph attacks. Compared to 2D spoofing attacks such as photograph and video, 3D mask attacks to face recognition systems is a considerably new subject. Even the impact of 3D mask attacks on existing recognition systems had not been analyzed before our study [74].

In the next chapter, we show how vulnerable the existing 2D and 3D face recognition systems are to spoofing mask attacks. Then, in Chapter 5, the countermeasures, which we have proposed up to now for the detection of 3D mask attacks, are explained.

Chapter 4

Impact of Mask Spoofing on Face Recognition

There are several types of spoofing attacks to face recognition systems such as photograph, video or mask attacks. To the best of our knowledge, the impact of mask spoofing on face recognition has been first analyzed in our study [74]. The reason for this delay is mainly due to the unavailability of public mask attacks databases. In this study, we use a 2D+3D mask database which was prepared for the research project TABULA RASA [111]. This chapter provides new results by demonstrating the impact of mask attacks on 2D and 3D face recognition systems. The results show that face recognition systems are vulnerable to mask attacks, thus countermeasures have to be developed to reduce the impact of mask attacks on face recognition. The results also show that 2D texture analysis provides more information than 3D face shape analysis in order to develop countermeasure techniques against high-quality mask attacks.

4.1 Introduction

The most common spoofing attacks to face recognition systems are achieved by using photographs and videos due to their convenience and low cost. It has been shown that face recognition systems are vulnerable to photograph and video attacks. Therefore, several countermeasures have been developed for the protection of face recognition systems against these 2D spoofing attacks.

Compared to 2D spoofing attacks, 3D mask attacks to face recognition systems is a considerably new subject. The main reason for the delay in mask spoofing studies is due to the unavailability of public mask databases. The preparation of a mask attacks database is much more difficult and expensive than the preparation of photograph or video attacks databases. Initially, to prepare a high quality mask, a 3D scanner is necessary to obtain the 3D model of the target person, which are generally high-cost devices. The procedure continues with manufacturing of the masks which is also an expensive procedure.

If a 3D mask is not able to spoof a recognition system, it is not a successful attack, and there is no need to develop a countermeasure against it. Therefore, in [74], we analyzed how well the spoofing performances of the masks used in our studies are. To the best of our knowledge, the spoofing performances of mask attacks on

both 2D and 3D face recognition were first analyzed in our study [74] using the mask database which was prepared within the context of the European Union (EU) research project TABULA RASA [111].

The mask database used in our studies was created by MORPHO [98]. This database includes many high-quality mask samples. It consists of 3D masks of 16 real subjects. The scans of subjects were acquired by a 3D scanner, and the masks were manufactured using a 3D printer. In addition to texture images, it includes 3D scans for both real and mask samples. Thanks to the nature of this database, in [74], we were able to conduct the benchmark evaluations for each of 2D, 2.5D and 3D face recognition.

The aim in the study [74] was not to propose a new face recognition method, but instead to show how vulnerable the selected baseline systems are to spoofing mask attacks. The results show that the masks used have very similar texture and especially 3D face shape characteristics to their target faces. They are very successful to spoof face recognition systems.

In this chapter, Section 4.2 gives brief information about the mask database which is used in our mask spoofing [74] and anti-spoofing studies [73, 75–77]. Section 4.3 explains the face recognition systems which are selected as baseline to test the performance of these systems under mask attacks. Section 4.4 discusses the experiments and analysis. Finally, conclusions are provided in Section 4.5.

4.2 The Mask Database

A mask is an object normally worn on the face, typically for protection, performance or entertainment. Additionally, masks can also be used for spoofing purposes.

There are several ways of mask manufacturing. Mask of a person can be prepared even by using papers. The company "Thats My Face" [132] provides colored masks (Figure 4.1). Masks are manufactured by mapping one frontal and one profile picture of the target person on a 3D model. However, since this model is not the exact 3D model of the target face, it does not show exact 3D face shape characteristic of the target person.

A mask used for 3D face spoofing purposes has to show very similar 3D shape characteristics to the target face to be considered as a successful attack. The mask database used in our studies was prepared to fulfill this objective. To obtain similar face shape characteristics to the target person, initially, scans of the subjects in the mask database were taken by a 3D scanner which uses a structured light technology. Then the 3D model (3D mesh) of each subject was sent to a 3D printer and the masks were manufactured by Sculpteo 3D Printing [110]. The material used for the

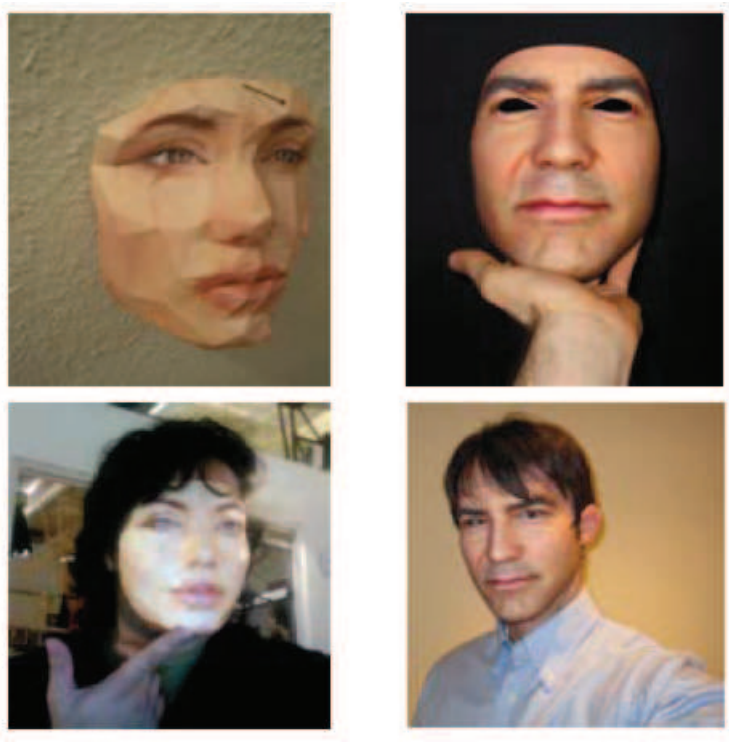

Figure 4.1: (upper row) Example samples for paper and fabric masks, (lower row) Masks in the upper row which are worn on the face. The pictures are taken from [132].

masks is polychrome mineral powder, which is standardly used for 3D printing.

The mask database is 2D+3D. For the sake of clarity, the database of real faces in 2D and 3D will be referred as DB-r2 and DB-r3, while the database of mask attacks will be referred as DB-m2 and DB-m3 in the rest of this chapter and the next chapter.

In the mask database, 20 subjects appear in total. The masks were manufactured for 16 of these subjects. For DB-r, average 10 scans of each subject were acquired. For DB-m, average 10 scans of each subject wearing either his/her own mask or masks of the other subjects that appear in the same database were acquired. Finally, 200 real face acquisitions from 20 subjects and 198 mask acquisitions from 16 masks are used for the evaluations. Figure 4.2 shows one example from this database for a real face access and the corresponding mask attack access.

In the mask database, DB-r and DB-m are partitioned in train and test sets. 8 subjects out of 16 subjects whose masks are manufactured, and 2 subjects out of 4 subjects whose masks are not manufactured are selected for DB-r. The samples of the selected subjects are assigned to the test set of DB-r, while the rest is used for the train set of DB-r. For DB-m, the mask attack accesses to the corresponding

Figure 4.2: Example from the mask database which is created by MORPHO. From left to right (upper row) The real face, the cropped texture image, the 3D scan after preprocessing, the cropped depth map estimated from the raw 3D scan (lower row) same images for the corresponding mask attack.

identities in the test set of DB-r are involved in the test set of DB-m, while the rest is used for the train set of DB-m. There is no overlap between the train and test sets, which makes the spoofing detection (explained in the next chapter) more challenging. Finally, there are 100 samples in each of the client (real accesses) test and train sets, and 99 samples in each of the impostor (mask attack accesses) test and train sets as shown in Table 4.1.

Table 4.1: Number of Images in the Mask Database for Train and Test Sets

	Train Set	**Test Set**
Client	100	100
Impostor	99	99

4.3 The Selected Face Recognition Systems

In this section, initially, we explain the pre-processing applied for the selected 3D and 2D face recognition techniques. Next, we give the details about these recognition techniques.

4.3.1 Pre-Processing

Both the selected 3D and 2D face recognition systems need pre-processing. The pre-processing applied for each selected system is explained below.

3D Face Recognition

The pre-processing for the selected 3D face recognition system is based on the method given in [39]. In order to crop the face region, the tip of the nose is detected, and the facial surface is cropped by a sphere with radius 80 mm, centered 10 mm away from the nose tip in +z direction. Note that the face looks towards +z direction. Next, the spikes are removed by thresholding, and then a hole filling procedure is applied. Finally, a bilateral smoothing filter is used to remove white noise while preserving edges. These pre-processed 3D scans (only shape, without texture) are used as input for 3D face recognition.

2D Face Recognition

For 2D face recognition, the texture images in the mask database are cropped as shown in Figure 4.2, and resized into 64×64 images. In this chapter, we aim to show how vulnerable the existing systems are to spoofing mask attacks by evaluating the performances of the selected systems with/without attacks. In the next chapter, we will show how a countermeasure improves the performance in presence of mask attacks by evaluating the performances of these systems with/without countermeasure.

Figure 4.2 shows an example for the texture images and 3D scans which are used in 2D and 3D evaluations, respectively.

4.3.2 Face Recognition Systems

In this part, the specifications of the selected 3D and 2D face recognition systems are explained.

3D Face Recognition

The 3D face recognition system selected as baseline for this study is introduced in [39]. It is also selected as the baseline system in TABULA RASA project [111]. It uses the pre-processed 3D mesh of the face as input. Three landmark points are previously annotated at the nose tip and outer eye corners for each sample in the database. Initially, a linear transformation is computed in a least squares sense (LSS), based on two sets of landmarks (landmarks of generic model and subject's face). Least squares means that the overall solution minimizes the sum of the squares of the errors made in the results of every single equation. The best fit in the LSS here is calculated by minimizing the squared distance between the point sets of generic model and subject's face. For this purpose, the obtained transformation that includes rotation, translation and isotropic scaling is applied onto the generic model, aligning it with the subject's face. Next, the alignment is further improved by Iterative Closest Point (ICP) method [13]. Afterwards, 140 previously selected

points on the generic model are coupled with the closest vertices on the face under analysis, and Thin Plate Spline (TPS) [16] warping is applied on the generic model resulting in warping parameters (WP) of size 140×3. WPs that represent the deviations from the common structure are given to the classifier for recognition. Finally, the distance between two face models is computed by taking the median of cosine distances between the corresponding feature vectors (WP), and recognition rates are computed. Figure 4.3 shows the feature extraction scheme on a sample model using this method, which is named WP.

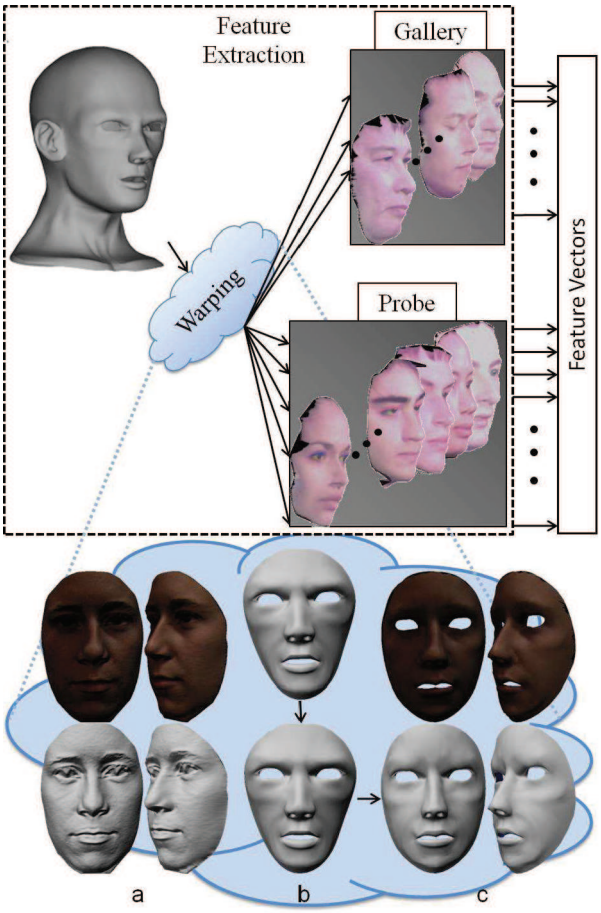

Figure 4.3: The feature extraction scheme and an illustration on a sample model: (a) The subject's face with and without texture (b) generic model before and after alignment (c) generic model after warping with and without texture. This figure is taken from [39].

2D Face Recognition

For 2D face recognition, Local Binary Patterns (LBP) [4] is selected as baseline. The success of LBP in face description is due to the discriminative power, computa-

tional simplicity of the operator, and its robustness to monotonic gray scale changes caused by, for example, illumination variations. The use of histograms as features also makes the LBP approach robust to face misalignment and pose variations to some extent. For 2D face recognition, we use the operator $LBP^{u2}_{8,2}$ on 8×8 blocks. The computation of $LBP_{P,R}$ is explained in Equations (3.1) and (3.2) in the previous chapter.

Uniform patterns are verified to be the fundamental patterns of local image texture. A local binary pattern is called uniform if the binary pattern contains at most two bitwise transitions from 0 to 1 or vice versa when the bit pattern is traversed circularly. The notation is $LBP^{u2}_{P,R}$. $u2$ stands for using only uniform patterns and labeling all remaining patterns with a single label.

As explained in the previous chapter, in Equation (3.9), U value is the number of spatial transitions (bitwise 0/1 changes) in the pattern. The patterns which satisfy $U \leq 2$ are selected as uniform patterns. Instead of using all patterns, sufficient information can be obtained by using only uniform patterns. The number of uniform patterns is $P \times (P-1) + 2$. So in our case; $LBP^{u2}_{P,R}$ results in a 59 features (59-bin histogram) from each image block, which corresponds to 3776 (i.e. $59 \times 8 \times 8$) features for each image.

Finally, the similarity between each image pair is computed with chi-square distance metric as recommended for LBP based algorithms in various studies [33, 52, 143]. Performances are evaluated using the similarity scores between image pairs. Equation (3.11) shows how chi-square distance between sample and model histograms is computed.

4.4 Experiments and Analysis

In this part, the evaluations are done for 2 modes. The first mode is the baseline mode: a standard biometric system with no spoofing and no countermeasure. The baseline performance is evaluated using DB-r. Performance is evaluated by verification all vs. all. Access from every identity in DB-r is tested against all other models in DB-r. The performance is measured by observing the rate of users rejected when authenticating against their own template (False Rejection Rate - FRR) and by the rate of users accepted when authenticating against someone else's template (False Acceptance Rate - FAR). The second mode is the evaluation of face recognition systems under mask attacks (baseline under attacks in Figure 4.4). Both DB-r and DB-m are used. When spoofing attacks are applied, performance is expected to degrade. In this mode, the FAR corresponds to the rate of attacks that are accepted by the system when spoofed. The FRR corresponds to the rate of real-access attempts that are incorrectly dismissed by the system as attacks.

For the evaluations regarding 2D and 3D face recognition systems here, only test set is used. Train set is used for classifier training inside the proposed countermeasures. Figure 4.4 shows the behavior of the 3D and 2D baseline systems with/without attacks. All results are presented in terms of detection error trade-of (DET) profiles which illustrate the behavior of a system as the decision threshold is changed, i.e. how the false rejection rate varies according to the false acceptance rate.

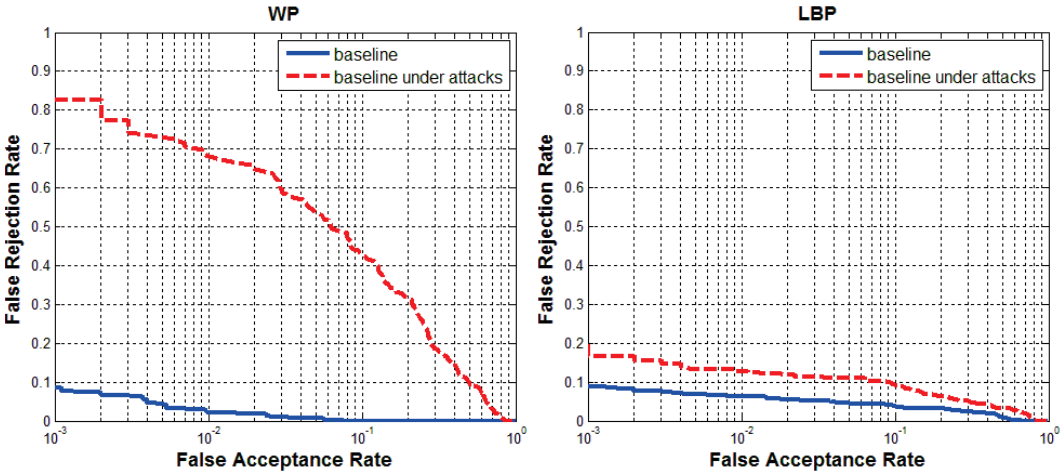

Figure 4.4: The DET Curves of the 3D and 2D face baseline biometric system with/without mask attacks, respectively.

Figure 4.4 shows that:

- Although the mask attacks are successful to spoof both 2D and 3D face recognition systems, the 3D face recognition system is more vulnerable to mask attacks compared to the 2D face recognition system (area between red and blue curves is much more for 3D compared to 2D face recognition system).
- Equal Error Rate (EER) at the baseline mode increases from 1.8% to 25.1% for 3D and from 4.7% to 9.9% for 2D face recognition system under attacks.
- 3D shape characteristics of a real face and corresponding mask attack are more similar compared to their texture characteristics. Hence, analysis on texture may reveal more information to detect mask attacks compared to analysis on 3D shape characteristic.
- Robustness against mask spoofing is observed to be both method and modality dependent as also concluded in [74].
- Face recognition systems are vulnerable to spoofing mask attacks hence, countermeasures are necessary to reduce their impact on face recognition.

For the baseline mode evaluations, we used the test set of DB-r, which contains 100 real samples from 10 subjects. In this study, we also report the baseline performances

of the selected systems on the Face Recognition Grand Challenge Database (FRGC) v1.0 [107] database in order to check if the selected systems still provide satisfactory baseline performances with more number of subjects. The scans of the subjects in the mask database were acquired with a high quality laser scanner (technology of MORPHO). The FRGC database was also prepared using the high quality laser scanner Minolta. Therefore, the scan quality in the FRGC is quite similar to the scan quality in our mask database. Furthermore, FRGC v1.0 includes 943 samples from 275 subjects and more challenging compared to the DB-r of the mask database. Table 4.2 shows the EER, verification rate at 0.001 FAR and rank-1 identification rates computed with the selected systems using both the mask database (the DB-r of the mask database) and the FRGC database.

Table 4.2: EER, Verification Rate at 0.001 FAR and Rank-1 Identification Rate (IR) for the 3D and 2D baseline systems using the Mask Database (MD) and the FRGC Database.

Techniques	**WP**		**LBP**	
	(MD)	(FRGC)	(MD)	(FRGC)
EER (%)	1.79	2.41	4.68	2.96
VR at 0.001 FAR (%)	91.33	87.70	90.89	90.03
IR (%)	100	94.01	98.89	94.50

Table 4.2 shows that slightly better performances are obtained in terms of identification and verification using the mask database compared to the ones obtained using the FRGC. For each face recognition technique, EER computed for the two databases are quite similar. Although there is a high increase in the number of subjects/samples when the FRGC is used for the evaluation, the performances of the selected baseline systems on the FRGC are still satisfactory, even quite similar to the results obtained using the mask database. These results show that the selected systems provide significant performances hence they are appropriate for this study, and the number of subjects/samples in the mask database is sufficient enough to obtain consistent results in this study.

4.5 Conclusions

In this study, a 2D+3D face mask attack database is used which was prepared for the TABULA RASA research project. It is used to evaluate the performances of the baseline face recognition techniques under spoofing attacks.

The novelty of this study is that it is the first time the impact of mask spoofing is analyzed on both 2D and 3D face recognition. Since it is possible to measure the baseline performances using the real accesses in the mask database, comparison between the baseline performance and the performance under spoofing attacks is possible, which is a significant advantage of this study. The results in our study

show that the face recognition systems are vulnerable to spoofing mask attacks. Robustness against mask spoofing is observed to be both method and modality dependent. The systems which are based on 3D face shape analysis is observed to be the most vulnerable systems to the mask attacks in case the masks used are prepared by using the 3D model of their target faces. Therefore, we can say that 2D face recognition systems are observed to be more robust against mask spoofing compared to 3D face recognition systems when high-quality masks are used for spoofing purposes. Since standard techniques are vulnerable to mask attacks, robust algorithms are necessary to mitigate the effects of spoofing on face recognition. In this study, we observe that analysis on texture may reveal more information to detect mask attacks compared to analysis on 3D face shape characteristic.

In the next chapter, initially, our countermeasure techniques, which are proposed to detect 3D mask attacks, are explained. Then, the countermeasure, which provides the best performance in mask face detection, is integrated to the selected 3D face recognition system in order to observe the positive impact of the countermeasure in recognition performances.

Chapter 5

Countermeasure Techniques Against Mask Attacks

There are several types of spoofing attacks to face recognition systems such as photograph, video or mask attacks. Recent studies show that face recognition systems are vulnerable to these attacks. In this chapter, countermeasure techniques are proposed to protect face recognition systems against mask attacks. The novel countermeasure techniques, which are based on the analysis on different shape, texture and reflectance characteristics of the real faces and the mask faces, are proposed to detect mask spoofing. In this chapter, the countermeasures are developed using both the 2D data (texture images) and the 3D data (3D scans) available in the mask database. The results show that each of the proposed countermeasures are succesful to detect mask spoofing and the fusion of these countermeasures further improves the results compared to using a single countermeasure. Due to the lack of publicly available mask database, studies on mask spoofing are limited. This chapter provides state-of-the art results by proposing novel countermeasures to protect face recognition systems against the attacks.

5.1 Introduction

The most common spoofing attacks are photograph and video attacks due to their convenience and low cost. Based on the observations that 2D face recognition (FR) systems are vulnerable to these attacks, researchers started to work on countermeasures to reduce their impact on recognition performances.

Proposed countermeasures against photo and video attacks are mainly based on liveness detection, motion analysis and texture analysis, which are explained in Section 2.2.1 in detail.

When 3D masks are introduced as attacks, some of these countermeasures proposed against 2D attacks are no more applicable. The study of Kollreider et al. [71] shows that a face recognition system relying on eye blinking and lip movements can be defeated by using photographic masks wrapped over face with eyes and mouth regions cut out. Also, since motion based countermeasures depend on different movements of 2D and 3D surfaces, they are not applicable when masks are used instead of photos or videos. It appears that the detection of 3D mask attacks is more challenging

compared to the detection of 2D facial attacks.

3D mask attacks to FR systems is a considerably new subject. The main reason for the delay in mask spoofing studies is due to the unavailability of public mask databases. To our knowledge, in the literature, there are two countermeasure studies against 3D mask attacks [66,142] excluding our studies. These two studies are based on reflectance analysis. They utilize 2D data (texture images) in their approach to detect 3D mask attacks. These two techniques are explained in Section 2.2.2 with their strengths and limitations in detail. In order to contribute this compelling research problem and fill the missing portions of the existing studies, we have proposed several countermeasure techniques against 3D mask attacks in [73], [76], [75] and [77].

The spoofing performances of the masks used and the countermeasure which uses 3D data (3D scan) instead of 2D data (texture image) as input to detect mask spoofing were first analyzed in our previous studies [73, 74], respectively, using the mask database which was prepared within the context of the European Union (EU) research project TABULA RASA [111]. The mask database used in our previous studies [73–77] was created by MORPHO [98]. The specifications of this database is given in the previous chapter in Section 4.2.

In Chapter 4, we analyzed how well the spoofing performances of the masks used in our studies are. The results of this study show that the masks used have very similar texture and especially 3D face shape characteristics to their target faces. They are very successful to spoof face recognition systems. In [73], we proposed to apply micro-texture analysis on both texture and depth images, and obtained 88.12% and 86% accuracy, respectively, for the classification of mask and real faces. The novelty of this work is that it was the first time 3D data was utilized to discriminate mask and real samples. In our next study [76], which is the continuation of [73], we applied fusion for the information extracted from both the texture and depth images, and obtained a higher classification accuracy of 93.5%. In addition to the increase in performance, it was the first time the performances of face recognition systems were analyzed with/without mask attacks and with/without the proposed countermeasure integrated to the recognition systems in [76]. By this way, it is possible to observe the positive impact of countermeasure on recognition performances in presence of mask attacks. In [75], we proposed a countermeasure based on reflectance analysis using the texture images in the same database. We obtained 94% classification accuracy in [75]. In [73], micro-texture analysis is applied on texture images, whereas in [77], we apply micro-texture analysis also on reflectance components of texture images as a new countermeasure. We observe that higher accuracy (95.98%) is obtained using reflectance component instead of texture image (original image) itself. This proves that reflectance image provides more appropriate information than original image to discriminate mask and real samples. In [77], we also analyzed fusion scenarios and obtained a classification accuracy of 98.99%, which was the best score we have obtained so far.

In this chapter, we provide an overview on our spoofing detection approaches which were introduced in the studies [73], [76] and [75] for the detection of mask attacks. In [77], we extended the works explained in these studies with some improvements, additional analysis, comparisons of performances of diverse countermeasures using the same protocol, and with a detailed analysis of the fusion scenarios. In this chapter, we explain this extended study, in which 98.99% classification accuracy is reported. This accuracy is the best accuracy that have been reported in the literature for mask spoofing detection up to now. Also, we integrate the countermeasure with the best performance to the selected 3D FR system in order to show the positive impact of the countermeasure on the systems under mask attacks, directly.

In the previous chapter, a brief information is given on the mask database used in our studies. Also, in Section 4.3, the selected 2D and 3D FR systems are presented, and then the impact of mask spoofing on these systems is evaluated. The results of the study explained in Chapter 4 show that countermeasures are necessary to mitigate the impact of spoofing mask attacks on the performances of the face recognition systems. In this chapter, we will explain our countermeasure techniques proposed for the detection of the mask attacks in order to protect face recognition systems against mask spoofing.

5.2 Countermeasure Techniques Against Mask Attacks

In this part, Section 5.2.1 gives brief information about the techniques that were used to develop the proposed countermeasures. Section 5.2.2 explains each of the proposed countermeasures.

5.2.1 Techniques used Inside the Proposed Countermeasures

Mask attack is a 3D attack that can be used to spoof both 2D and 3D FR systems. Most of the existing 3D scanners do not provide only 3D scan, they also capture texture image. Figure 4.2 shows an example for the two outputs of a scanner. Thus, when there is only one camera for 2D and one scanner for 3D FR system, a countermeasure which uses texture images as input can be used to protect both 2D and 3D FR systems if texture images are provided as default output of a scanner. In the present study, we propose four countermeasures against 3D mask attacks, which use either the depth maps or texture images as input (Figure 5.2).

In this section, we first explain the pre-processing applied for the proposed countermeasures. Then, we give a detailed information about the techniques that were used to develop the proposed countermeasures.

5.2.1.1 Pre-Processing for the Countermeasures

There are slight alignment differences between faces in the mask database. For the countermeasures, initially, all 3D faces in DB-r3 and DB-m3 are aligned to a generic face using LSS alignment, which makes the alignment of all faces identical.

In this study, we want to benefit from the information that the mask surface is smoother than the real face surface to detect mask attacks. Therefore, the depth maps are estimated from the raw aligned 3D scans. Next, 2D cropping is applied to extract face region from both the texture images and depth maps. Then all images are resized into 64×64 grayscale image.

In [77], we improved our cropping code compared to the ones used in our previous studies. The final version of the texture images and depth maps used for the countermeasures proposed in this study are shown in the second and fourth columns of Figure 4.2, respectively.

5.2.1.2 The Variational Retinex Algorithm

For the countermeasures proposed in this study, the image is decomposed into reflectance and illumination components using the variational retinex algorithm explained in the studies [6, 67].

In this part, we first give information about minimizing energy functions. Then, we explain the variational retinex algorithm [6, 67].

Minimizing Energy Functions

The concept of minimizing the energy of a given system is used in image processing. Minimizing energy functions often includes solving partial differential equations, more specifically, Euler-Lagrange differential equations.

In the Euler-Lagrange problem, we usually have a continuous real-valued function $y = f(x)$ with continuous derivative $y\prime = df/dx$. Considering x, y, and $y\prime$ as three independent variables, a new function $g(x, y, y\prime)$ is defined. Using this function, the energy function is defined as: $E = \int g(x, y, y\prime)dx$. The energy function E has a minimal value if Euler-Lagrange equation:

$$\frac{\partial g}{\partial y} - \frac{\partial}{\partial x}\left(\frac{\partial g}{\partial y\prime}\right) = 0 \tag{5.1}$$

is satisfied. The left hand side of this equation is denoted as ∇E. Here f is introduced as a function of one independent variable x, the same concept is applied when f is a function of n independent variables: $x1, x2, \ldots, xn$. In particular, when $u = f(x, y)$, function of two independent variables x and y, Euler- Lagrange equation becomes:

$$\nabla E = \frac{\partial g}{\partial u} - \frac{\partial}{\partial x}\left(\frac{\partial g}{\partial u_x}\right) - \frac{\partial}{\partial y}\left(\frac{\partial g}{\partial u_y}\right) = 0 \tag{5.2}$$

The variational retinex algorithm is developed by defining and minimizing an energy function.

The Variational Retinex Algorithm

An image can be considered as a two dimensional function $S(x, y)$, where (x, y) denotes a pixel on the image. The value of the function $S = S(x, y)$ represents the intensity of the light at the pixel (x, y). As stated in [6], the intensity S may be characterized by two components which are;

- the amount of source illumination falling on the object, the illumination component $L(x, y)$.
- the amount of illumination reflected by the object, the reflectance component $R(x, y)$.

$S(x, y)$ is computed using the illumination and reflectance components as shown in Equation (5.3).

$$S(x, y) = L(x, y) \times R(x, y) \tag{5.3}$$

In [6], it is stated that if images are assumed to be composed of illumination and reflectance components, generating the retinex effect means being able to separate one component from another. A first step taken by most algorithms in such sort of problems is the conversion to the logarithmic domain by $s = log(S)$, $l = log(L)$, and $r = log(R)$. In the logarithmic domain, the relation between these three images becomes: $s = l + r$.

In [67], Kimmel et al. make the following assumptions:

1. The logarithmic illumination l varies spatially smoothly.
2. The logarithmic reflectance r consists of constant or smooth parts and discontinuous jump parts.
3. l is greater than or equal to the logarithmic intensity s ($l \geq s$).
4. l is close to s (i.e. l does not deviate far away from s).

Based on the assumptions listed above, in the studies [6, 67], the energy function is defined as follows:

$$E(l) = \int (|\nabla l|^2 + \alpha(l - s)^2 + \beta|\nabla(l - s)|^2)dxdy \tag{5.4}$$

where α and β are positive constants. Since S is the given image, s here is constant. In this equation;

- The first penalty term ($|\nabla l|^2$) forces spatial smoothness on l.
- The second penalty term $(l-s)^2$ forces a proximity between l and s. The difference between these images is exactly r, which means that the norm of r should be small. Simultaneously, it forces the solution l to be $l \geq s$. In [67], it is stated that in practice this term should be weak enough not to attract l down too much towards s. This is why the parameter α should be very small.
- The third term forces r to be spatially smooth. In [67], it is stated that the parameter β should be a very small value to preserve the discontinuous jumps of r. Note that spatially smooth r contradicts spatially smooth l since $r+l=s$. However in practice adding this penalty term kicks in mainly on sharp edges and handles situations where the illumination is not smooth (as well as cases of direct light sources and specularities).

The integrand of this energy function is:

$$\begin{aligned} g(l, l_x, l_y) &= |\nabla l|^2 + \alpha(l-s)^2 + \beta|\nabla(l-s)|^2 \\ &= (l_x^2 + l_y^2) + \alpha(l-s)^2 + \beta((l_x - s_x)^2 + (l_y - s_y)^2) \end{aligned} \tag{5.5}$$

Euler-Lagrange equation becomes:

$$\begin{aligned} \nabla E &= \frac{\partial g}{\partial l} - \frac{\partial}{\partial x}\left(\frac{\partial g}{\partial l_x}\right) - \frac{\partial g}{\partial y}\left(\frac{\partial g}{\partial l_y}\right) \\ &= 2\alpha(l-s) - \frac{\partial}{\partial x}\left(2l_x + 2\beta(l_x - s_x)\right) - \frac{\partial}{\partial y}\left(2l_y + 2\beta(l_y - s_y)\right) \\ &= 2\alpha(l-s) - 2l_{xx} - 2\beta(l_{xx} - s_{xx}) - 2l_{yy} - 2\beta(l_{yy} - s_{yy}) \\ &= 2\left[\alpha(l-s) - \Delta l - \beta\Delta(l-s)\right] \\ &= 0 \end{aligned} \tag{5.6}$$

which means $\alpha(l-s) - \Delta l - \beta\Delta(l-s) = 0$. In [6], to solve this equation, the idea of the steepest descent is applied with an auxiliary variable t:

$$\frac{dl}{dt} = -\nabla E = \Delta l + \beta\Delta(l-s) - \alpha(l-s) \tag{5.7}$$

To find a local minimum of a function using steepest descent, one takes steps proportional to the negative of the gradient of the function at the current point. In our evaluation, l is computed via steepest descent as follows:

$$l_n = l_{n-1} - dt \cdot \nabla E \tag{5.8}$$

Finally, projecting onto the constraint $l \geq s$ is done by $l_n = max(l_n, s)$.

In our experiments, the values 0.0001 and 0.1 are used for α and β, respectively, as suggested in [6, 67]. The initial value of l (l_0) is taken as s. The step size dt and the total number of iterations are selected as 0.05 and 5000, respectively. After the

iterations, optimum l is obtained, and r is computed from $r = s - l$. Finally, the reflectance and illumination components are evaluated from $R = e^r$ and $L = e^l$, respectively.

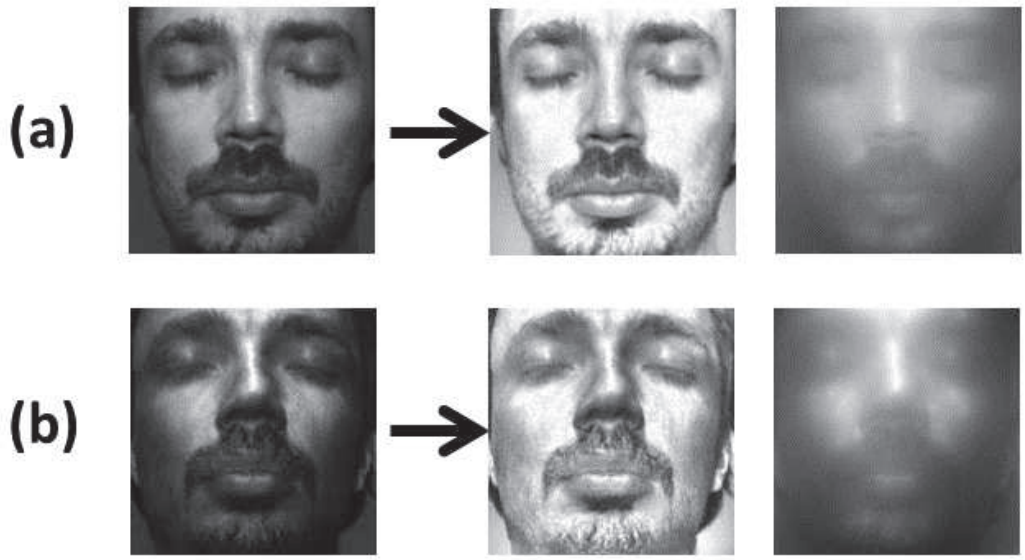

Figure 5.1: Example from the mask database which is created by [98] (a) The real face with texture, the reflectance image and the illumination image of the real face (b) Same images associated with the mask of the same person.

Figure 5.1 shows an example from the mask database for a real face and corresponding mask attack. First column shows the original images, second column and third column show the reflectance and illumination images, respectively, which are computed using the variational retinex algorithm.

5.2.1.3 Micro-Texture Analysis Technique

The micro-texture analysis, which was first proposed in [87] to detect 2D face attacks, is used to detect 3D mask attacks here. In [87], it is applied on texture images, whereas in this chapter, we apply this technique not only on texture images but also on depth maps estimated from 3D scans and on reflectance components of texture images.

This LBP based micro-texture analysis technique emphasizes the micro-texture differences in the feature space. It aims at learning the differences between real and fake face, and designs a feature space which emphasizes those differences. The original LBP forms labels for the image pixels by thresholding the 3×3 neighborhood of each pixel with the center value and considering the result as a binary number. The LBP operator has been extended to use neighborhoods of different sizes as ex-

plained in Chapter 3. Equations (3.1) and (3.2) show how $LBP_{P,R}$ is computed. Furthermore, as explained in the previous chapter, uniform patterns are verified to be the fundamental patterns of local image texture. The notation is $LBP^{u2}_{P,R}$, where $u2$ stands for using only uniform patterns and labeling all remaining patterns with a single label.

In [87], authors claim that micro-texture details that are needed to discriminate a real face from face print can best be detected using combination of different LBP operators. Thus, they derive an enhanced facial representation using multi-scale LBP operators. Their proposed representation computes LBP features from 3×3 overlapping regions to capture the spatial information and enhances the holistic description by including global LBP histograms computed over the whole image. This is done as follows: the face is cropped and resized into a 64×64 pixel image. Then, $LBP^{u2}_{8,1}$ operator is applied on the face image and the resulting LBP image is divided into 3×3 overlapping regions (with an overlapping size of 14 pixels). The local 59-bin histograms from each region are computed and collected into a single 531-bin histogram. Then, two other histograms are computed from the whole face image using $LBP^{u2}_{8,2}$ and $LBP^{u2}_{16,2}$ operators, yielding 59-bin and 243-bin histograms that are added to the 531-bin histogram previously computed. In [87], the length of the final enhanced feature histogram is reported as 833 (i.e. $531 + 59 + 243$).

5.2.1.4 Classification Technique

Mask face detection is a two-class classification problem. Since SVM [23] are proven to be a powerful tool for discriminating two classes of data, we adopted an SVM classifier for this purpose. SVM finds the maximum margin hyper-plane to separate the training data in feature space and a decision for a new test data x is classified. In our experiments, we adopted linear kernel since our feature vectors are high-dimensional and are hence likely to be linear separable.

5.2.2 The Proposed Countermeasures

Four countermeasures are proposed in this study to discriminate mask and real samples. Three of them use the 2D data (texture images), and the remaining one uses the 3D data (depth maps estimated from the raw 3D scans) available in the mask database as input.

The flowchart of the countermeasures proposed in this chapter are shown in Figure 5.2. In this figure, the micro-texture analysis (explained in Subsection 5.2.1.3) applied on texture images is called CM1, applied on reflectance images is called CM2, applied on depth maps is called CM4, and finally the countermeasure for which the pixel intensity values on reflectance images are used directly by the classifier is called CM3 (CM denotes countermeasure).

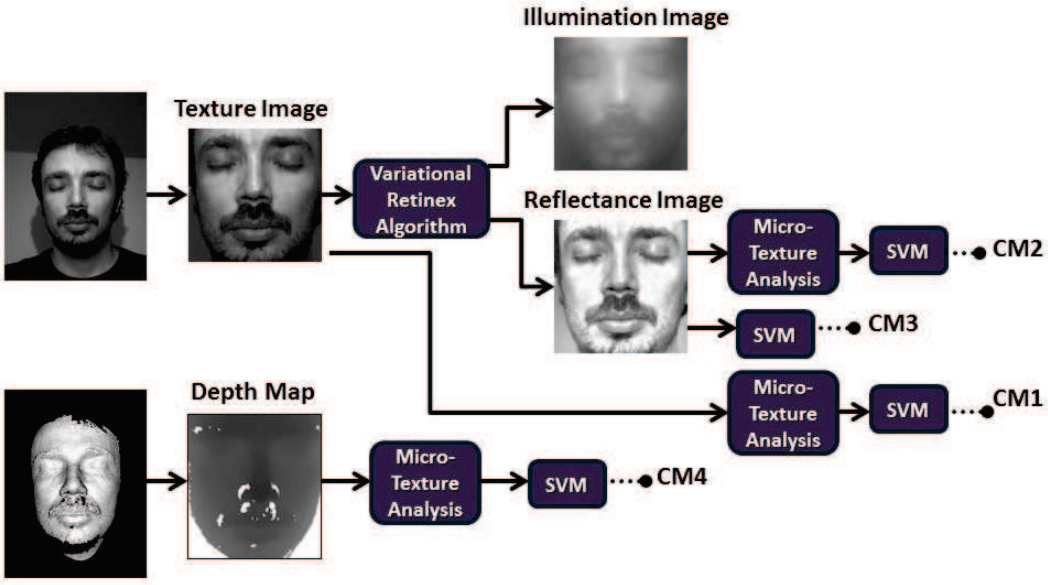

Figure 5.2: The flowchart of the proposed countermeasures.

CM1 and CM4 are first introduced in our study [73], and CM3 is first introduced in our study [75]. In the present study, we provide an overview on our spoofing detection approaches introduced in the studies [73, 75]. We extend the works explained in these studies with some improvements (e.g. better cropping, usage of non-normalized images instead of normalized images), additional analysis, comparisons of performances of diverse countermeasures using the same protocol, and with a detailed analysis of the fusion scenarios. Also, CM2 is first introduced in our recent study [77]. It is a new countermeasure providing very satisfactory accuracy to classify mask and real faces. The results of CM2 show that reflectance component of an image provides more appropriate information than original image itself for mask detection. From the fusion results, we also observed that it provides complementary information on mask detection.

5.2.2.1 CM1: Micro-Texture Analysis on Texture Images

Captured image from mask may visually look very similar to the image captured from live face (e.g. the texture images in the second column of Figure 4.2). A close look at the differences between faces in DB-r2 and DB-m2 reveals that their surface properties are different. For mask manufacturing 3D printers are used, hence they may contain printing quality defects that can be detected with micro-texture patterns. For CM1, micro-texture analysis is applied on texture images, and the feature histogram of length 833 is obtained. Finally, linear SVM classifier is applied to detect mask and real faces.

5.2.2.2 CM2: Micro-Texture Analysis on Reflectance Images

For CM2, initially, the illumination and reflectance components (Figure 5.2) of the texture images are obtained using the variational retinex algorithm introduced in Subsection 5.2.1.2. Then, micro-texture analysis is applied on reflectance components of texture images rather than texture images itself. The reason of this analysis on reflectance images is that a close look at the differences between the reflectance images of the real and mask faces reveals that the texture characteristics on their reflectance components are also different. The feature vectors of length 833, which are obtained by applying micro-texture analysis on reflectance images, are used as input by linear SVM classifier. This feature vector gives information from the reflectance image in the image texture level.

5.2.2.3 CM3: Pixel Intensity Analysis on Reflectance Images

Our observations on the reflectance components of mask and real faces reveal that reflectance characteristics of mask and real face samples are different especially at some specific regions of the face (eyelashes, eyebrows and moustache). Based on these observations, in this study, we use the intensity values on reflectance component of each image as input for linear SVM classifier. Since the intensity values on reflectance images are between 0 and 1 ($R(x, y) \in [0, 1]$), we stretched it to the interval [0, 255] by multiplying R with 255. The reflectance component, which is in the size of 64×64 pixel image, is reshaped as [1 4096] ($64 \times \times 64 = 4096$). The resultant vector is the feature vector providing information in the pixel intensity level. Finally, linear SVM classifier is applied to detect real and mask faces.

5.2.2.4 CM4: Micro-Texture Analysis on Depth Maps

The 3D shape of high quality mask is also very similar to the 3D shape of corresponding real face (e.g. the 3D scans in the third column of Figure 4.2). Our analysis on DB-r3 and DB-m3 show that the mask scan is smoother than the real face scan. Especially the parts of the face with facial hair are quite different. Since there is no real facial hair (e.g. mustache, eyebrow) on the masks, the 3D scan of mask is smoother in these parts compared to the real face scan. When high quality scanners are used for acquisition, although there is a decrease in the number of holes, it is still possible to observe some holes on the scan especially at the parts of the face with facial hair. Thus, in our study, micro-texture analysis is also applied on the depth maps which are estimated from the raw 3D scans, and the other feature histogram of length 833 is obtained. Finally, linear SVM classifier is applied to detect real and mask faces.

5.3 Experiments and Analysis

Section 5.3 shows the experiments and results of all the proposed countermeasures together with the fusion scenarios for comparison purposes. We first show the stand-

alone classification performances of the proposed countermeasures together with the fusion scenarios. Then, we integrate the countermeasure providing the best performance to the selected 3D FR system in order to observe the improvement in the recognition performance of the system in presence of mask attacks.

5.3.1 Stand-Alone Classification Performances of the Countermeasures

In the present study, we apply the proposed countermeasures (CM1, CM2, CM3, CM4) using the same database with the same train-test sets, hence an exact comparison between these countermeasures is possible. Train set is used for classifier training. This classifier is subject to two kind of errors:

- FLR (False Living Rate), that represents the percentage of fake data misclassified as real. (similar to FAR)
- FFR (False Fake Rate), which computes the percentage of real data assigned to the fake class. (similar to FRR)

The lower these two errors, the better the performance of the countermeasures. In this section, we first evaluate the performances of the single countermeasures, and then evaluate the performances for the fusion scenarios. The Region of Convergence (ROC) curves in Figure 5.3 shows the stand-alone classification performances of the four countermeasures together with the fusion based countermeasure providing the best performance in Table 5.2.

Area Under Curve (AUC), EER and best accuracy results using CM1, CM2, CM3, and CM4 are shown in Table 5.1.

Table 5.1: AUC, EER and Accuracy Results Using the Four Countermeasures

Countermeasures	**AUC**	**EER(%)**	**Accuracy(%)**
CM1	0.956	9.04	91.46
CM2	0.980	**5.02**	**95.98**
CM3	**0.984**	9.04	93.47
CM4	0.919	18.59	82.91

Table 5.1 and Figure 5.3 show that;

- The best performances in terms of EER and accuracy are obtained using CM2, and the best performance in terms of AUC is obtained using CM3.
- The best performances are obtained with the countermeasures based on reflectance analysis (CM2 and CM3) compared to the performances obtained with CM1 and CM4. This shows that reflectance characteristics of the real and mask faces in the mask database provide more appropriate information than their texture and smoothness characteristics.

- CM4, which is based on smoothness analysis, provides worse results compared to the other countermeasures. However, the performance of CM4 can be still considered as satisfactory.
- 2D data (texture images) provide more information than 3D data (depth maps) to detect mask spoofing.

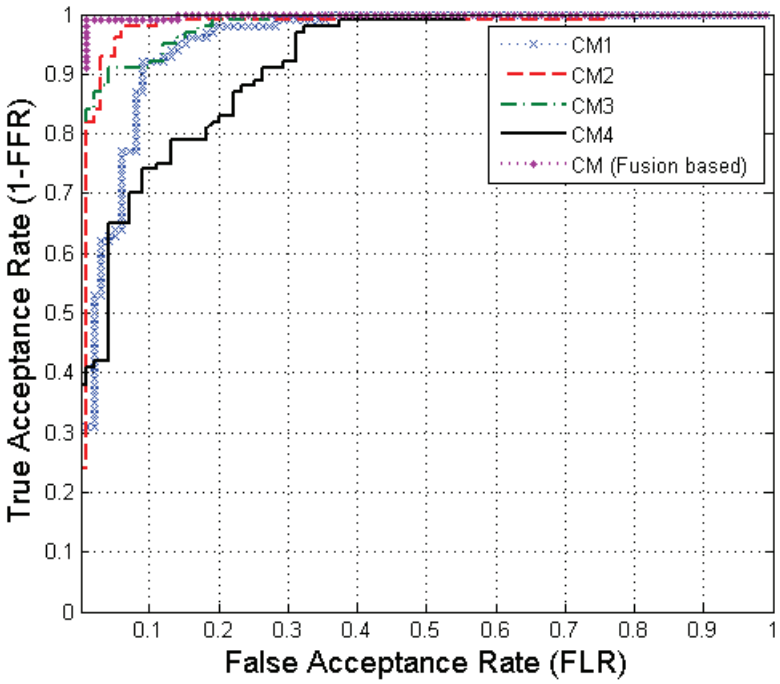

Figure 5.3: The Classification Performances of the Countermeasures.

After evaluating the performances of the single countermeasures, we analyze the performances for the fusion scenarios.

For feature level fusion, the feature histograms computed from different types of images (texture, reflectance and depth) are concatenated and the classifier is applied on the resultant feature histogram. In Table 5.2, the feature level fusion of 2 countermeasures, 3 countermeasures and finally all the 4 countermeasures are reported for which the length of the final feature histograms are 1666, 2499 and 3332, respectively. Once the enhanced histogram is computed, a linear SVM classifier is used to determine whether the image corresponds to a live face or not.

For score level fusion, linear SVM classifier is applied using the features computed from each type of images (texture, reflectance and depth) separately, and then Z-score normalization is applied for each score group. Finally, the weighted score level fusion is used for combining the outputs of the individual SVMs to determine

whether the image corresponds to a live face or not.

AUC, EER and best accuracy results are shown in Table 5.2 for the fusion scenarios.

Table 5.2: AUC, EER and Accuracy Results for the Fusion Scenarios of the Proposed Countermeasures

Countermeasures Involved in Fusion	**Feature Level Fusion**			**Score Level Fusion**		
	AUC	**EER** (%)	**Acc.** (%)	**AUC**	**EER** (%)	**Acc.** (%)
CM1, CM2	0.994	3.01	97.49	0.988	3.01	97.49
CM1, CM3	0.985	9.04	93.97	0.993	5.02	96.48
CM1, CM4	0.972	9.04	92.96	0.976	8.04	94.47
CM2, CM3	0.984	9.04	93.47	0.993	5.02	96.48
CM2, CM4	0.994	3.01	97.49	0.992	4.02	96.98
CM3, CM4	0.986	8.04	92.96	0.994	5.02	95.98
CM1, CM2, CM3	0.985	9.04	93.47	**0.998**	**2.01**	**98.99**
CM1, CM2, CM4	**0.998**	**2.01**	**97.99**	0.993	5.02	96.48
CM1, CM3, CM4	0.987	8.04	93.47	0.997	2.01	97.99
CM2, CM3, CM4	0.986	8.04	93.47	0.997	2.00	98.49
CM1, CM2, CM3, CM4	0.987	8.04	93.47	0.997	2.01	98.49

From the reported results in Table 5.2, we can remark the followings:

- Both score and feature level fusion of the countermeasures improve the performance compared to using single countermeasure. For instance, CM4 provides a detection accuracy of 82.9% whereas when CM4 and CM1 are fused, the accuracy is improved to 92.96% for feature and 94.47% for score level fusion. This proves that when both the texture images and depth maps are provided by 3D scanners, more robust countermeasures can be obtained by fusion.

- For feature level fusion, the best performances are obtained by the fusion of CM1, CM2 and CM4. In this part, we observed that when we concatenate the same type of features (micro-texture features of length 833 for each of CM1, CM2 and CM4), we observe a significant increase in the performance. In CM3, the features are pixel intensity values (features of length 4096). Therefore, when we apply feature level fusion using CM3 with the other countermeasures, the positive impact of CM3 in the performances was not observable as shown in Table 5.2.

- For score level fusion, the best performances are obtained by the fusion of CM1, CM2 and CM3. All these countermeasures (CM1, CM2 and CM3) uses texture images as input (reflectance image is computed from texture image). This proves that 2D data provides very beneficial information for mask spoofing detection.

- CM3 increases the performances when it is used in score level fusion, whereas the impact of it in feature level fusion is not remarkable.
- Although CM1, CM2 and CM3 provide very satisfactory results alone, the score level fusion of these countermeasures provides the best performance compared to all other scenarios in Table 5.1 and 5.2. Therefore, in Figure 5.3, the ROC curve of this fusion based countermeasure is shown as the best one.
- Since existing 3D scanners provide both 3D scan and corresponding texture image, more robust countermeasures can be developed by fusion of these two type of outputs (2D and 3D data).

5.3.2 Integration of the Countermeasure to 3D Face Recognition System

In this subsection, we integrate the countermeasure, which provides the best performance in the previous subsection (fusion of CM1, CM2 and CM3), to the 3D FR system selected as baseline.

The evaluations are done for 4 modes. The first two modes are the baseline mode and the mode under attacks, which are explained in Subsection 4.4. The third mode illustrates performance when the countermeasure is applied against the attacks, that results in an improved performance with respect to the second mode. For the samples which are detected as attack by the countermeasure, a least similarity score is assigned to those samples in verification tests. Last mode evaluates the performance of the baseline system together with the countermeasure in the normal operation mode of system, i.e., without attacks. The inclusion of the countermeasure may degrade the baseline performance when not confronted to attack (e.g. the countermeasure may consider as fake some real users.).

For evaluations, we fix 3 different evaluation points at FFR = 1%, 5%, and 10% (FFR and FLR were defined in the previous subsection). Once fixed, we incorporate the countermeasure as a first step into the baseline biometric systems oriented to discard fake data, and generate the performance evaluations for the 4 modes explained above.

Figure 5.4 shows the behavior of the 3D face baseline system with/without attacks and with/without the countermeasure. The three figures represent the overall system performance under spoofing attacks when three different operating points (FFR = 1%, 5%, and 10%) are used for adjusting the countermeasure.

It is clear from Figure 5.4 that the 3D FR system is vulnerable to mask attacks (more area between blue and red curves indicates more vulnerability to the attacks). Performance enhancement is obtained almost all regions of DET plots in Figure 5.4 when the countermeasure is introduced in presence of mask attacks (black curve

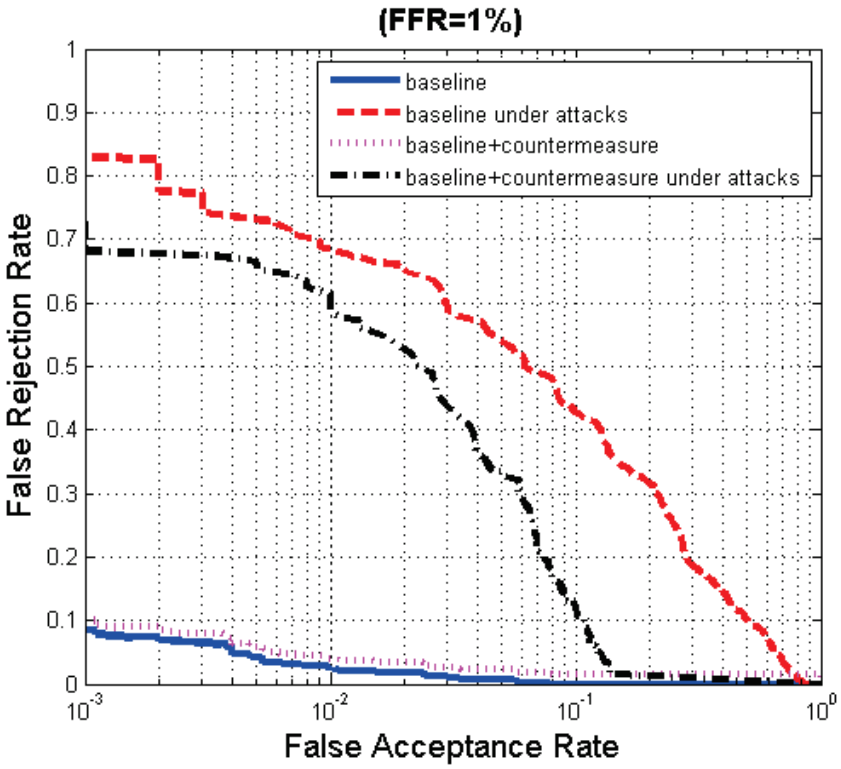
(FFR=1%)
baseline
baseline under attacks
baseline+countermeasure
baseline+countermeasure under attacks
False Rejection Rate
False Acceptance Rate
0
0.1
0.2
0.3
0.4
0.5
0.6
0.7
0.8
0.9
1
10^-3
10^-2
10^-1
10^0

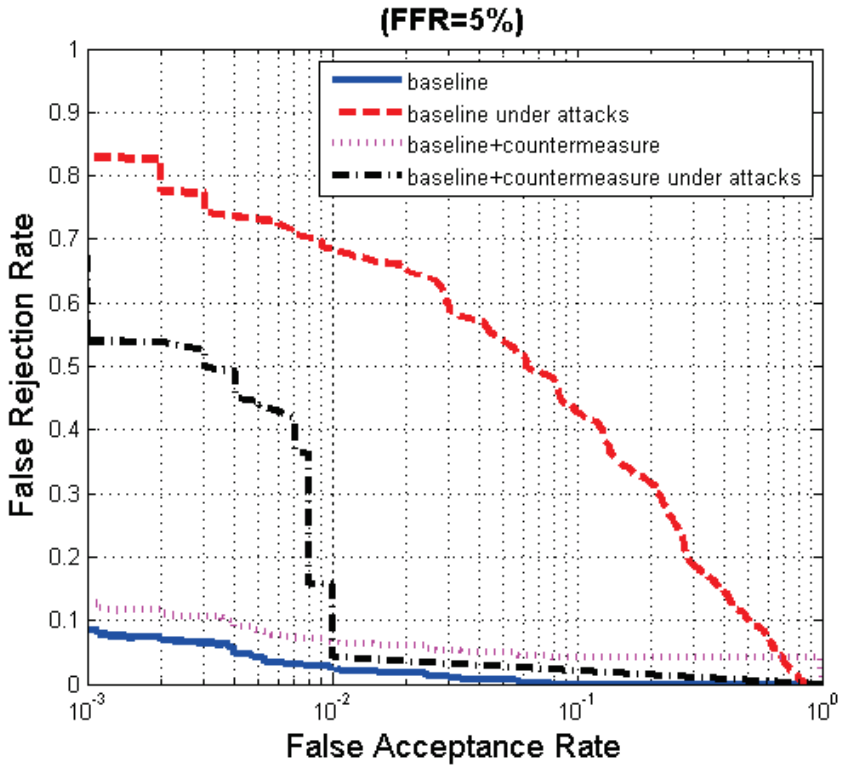
(FFR=5%)
baseline
baseline under attacks
baseline+countermeasure
baseline+countermeasure under attacks
False Rejection Rate
False Acceptance Rate
0
0.1
0.2
0.3
0.4
0.5
0.6
0.7
0.8
0.9
1
10^-3
10^-2
10^-1
10^0

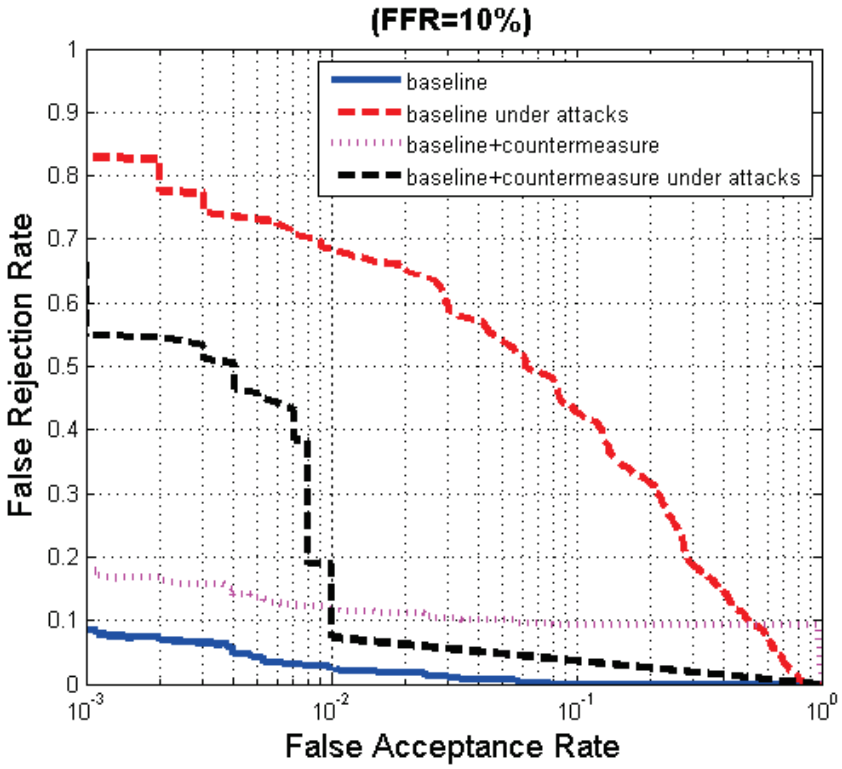

Figure 5.4: The DET Curves of the 3D face baseline biometric system when integrating the countermeasure.

compared to red curve). If we take an operating point where FFR = 1%, then FRR of the 3D FR system under attacks drops from around 65% to around 50% at FAR = 2%. For both of the two other plots (at FFR = 5% and 10%), the introduction of the countermeasure lowers FRR from around 65% to 4% and 7%, respectively, at FAR = 2%. The performance of the countermeasure is observed to be better at FFR = 5% compared to the cases at FFR = 1% and 10%. Finally, the inclusion of the countermeasure improves the results of 3D FR system under attacks, whereas it degrades baseline performances of the system when not confronted to attack (pink curve compared to blue curve).

5.4 Conclusions

In this study, a 2D+3D mask attack database is used to evaluate the performances of the proposed countermeasures for the protection of face recognition systems against mask attacks.

The novelty of this study is that it is still one of the few studies that proposes countermeasures against 3D mask attacks. The analysis are done on depth maps, texture images and reflectance components of texture images, and 4 different coun-

termeasures are proposed. Three of the proposed countermeasures use 2D data (texture images), and the remaining one uses 3D data (depth images) as input. These countermeasures can be used to protect both 2D and 3D FR systems against mask attacks. The results of this study show that analysis on reflectance images provide the best results compared to analysis on texture and depth images. All of the 4 countermeasures provide satisfactory information hence can be used as independent sources to discriminate masks from real faces. However with the fusion of these countermeasures, we observe a significant improvement in the performances. For instance, in this chapter, a classification accuracy of 99% (almost perfect accuracy) is achieved for real face vs. mask face by fusion.

Up to now, we have analyzed several characteristics of real and mask faces, and obtained almost perfect results on this mask database. The limitation of our study is that we were able to test the performances of the proposed countermeasures using the masks made from one type of material, which is polychrome mineral powder. When masks made from different materials are used, we may obtain different performance accuracy. Our future works are first to test the performances of the proposed countermeasures using masks made from different materials in order to observe if we can still obtain satisfactory results, and then to propose new countermeasures for more challenging mask databases with higher number of subjects as soon as available.

Chapter 6

Impact of Nose Alterations on Face Recognition

Numerous major challenges in face recognition, such as pose, illumination, expression and aging, have been investigated extensively. All those variations modify the texture and/or the shape of the face in a similar manner for different individuals. However, studies on alterations applied on face via plastic surgery or prosthetic make-up which can be in countless different ways and amounts, are still very limited. In this chapter, we analyze how such changes on nose region affect the face recognition performances of several key techniques. For this purpose, a simulated face database is prepared using FRGC v1.0 in which nose in each sample is replaced with another randomly chosen one. Since this is a 3D database, the impact analysis is not limited to only 2D, which is one of the novelties of this study. Performance comparisons of three 2D and four 3D algorithms are provided. In addition, differently from previous works, baseline results for the original database are also reported. Hence, the impact which is purely due to the applied nose alterations can be measured. The experimental results indicate that with the introduction of alterations both modalities lose precision, especially 3D.

6.1 Introduction

Plastic surgery is considered to be a relatively new challenge in face recognition when compared to pose, expression or illumination variations. With the increasing number of people resorting to plastic surgery for correction of feature defects, cosmetic reasons or even law evasion, it becomes of interest for the biometric community to investigate and prevent the impact of facial alterations on recognition performances. Yet, very few studies exist which address this problem.

In this chapter, we focus on the nose modifications and analyze their effects on success rates of different face recognition methods. In the next chapter, we propose a new approach robust to nose alterations. According to the statistics published by The American Society for Aesthetic Plastic Surgery in 2010 [46], nose reshaping (rhinoplasty) is the second most common surgical procedure on face after cosmetic eyelid surgery (blepharoplasty).

On the other hand, plastic surgery is just one of many ways to change the appearance of the nose. For example, latex/silicone-based prosthetic appliances can be simply

purchased as off-the shelf products. Alternatively, makeup using wax or putty can also alter the nose shape very easily. Three nose alteration examples for the three aforementioned methods are given in Figure 6.1.

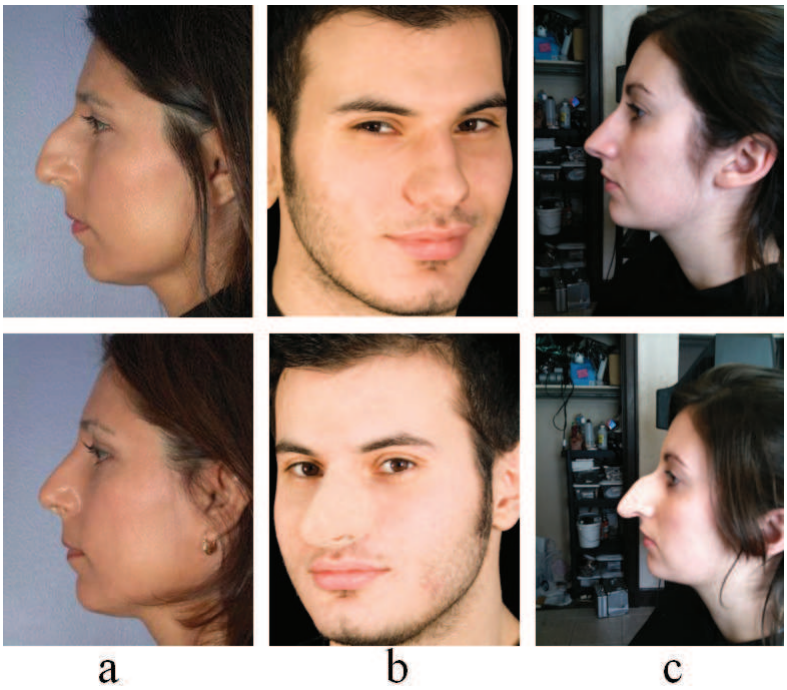

Figure 6.1: Examples of nose alterations with before (upper row) and after (lower row) photos: (a) plastic surgery [133] (b) latex appliance [120] (c) makeup using wax [19]

To the best of our knowledge, the impact of facial alterations, specifically due to plastic surgeries, on face recognition was first analyzed in [126] where the effect of plastic surgery is evaluated on six recognition algorithms. The database used consisted of 506 subjects with 2 images: before and after the plastic surgeries. Later, this work was extended in [127] by augmenting the database up to 900 subjects and additionally including a different non-surgery database for performance comparison. The results showed that the evaluated appearance, feature and texture-based algorithms were unable to effectively mitigate the decline caused by plastic surgery procedures.

The shortcomings of these studies [126, 127], which will be addressed throughout this chapter, are as follows:

- Due to the fact that a single image is provided before the plastic surgery procedure, a non-surgery vs. non-surgery recognition experiment had to be conducted on a separate database with different subjects. Unfortunately, for face recognition algorithms, the accuracy can vary widely depending on the difficulty of the database. Hence, an authentic comparison is not possible.

Figure 6.2: Examples of facial hair, expression and makeup variations on the facial images between before (upper row) and after (lower row) plastic surgery procedure

- In the plastic surgery database, the before and after images differ not only as a result of the procedure, but also due to expressions, makeup and facial hair variations (Figure 6.2). This leads to an additional decrease in the performances which clouds the true measurement of the plastic surgery effect.
- Since this is an image database, the analyses are restricted to 2D. However, 3D face recognition gains a rising popularity as it offers superiority over to its 2D counterpart by being intrinsically robust against illumination and pose variations. For this reason, the impact of the facial alterations on 3D algorithms should also be investigated.

In this study, these limitations are eliminated by creating a synthetic database using FRGC v1.0 [107] for which nose regions are randomly exchanged between subjects. In this way, a 2D+3D database is obtained for nose alterations and since the conditions and the subjects are identical for the original and the simulated databases, measuring the exact impact of the applied changes is possible.

6.2 Simulating Nose Alterations

The nose region can be altered in many ways using plastic surgery, prosthetic appliances or makeup and it can be made bigger, smaller, wider or thinner. In order to simulate these changes and preserve the authenticity of the facial shape, noses in the database are replaced by randomly chosen ones from different subjects. For this purpose, a Thin Plate Spline (TPS) based method is implemented.

A metamorphosis technique for 3D plastic surgery simulation was proposed in [81], where three morphing operations: augmentation, cutting and lacerating were simulated. Later in [112], an automatic virtual plastic surgery system was presented

which similarly to our approach, replaced an individual's facial features with corresponding features of another individual and fused the replaced features with the original face, but only in 2D. In a more recent work [17], effective patient specific improvements for facial attractiveness are automatically suggested using 3D scans of the patients and the results are simulated by merging the target feature of the most similar face in the 3D database of attractive faces with the patient's face.

In this study, beautification of the faces is not a concern. What we aim is to change nasal regions in the database as realistically as possible and create nose variations for all subjects. Therefore, a target list is randomly generated to transfer noses (from another person) for each sample in the database. For this purpose, firstly, nose regions of all facial scans are automatically segmented in a similar manner to [63] where an annotated generic face model is deformed to fit the target models and the annotations are transferred.

Next, nose deformations are applied using TPS method [16] in 3D. Prior to warping, the target model is aligned with the source model using 4 of 5 landmark points around the nose (Figure 6.3), excluding the nose tip. A linear transformation that includes rotation, translation and isotropic scaling is computed in a least square sense, based on the two sets of landmarks and applied onto the source model. Subsequently, using all 5 point pairs a coarse TPS approximation is computed.

In the final step, for one-fifth of the vertices on the target nose, the closest vertices on the source nose are found and coupled to be utilized in a second and denser TPS warping, which results in the source nose completely transforming into the target nose. The proposed method is illustrated in Figure 6.3.

The original database FRGC v1.0 consists of 943 multimodal samples from 275 subjects and the simulated 3D database is of the same size. For simulated samples in 2D, the synthesized 3D models with the corresponding original texture mapped on. However, due to some mismatches in 2D and 3D samples in the original database, 39 samples had to be removed, leaving us with a database of 904 samples from 268 subjects.

In order to evaluate the visual plausibility of the created database, an online survey was conducted, for which the participants were asked to classify the randomly displayed facial images (with or without texture) as original or simulated. According to a total number of 81 participations, success rate is found to be 60.68% for the images displayed with texture. For the other ones, the performances deteriorate as expected (58.77%) since the texture gives a better hint about originality. Being very close to the average performance of a random classifier (50%), this result indicates very low distinguishability, and hence a highly realistic look for the simulated noses.

For the sake of clarity, the original databases in 2D and 3D will be referred as DB-o2

and DB-o3, while the simulated nose alteration databases will be referred as DB-s2 and DB-s3, in the rest of this chapter and the next chapter.

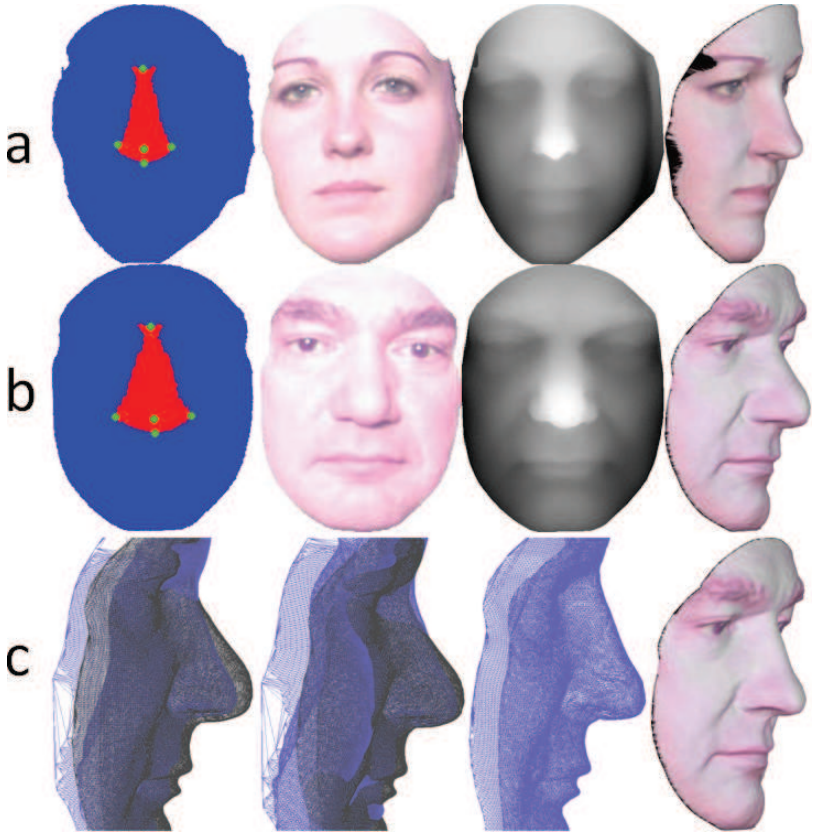

Figure 6.3: From left to right: (a) Nose region with landmark points, color map, depth map and profile view for the target model (b) Same images for the source model (c) Two models superimposed before and after alignment, resulting mesh after warping and profile view for the synthesized model

6.3 Experiments and Analysis

The effect of the applied nose alterations on face recognition performances are evaluated with three different scenarios in both 2D and 3D which are determined according to the study of [127] for comparison purposes.

Initially, all four databases, DB-o2, DB-o3, DB-s2 and DB-s3 are partitioned in non-overlapping train and test datasets. This is done by randomly selecting 40% of the subjects and assigning their samples to the train set, while the rest is used for testing. The partitioning is repeated 10 times and verification and identification performances are computed over these 10 trials.

For verification tests, the Receiver Operating Characteristic (ROC) curves which plot Verification Rates (VR) as a function of False Acceptance Rates (FAR) are reported together with the verification rates at 0.001 FAR.

For identification tests, the first sample of every individual in the test set is used as gallery and the rest as probes. The rank-1 recognition rates are reported.

- **Experiment 1 - Performance on the original database:** It is important to compute the performances on the original datasets in terms of having a baseline. In this way, the impact of the applied changes can be measured accurately. For this purpose, 2D and 3D algorithms are evaluated on DB-o where the similarities are calculated between each original image pair.
- **Experiment 2 - Performance on the simulated database:** In this scenario, the similarity scores between every DB-o and DB-s sample pairs are calculated and used to evaluate recognition performances. For the train set, for each subject selected, half of the corresponding images are taken from DB-o and the rest from DB-s. This experiment is identical to Experiment 1, except the probe images are now replaced by their modified versions.
- **Experiment 3 - Performance on the simulated database with training on an external database:** Face recognition algorithms are usually trained using different databases. Therefore in this scenario, Experiment 2 is repeated, but the training partition is composed of samples from an external database, namely Texas 3D Face Recognition Database [53]. Briefly, the Texas 3D Face Recognition (Texas 3DFRD) database is a collection of 1149 pairs of facial color and range images of 105 subjects. In order to obtain a train set of similar subject and sample numbers as in Experiments 1 and 2, a subset of Texas 3DFRD is compiled with 350 color and range images of 103 subjects, without expressions.

6.3.1 Impact on 2D Face Recognition

Three key methods are chosen to be evaluated for 2D face recognition: Principal Component Analysis (PCA), Linear Discriminant Analysis (LDA) [12] and Local Binary Pattern (LBP) [4]. PCA and LDA are appearance-based approaches which are widely used for dimensionality reduction and feature extraction. On the other hand, LBP is a texture-based algorithm for describing local structures.

The plastic surgery database in [127] has images after several types of surgery operations such as forehead surgery, ear surgery, eyelid surgery, nose surgery, skin resurfacing, face lift etc. However, since the results are reported for each surgical operation separately, we can compare our results with the reported rank-1 identification accuracies for nose surgery (rhinoplasty) as shown in Table 6.1.

According to this comparison, it is observed that even the evaluated databases are completely different, very similar identification results are achieved with both PCA and LDA. Observing such consistent results with a real plastic surgery database indicates high accuracy for our synthetic database.

Table 6.1: Rank-1 identification accuracies for 2D FR algorithms for Experiment 1, 2 and 3

Algorithm	**Exp. 1**	**Exp. 2**	**Exp. 3**	**Exp. 3 [127]**
PCA	40.24%	30.02%	24.74%	23.1%
LDA	64.74%	51.56%	28.94%	24.1%
LBP	92.90%	88.52%	88.52%	44.8%

However, this is not the case for LBP. Very different identification rates are obtained, mainly due to two main reasons: The significant variance between the pre-surgery and post-surgery images in [127] (as shown in Figure 6.2) and the fact that in our case, the only variation is due to the nose alteration and hence the change in the image texture is minimal.

Table 6.2: Verification rates at 0.001 FAR for 2D FR algorithms for Experiment 1, 2 and 3

Algorithm	**Exp. 1**	**Exp. 2**	**Exp. 3**
PCA	27.50%	21.18%	11.66%
LDA	50.69%	40.11%	15.30%
LBP	81.51%	71.72%	71.72%

The verification rates at 0.001 FAR and the ROC curves for all three algorithms are given in Table 6.2 and Figure 6.4, respectively. For LBP, the rates are identical for Experiments 2 and 3, since no training is required.

According to the results in Table 6.1 and Table 6.2, best performance is obtained using LBP method for both identification and verification with a marked difference. This shows that being a texture based method, LBP is much more appropriate than appearance based methods, PCA and LDA in case of nose alterations. With LBP, the relative difference between the results of Experiment 1 and 2 for identification and verification are found as 4.71% and 12.01%, respectively.

Robustness of LDA is observed to be higher than PCA, with 20% decrease for both verification and identification scenarios. Whereas, PCA suffers 25.40% and 22.98% loss in identification and verification accuracies, respectively.

Utilization of an external database worsens the results even further for both identification and verification experiments.

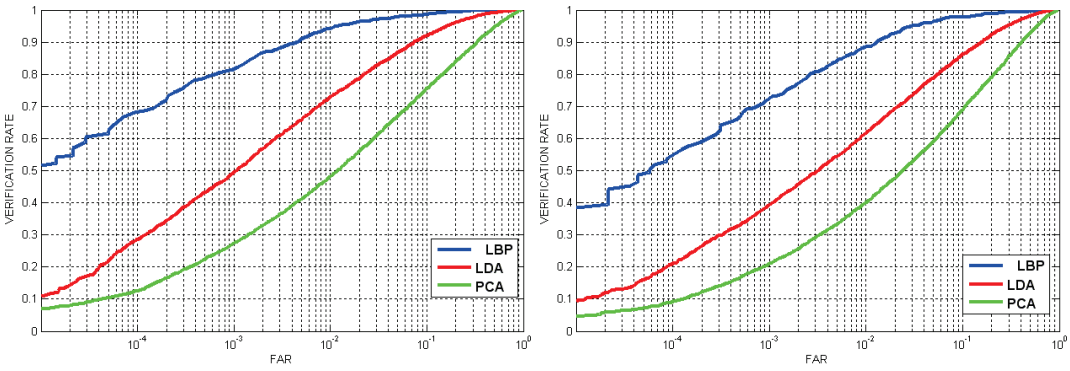

Figure 6.4: Verification rates for all 2D FR algorithms by Experiment 1 (left) and Experiment 2 (right).

6.3.2 Impact on 3D Face Recognition

For the evaluation of 3D face recognition systems, 4 algorithms are selected where the facial surfaces are represented as depth maps or point clouds.

Depth maps can be involved in most of the existing 2D techniques, including subspace methods. In this part of the study, similar to the 2D evaluations, PCA and LDA are selected to be evaluated.

Additionally, two different approaches are implemented for 3D face recognition using point clouds. In this representation, faces are required to be registered prior to similarity measurements.

For this reason in the first technique, the faces are aligned with a generic face model using 3 landmark points (2 outer eye corners and the nose tip) and then the depth values are regularly sampled. The similarity (in this case distance) between two faces is obtained by averaging the z-distances of all vertices. In this way, the volume difference (VD) between two facial surfaces is approximated.

For the second approach (WP), we implemented the method presented in Chapter 4 which employs the TPS warping parameters as biometric signatures.

The achieved rank-1 identification rates and the verification rates at 0.001 FAR by all 3D algorithms on databases DB-o3 and DB-s3 are given in Table 6.3 and Table 6.4. As is the case with LBP, since the two point cloud methods do not require any training, rates for Experiments 2 and 3 are the same.

For identification, the best performing and most robust algorithm is observed to be WP, followed by LDA on range images. Both PCA and VD suffer a drastic decline (25%) when nose alterations are introduced.

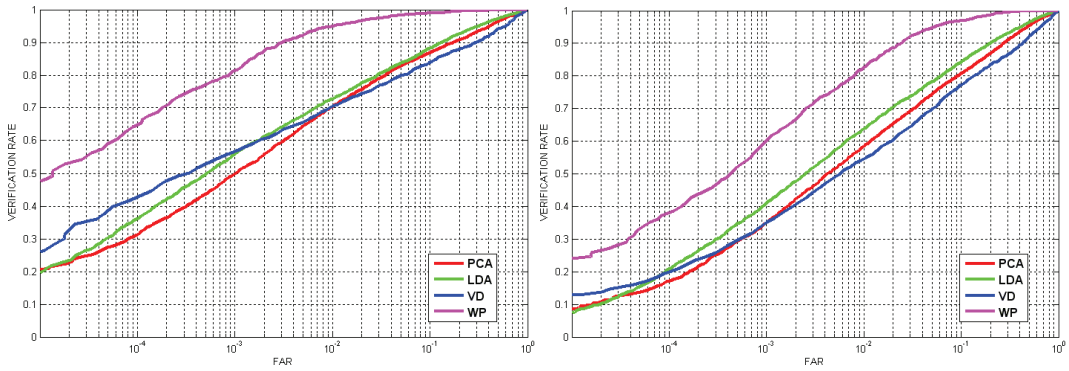

Figure 6.5: Verification rates for all 3D FR algorithms by Experiment 1 (left) and Experiment 2 (right).

Table 6.3: Rank-1 identification accuracies for 3D FR algorithms for Experiment 1, 2 and 3

Algorithm	**Exp. 1**	**Exp. 2**	**Exp. 3**
PCA	64.11%	48.40%	33.96%
LDA	68.47%	58.15%	42.03%
VD	68.26%	51.95%	51.95%
WP	94.46%	86.64%	86.64%

Likewise, analysis concerning the verification rates reveals that LDA and WP are least affected from nose alterations. However in verification, deteriorations are much more visible for all four methods.

Table 6.4: Verification rates at 0.001 FAR for 3D FR algorithms for Experiment 1, 2 and 3

Algorithm	**Exp. 1**	**Exp. 2**	**Exp. 3**
PCA	49.85%	35.22%	17.42%
LDA	56.67%	42.18%	17.74%
VD	56.97%	35.23%	35.23%
WP	81.18%	60.79%	60.79%

Similar to the case observed in 2D experiments, utilization of an external database has a negative effect on the recognition accuracies. Algorithms have better performances when they are trained on both pre- and post-alteration images.

6.4 Conclusion

As means of altering facial shape proliferate, its impact on recognition performances becomes crucial to measure and prevent. Today, more and more people undergo plas-

Figure 6.6: Two examples of nose alterations with and without textures (upper row: originals lower row: altered).

tic surgeries (From 2009-2010, there was almost a 9% increase in the total number of cosmetic surgical procedures and since 1997, there has been over 155% increase in the total number of cosmetic procedures [46].) not only for medical reasons but also to improve their appearance or even to hide their true identity. Easy-to-use appliances and makeup products are within reach of everyone who seeks ways to evade recognition.

In this study, a synthetic nose alteration database is obtained for which the nose of every subject in FRGC v1.0 is transfigured by replacing it with another randomly selected one. It is utilized to evaluate the performances of face recognition algorithms in presence of nose alterations.

The novelty of this contribution is that the analyses are not restricted to 2D images. Thanks to the nature of the simulated database, the effect of the applied modifications can be determined also in 3D. Additionally, since it is possible to measure the original performances on FRGC v1.0, an authentic comparison between pre- and post-alteration performances can be provided, which is a significant advantage of this study when compared to the previous ones.

The results reveal that the evaluated algorithms are not robust to the variations caused by nose alterations, especially for the purpose of verification. Furthermore, comparing verification performances of 2D and 3D algorithms show that 3D is much more vulnerable against the nose variations. On the other hand, robustness in identification is observed to be more method dependent then modality.

Robust face recognition algorithms are necessary to mitigate the effects of facial modifications. In the next chapter, we propose a block based face recognition approach robust to nose alterations. Our future research direction is to develop such face recognition methods robust to facial alterations. Additionally, we would like to measure the efficiency of nose alterations for face spoofing purposes.

Chapter 7

Face Recognition Robust to Nose Alterations

Face recognition robust to alterations applied on face via plastic surgery or prosthetic make-up can be still considered as a new topic. In this chapter, a block based face analysis approach is proposed which provides a fairly good recognition performance together with the advantage of robustness to such kind of alterations. For this study, a simulated nose alteration face database is used which is prepared using FRGC v1.0. Since this is a 3D database, the approach can be tested both in 2D and 3D, which is one of the contributions of this study. Furthermore, differently from previous works, baseline results for the original database are reported. The impact which is purely due to the applied nose alterations is measured using both the proposed approach and the standard techniques which are based on holistic description for comparison. The results indicate that although both 2D and 3D modalities lose precision due to alterations, the proposed approach is superior in terms of both the recognition performance and robustness to alterations compared to standard techniques.

7.1 Introduction

The number of people resorting to plastic surgery for correction of feature defects or cosmetic reasons has been increased a lot in recent years. Therefore researchers started to work on preventing the impact of facial alterations on recognition. However, there are only a few studies which are proposed to prevent the impact of facial alterations on face recognition.

An evolutionary granular approach is proposed in [15] for matching a post-surgery face image with a pre-surgery face image and 15% improvement in identification performance is reported. Furthermore, two new methods, FARO and FACE, based on fractals and a localized version of correlation index, respectively, are implemented in [90] which claims that the performance of these two algorithms compare favorably against standard face recognition methods such as PCA and LDA in case of plastic surgery changes. Singh et al. adopted the near set theory to classify facial images that have previously undergone some feature modifications in [125].

To the best of our knowledge, the impact of plastic surgeries on face recognition was first analysed by Singh et al. in [126,127] where the effect of plastic surgery is evaluated on several recognition algorithms. In the previous chapter, the shortcomings in

the studies [126,127] are explained. In our previous study [40] (explained in Chapter 6), these limitations are eliminated by creating a synthetic database using FRGC v1.0 for which nose regions are exchanged between subjects in the same database. In this way, a 2D+3D database is obtained for nose alterations and since the conditions and the subjects are identical for the original and the simulated databases, measuring the exact impact of nose alterations is possible.

Our previous study [40] focuses on the nose modifications and analyze their effects on success rates of several face recognition methods both in 2D and 3D face recognition using the simulated nose alteration database.

In this chapter, we focus on developing a new approach which reduces the impact of nose alterations on recognition performances. The proposed approach is based on local description. Principal Component Analysis (PCA) [12], Linear Discriminant Analysis (LDA) [12] and Local Binary Pattern (LBP) [4] are standard techniques in face recognition. These techniques are applied generally over the whole image to extract image features as in the studies [40,126,127]. In this study, these techniques are applied over image blocks to extract block features. Dissimilarity between an image pair is computed using the dissimilarities which are previously computed for each block pair of these images in the most optimum way to maximize the recognition performances. This study aims to reduce the performance decrease caused by nose alterations.

The rest of the chapter is organized as follows: Section 7.2 describes the proposed approach. Section 7.3 gives the experimental results to show the effect of nose alterations in 2D and 3D face recognition. In this section, the results are reported using both the proposed approach and the standard techniques which are based on holistic description for comparison purposes. Finally, the conclusions are provided in Section 7.4.

7.2 Block Based Face Recognition Approach Robust to Nose Alterations

The proposed approach analyzes images by dividing them according to a regular square grid. Initially, cropping of all texture and range images (depth maps) in DB-o and DB-s is done. Then, all cropped images are resized with the parameter [300 300] since in our case, all these images in both DB-o and DB-s have pixel size more than [300 300]. After resizing, they are divided into 36 blocks each of which has size [50 50] (Figure 7.1). These parameters should be adjusted according to the image sizes in the selected databases.

In our study, the techniques PCA, LDA, and LBP are used only to extract features of the image blocks. For each image pair, using these extracted features, dissim-

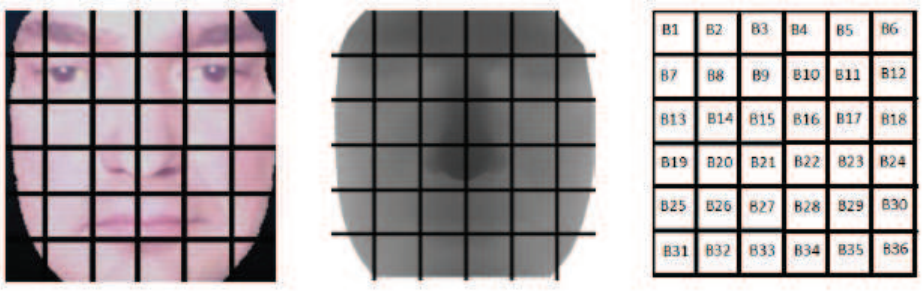

Figure 7.1: (a) Texture image divided into 36 blocks (b) Depth map divided into 36 blocks. (c) Image showing the ordering of blocks (BI represents Block I).

ilarities between blocks of the first image and corresponding blocks of the second image are computed, separately. This process provides 36 dissimilarity results for one image pair. Distribution of these dissimilarity results is analyzed for both DB-o and DB-s. According to our analysis, the blocks which deteriorate the recognition performances are decided not to be involved in resultant dissimilarity computation between the image pairs by applying a special technique which is explained in the next paragraphs.

Figure 7.2 shows an example to our analysis by using an original image in gallery (Image 1), another image of the same person for original vs. original comparison (Image 2) and a synthetic image which is in fact Image 2 after nose alteration for original vs. synthetic comparison (Image 3). The figure shows dissimilarity results computed for each of 36 blocks. PCA is applied to extract the block features. Dissimilarity results between the blocks of Image 1 and Image 2 are computed for original vs. original comparison (Or. vs. Or. in Figure 7.2). Dissimilarity results between the blocks of Image 1 and Image 3 are computed for original vs. synthetic comparison (Or. vs. S. in Figure 7.2). From Figure 7.2, it is clear that dissimilarity results for the two comparisons are similar at most of the block numbers except the ones which have undergone nose alteration. For instance, very high dissimilarity is obtained for Or. vs. S. compared to Or. vs. Or. comparison at Block 15 which represents the nose region affected from nose alteration. Also Figure 7.2 shows that the lowest dissimilarities are observed at the blocks which represents just the skin part (e.g. Block 18) and higher dissimilarities are observed usually at the dense-textured blocks (e.g. Block 8). According to these analysis for Or. vs. Or. and Or. vs. S. comparison cases, we developed our approach.

In the proposed approach, after dissimilarities are computed for each block pair, respectively, they are sorted from minimum to maximum. D_i represents the i^{th} minimum dissimilarity result inside the total 36 dissimilarity results.

Equation (7.1) shows how the results are obtained inside the proposed approach.

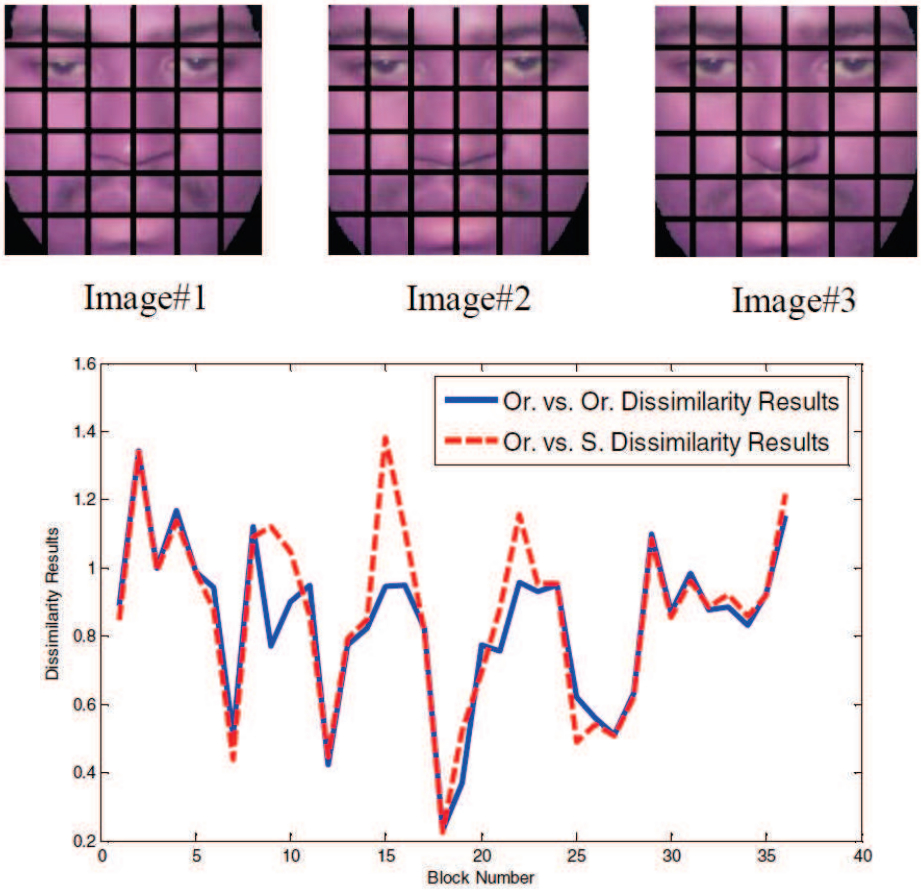

Figure 7.2: Dissimilarity Results obtained for original vs. original comparison between Image 1 and Image 2 and original vs. synthetic comparison between Image 1 and Image 3.

$$RD(k) = \frac{1}{k}\sum_{i=1}^{k} D_i \qquad k = 1, ..., 36 \tag{7.1}$$

For the first computation (k=1), only the block pair with minimum dissimilarity (D_1) is involved in the resultant dissimilarity computation between an image pair, which is represented as RD in Equation (7.1). For next computations ($k > 1$), each time, the next minimum dissimilarity is added to the array and the resultant dissimilarity is computed as mean of the dissimilarities in this array. This means that at the last computation ($k = 36$), the dissimilarity results computed for all block pairs ($D_1, \ldots, D_{36}$) are used in Equation (7.1) to compute the resultant dissimilarity between an image pair. The resultant dissimilarities are computed for each image pair and then recognition performances are evaluated from these results.

Figure 7.3 shows the 36 identification rates which are computed by using the depth

maps in our database for one non-overlapping training and testing partitioning. In this study, RD is assumed as the dissimilarity between an image pair and the distance matrix is obtained using the dissimilarities that are computed for all image pairs. From the distance matrix, rank-1 identification rates are computed for increasing k values. The x axis in this figure represents the number of block pairs involved in resultant dissimilarity computation between image pairs (k in Equation (7.1)). Three outcomes can be extracted from Figure 7.3:

- In case significant number of block pairs are not involved in the resultant dissimilarity computation ($k < 15$), a rapid decline is observed in performances.
- In case the block pairs with higher dissimilarities are not involved in the resultant dissimilarity computation ($15 < k < 36$), better performance can be observed even for DB-o compared to the case for which all block pairs are used ($k = 36$). (Best performance for DB-o is observed at $k = 23$ for the example in Figure 7.3.)
- It is obvious that the increase in the performance ($\frac{max(IR(k))-IR(36)}{IR(36)}$; where IR represents Identification Rates) is much more for DB-s compared to DB-o.

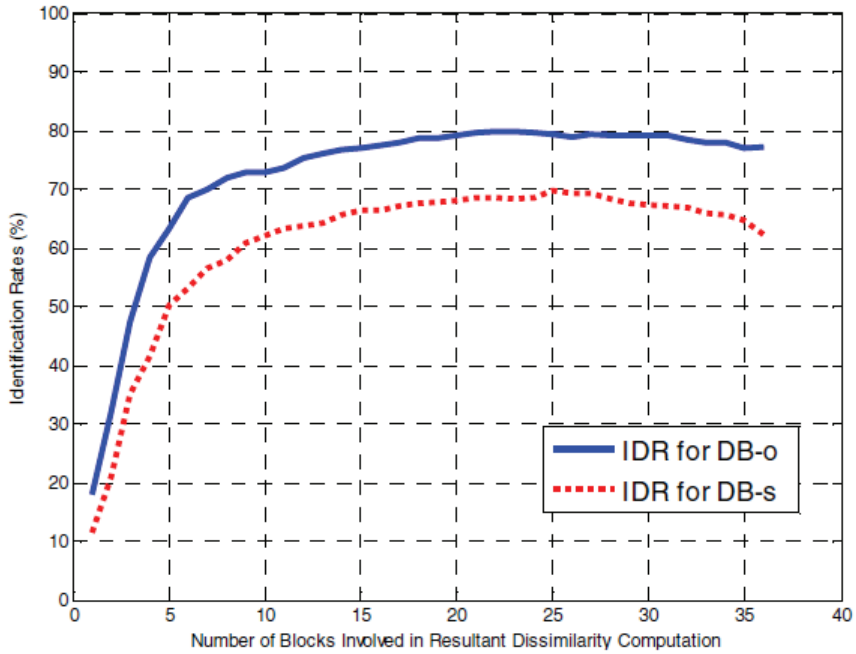

Figure 7.3: An example showing the identification rates computed at each of 36 successive computations using depth maps.

The proposed approach is mainly based on these outcomes. Due to the impact of facial alterations, the increase in the performance is observed as always higher for DB-s under the same conditions for DB-o and DB-s. Therefore, in this study the

maximum identification rate obtained after successive computations (the rate at $k = 23$ for DB-o and at $k = 25$ for DB-s for the example in Figure 7.3) is selected as the resultant performance rate of the system. Based on the first outcome, in the proposed approach, computations are started using the first 15 minimum dissimilarities instead of using only the first minimum one in order to reduce the computation time. Note that in this method, we do not eliminate exactly the altered blocks, we eliminate the blocks with higher dissimilarities. Therefore there is no need to know which part of the face has plastic surgery and the method can be applied for any operation.

Table 7.1 shows the identification rates obtained for DB-o and DB-s using the example in Figure 7.3 for three cases. PCA is used to extract features. Case 1 is the case for which dissimilarities of all block pairs (D_1, ..., D_{36}) are used to compute the rate with block based face analysis (rate at $k = 36$). Case 2 is the proposed approach, for which maximum rate obtained after successive computations is selected as the rate of system (maximum rate at $15 < k < 36$). Finally, Case 3 is the case for which standard PCA (based on holistic description) is used to compute the rate.

Table 7.1 shows the superiority of the proposed approach in terms of both recognition performances and robustness to nose alterations. The identification rates computed with standard PCA (Case 3) are reported to make a comparison between the standard and the proposed approach. The same train-test partitioning is used for all cases. From the table, it is clear that block based analysis of images (both Case 1 and 2) improves the results significantly compared to Case 3, which is a holistic approach. However, using the proposed approach, for which only the blocks that maximizes recognition performances are used (Case 2), it is clear that the best performance rates are obtained for both DB-s and DB-o with the advantage of the most robust result to alterations, which is the main target of this study.

Table 7.1: Rank-1 identification accuracies obtained for three cases using the same data of the example in Figure 7.3.

Algorithm PCA	**DB-o**	**DB-s**	**Performance Decrease**
Case1	77.32%	62.37%	19.34%
Case2	79.90%	69.85%	12.58%
Case3	58.51%	45.88%	21.59%

7.3 Experiments and Analysis

In this part, the results of the proposed method are compared with the results of standard techniques used in the studies [40, 126, 127], in which the impact of facial alterations on recognition performances is measured.

Initially, all four databases, DB-o2, DB-o3, DB-s2 and DB-s3 are partitioned in non-overlapping train and test datasets. This is done by randomly selecting 40% of the subjects and assigning their samples to the train set, while the rest is used for testing, similarly to the studies in [40, 127]. The partitioning is repeated 10 times and verification and identification rates are computed over these 10 trials.

For verification tests, the verification rates at 0.001 FAR are reported. For identification tests, the first sample of each individual in the test set is used as gallery and the rest as probes. The rank-1 recognition rates are reported.

The effect of the applied nose alterations on face recognition performances is evaluated with two different scenarios in both 2D and 3D which are determined according to the study of Singh et al. [127] for comparison.

- **Experiment 1 - Performance on the original database**: It is important to compute performances on the original datasets in terms of having a baseline. In this way, the impact of the applied changes can be measured accurately. For this purpose, 2D and 3D algorithms are evaluated on DB-o where the dissimilarities are calculated between each original image pair.
- **Experiment 2 - Performance on the simulated database**: In this scenario, the similarity scores between every DB-o and DB-s sample pairs are calculated and used to evaluate recognition performances. For the train set, for each subject selected, half of the corresponding images are taken from DB-o and the rest from DB-s. This experiment is identical to Experiment 1, except the probe images are now replaced by their modified versions.

Results of Experiment 1 and 2 are reported using both the proposed approach and the holistic approach, in which the key techniques (PCA, LDA, LBP) are applied over the whole image which are resized as [50 50]. This selection of the resizing parameter for the holistic approach in this study is based on the following reason:

- The key techniques are applied on plastic surgery database in [127] and results that are close to the reported results in [127] are obtained with this resizing parameter.

7.3.1 Evaluation on 2D Face Recognition

In this part, three key methods, PCA, LDA, and LBP, are applied over the image blocks for the proposed approach; whereas they are applied over the whole image for the holistic approach, which is in fact the approach generally used for standard techniques. PCA and LDA are appearance based approaches. LBP is a texture based algorithm for describing local structures.

The plastic surgery database in [127] has images after several types of surgery operations such as forehead surgery, ear surgery, eyelid surgery, nose surgery, face lift

etc. In this part, the proposed approach is tested also using this real plastic surgery database to compare our results with the reported results in [127]. However, since this database includes only one image before the plastic surgery, it is not possible to compute exact baseline performances. Hence using this database, it is also not possible to show the robustness of our approach to plastic surgery due to the lack of baseline scores. Therefore in Table 7.2, only the success of our approach in terms of recognition performance is shown.

The first column of Table 7.2 shows the results reported in [127], second column shows the results we obtained using the same techniques just to verify the parameters we selected for each technique are appropriate or not, and last column shows the results obtained with the proposed approach. Since the results in column 1 and 2 are consistent; the same parameters are selected to be used in this study to make an authentic comparison between the proposed approach and the holistic approach. Inside the PCA, LDA and LBP methods used in [40,126,127], only the LBP applied in [40] is not based on holistic description. However, in this study, LBP based on holistic description [4] is selected to be used to make the comparison just between the proposed and the holistic approach. From Table 7.2, performance increase with the proposed approach is obvious for all methods.

Table 7.2: Rank-1 identification accuracies for 2D FR algorithms for Experiment 2 on Real Plastic Surgery Database (P. A is proposed approach, H.A is holistic approach).

Algorithm	**Exp. 2** (Results in [127])	**Exp. 2** (H. A.)	**Exp. 2** (P. A.)
Case1	29.1%	29.01%	39.94%
Case2	38.6%	36.14%	44.24%
Case3	47.8%	46.87%	51.28%

The rank−1 recognition rates and the verification rates at 0.001 FAR are given in Table 7.3 and 7.4, respectively, for both the proposed and holistic approach. The train−test partitioning are the same to make an exact comparison.

The relative difference between results of Experiment 1 and 2 shows robustness of the methods to nose alterations. According to the results in Table 7.3 and 7.4, best performance is obtained using LBP method for both identification and verification. It is also more robust to nose alterations compared to PCA and LDA with both of the approaches.

This shows that LBP is much more appropriate than PCA and LDA in presence of nose alterations as also concluded in [40]. Robustness of LDA is observed to be higher than PCA, for both verification and identification.

Table 7.3: Rank-1 identification accuracies for 2D FR using two approaches for Experiment 1 and 2

Algorithms	**Holistic Approach**		**Proposed Approach**	
	Exp. 1	**Exp. 2**	**Exp. 1**	**Exp. 2**
PCA	44.60%	31.62%	79.24%	64.62%
Perf. Decrease	29.10%		18.45%	
LDA	69.90%	55.67%	80.36%	68.33%
Perf. Decrease	20.36%		14.97%	
LBP	77.08%	70.05%	81.27%	76.33%
Perf. Decrease	9.12%		6.08%	

Table 7.4: Verification rates at 0.001 FAR for 2D FR using two approaches for Experiment 1 and 2

Algorithms	**Holistic Approach**		**Proposed Approach**	
	Exp. 1	**Exp. 2**	**Exp. 1**	**Exp. 2**
PCA	31.75%	21.06%	69.29%	52.75%
Perf. Decrease	33.67%		23.87%	
LDA	55.54%	41.60%	70.27%	57.86%
Perf. Decrease	25.10%		17.66%	
LBP	60.74%	53.30%	72.39%	66.26%
Perf. Decrease	12.25%		8.47%	

The effect of the proposed approach in terms of the increase in recognition performances is most obvious for PCA. Performance is almost doubled for both identification and verification. On the other hand, there is also an increase in the performance for LBP with the proposed approach, however it is less compared to PCA and LDA. From Table 7.3 and 7.4, it is also clear that using the proposed approach, the decrease in the performance due to facial alterations is lower compared to the results obtained with the holistic approach for all three techniques. This proves that the proposed approach both increases the recognition performances and provides more robust results to facial alterations compared to the holistic approach.

7.3.2 Evaluation on 3D Face Recognition

For the evaluation on 3D face recognition, 2 algorithms are selected where the facial surfaces are represented as depth maps. Depth maps can be involved in most of the existing 2D techniques, including subspace methods. In this part, similar to the 2D evaluations, PCA and LDA are used. The achieved rank-1 identification rates and the verification rates at 0.001 FAR on DB-o3 and DB-s3 are given in Table 7.5 and 7.6.

For both identification and verification, using both of the approaches, LDA provides

better performing and more robust result compared to PCA on depth maps. Similar to analysis on texture images, again the proposed approach provides both better performances and also more robust results compared to the holistic approach. This proves the superiority of our approach also on depth maps. From the analysis on both texture and range images, it is observed that in verification, performance decrease is much more visible for all the methods. Also, with the holistic approach, much better results are obtained on range images compared to texture images for PCA. With the proposed approach, results on texture and range images are closer for PCA.

Table 7.5: Rank-1 identification accuracies for 3D FR using two approaches for Experiment 1 and 2

Algorithms	**Holistic Approach**		**Proposed Approach**	
	Exp. 1	**Exp. 2**	**Exp, 1**	**Exp. 2**
PCA	62.37%	47.46%	81.05%	69.58%
Perf. Decrease	23.91%		14.15%	
LDA	66.48%	56.55%	83.32%	75.12%
Perf. Decrease	14.94%		9.84%	

Table 7.6: Verification rates at 0.001 FAR for 3D FR using two approaches for Experiment 1 and 2

Algorithms	**Holistic Approach**		**Proposed Approach**	
	Exp. 1	**Exp. 2**	**Exp, 1**	**Exp. 2**
PCA	47.91%	31.86%	71.24%	54.34%
Perf. Decrease	33.50%		23.72%	
LDA	54.56%	39.61%	72.49%	60.35%
Perf. Decrease	27.40%		16.75%	

7.4 Conclusion

In this study, a synthetic nose alteration database is used which is prepared using FRGC v1.0. It is used to evaluate the performances of the proposed approach and compare the results with the standard recognition methods.

The novelty of this study is that the analyses are not restricted to 2D, the effect of the applied modifications can be determined also in 3D. Also, since it is possible to measure the original performances on FRGC v1.0, an authentic comparison between pre- and post-alteration performances can be provided, which is an advantage of this study when compared to the previous ones.

The results in [40, 126, 127] show that the standard recognition methods are not robust to the variations caused by nose alterations, especially for the verification case. Robustness to nose alterations is also observed to be method dependent. Robust algorithms are necessary to mitigate the effects of facial alterations. Therefore, in this chapter, a new approach is proposed which provides more robust results compared to the standard methods. It is simply a block based face analysis method, for which only the blocks of images that maximize recognition performance are used in dissimilarity computation between image pairs by applying a special technique.

Our future research direction is to propose novel countermeasure techniques, which mitigate the impact of facial alteration on recognition performances.

Chapter 8

Facial Cosmetics Database and Impact Analysis on Face Recognition

Facial cosmetics, also called makeup, change the perceived appearance of a face and therefore have an impact on automatic face recognition. In this chapter, to evaluate their impact in detail, the face as a whole and its most significant makeup application areas as skin, eyes and mouth are investigated separately. After specifying makeup application, a makeup categorization approach is developed in order to classify the applied products according to their effect on human perception. To evaluate the impact of facial cosmetics, a database of multiple images with and without makeup for each person is built.

8.1 Introduction

Facial cosmetics are a common part of the daily life in many cultures since Ancient Egypt [7] and change the perception of a face. The impact of facial cosmetics on the perception of a face is shown in Figure 8.1.

Research on the impact of facial cosmetics is limited, mainly because of the lack of public database which contains multiple images with and without facial cosmetics for a significant number of women. In [119], the authors develop a system which detects the most suitable makeup for a given human face. Unfortunately, they cannot provide public access to the database which they used for their study. Some databases (e.g. [114], [42]) provide images with facial cosmetics but there are no corresponding images without facial cosmetics hence these databases are inappropriate for the evaluation of face recognition.

In facial cosmetics studies, it is inevitable to know what the ordinarily used facial cosmetics are, where they are applied and which effect they cause. So far, no exhaustive specification exists.

Facial cosmetics can be applied in different ways. In order to evaluate the impact of facial cosmetics, an objective categorization approach beyond subjective opinions and preferences is needed.

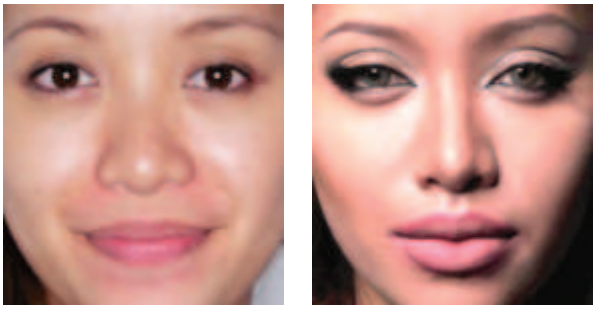

(a) Before (b) After

Figure 8.1: Impact of Facial Cosmetics on the Perception of a Face. This figure is taken from [138].

As facial cosmetics change the perception of face, they play an important role in human face recognition [136].

Automatic face recognition evolved into an important topic over the last decades since its relevance in security applications, intelligent robotics and entertainment industry continue to emerge.

One rare investigation of the facial cosmetics challenge in face recognition can be found in [29]. The authors state that facial cosmetics have an impact on the performances of face recognition systems. They mention about the need for a better understanding of the altering effects of facial cosmetics and the development of robust algorithms. Since the database used in their study is not publicly available, the obtained results are not reproducible. Also, the amount of applied facial cosmetics and the cosmetics' application area are not evaluated in detail.

The goal of this work is to contribute to studies related to facial cosmetics by providing a suitable database as well as an objective classification of facial cosmetics. The database contains multiple images with and without facial cosmetics for each person and provides detailed information about the application area and amount of applied cosmetics for each image. In this study, preliminary tests concerning the impact of facial cosmetics on face recognition are conducted. For those tests, the popular and efficient face recognition technique Local Binary Patterns (LBP) [4] is used for evaluation. Since LBP is texture-based technique and facial cosmetics have an influence on the texture, it is appropriate to analyze the impact of facial cosmetics on face recognition with this technique.

This chapter is organized as follows. In Section 8.2, the construction and structure of the facial cosmetics database are presented. Section 8.3 discusses a specification and classification approach of applied facial cosmetics. Preliminary tests concerning the impact of facial cosmetics on face recognition are presented in Section 8.4. The

conclusion is given in Section 8.5.

8.2 Facial Cosmetics Database

This section explains the construction of the proposed database, which can be used for diverse study related to facial cosmetics. It contains multiple images with and without facial cosmetics for each person. The subjects belong mainly to the Caucasian race and are between 20 and 30 years old. Hispanics, Asian and African Americans are also sparsely represented. In Section 8.4.2, the database is used to evaluate the impact of facial cosmetics on face recognition.

8.2.1 Specification of the Database

The database contains frontal facial images with little expression. It provides one reference image and one or more progressive makeup series per person. The latter is a series of images, where at each succeeding image more makeup is applied. The series always starts with a no makeup image as visualized in Figure 8.2. All kinds of makeup varying from slight to heavy are represented. The reference image does not belong to any makeup series and is taken in an other setting, resulting in variations of illumination, skin and hair conditions. As it can be observed from Figure 8.2, the reference image shows a different tone of skin, less dark circles under the eyes and a change in eyebrows's shape.

Figure 8.2: Reference Image and Makeup Series Images in their Original Form

Many applications require preprocessed images. Therefore, each image is available in its original and preprocessed version in the database. Preprocessing includes rotation and cropping as shown in Figure 8.3.

The facial subareas, eyes and mouth, are altered the most by facial cosmetics. In order to evaluate them separately, eyes and mouth regions are extracted and stored as separate images. The mouth images are rotated as well to ensure that the mouth corners are exactly at the same position in each image.

8.2.2 Acquisition of Images

It is important to collect images which are taken under similar conditions to real world scenarios (e.g. surveillance camera, snapshots). To achieve this, makeup

Figure 8.3: Reference Image and Makeup Series Images in their Rotated and Cropped Form

tutorial videos are used as source. Makeup tutorials are well suitable to obtain progressive makeup series. Most used videos were taken from YouTube, some of them were taken from websites of facial cosmetic companies. More information is available at $http://fcd.eurecom.fr/$. YouTube is a convenient source. Since many persons inherit an own channel, multiple videos of the same person can be found quickly. The number of online videos increases daily.

To ensure different conditions for reference and test images as described in Section 8.2.1, at least two videos are required for each person.

8.2.3 Structure of the Database

Each image in the database contains detailed information in its filename of form XXXX-N-ABCDEFGH. XXXX and N specify the identification number of the person and the identification number of the video related to the person, respectively. ABCDEFGH refers to an 8-digit makeup code which is described in Table 8.1. The makeup code specifies the quantity of applied makeup at eight different locations (see Figure 8.4).

The database currently contains 389 images. 50 of them are reference images and 339 of them belong to makeup series. 109 of the makeup serie images are classified into the makeup category 'no', 147 into 'slight', 54 into 'intermediate' and 79 into 'heavy', which are described in Section 8.3.2.2. Each image is available in its original (Figure 8.2) and cropped form (Figure 8.3). The sizes of the face, eyes and mouth images are 150×140 pixel, 60×140 pixel and 40×70 pixel, respectively. For each original form of an image, the coordinates of the eye centers and mouth corners are manually annotated and provided in a textfile.

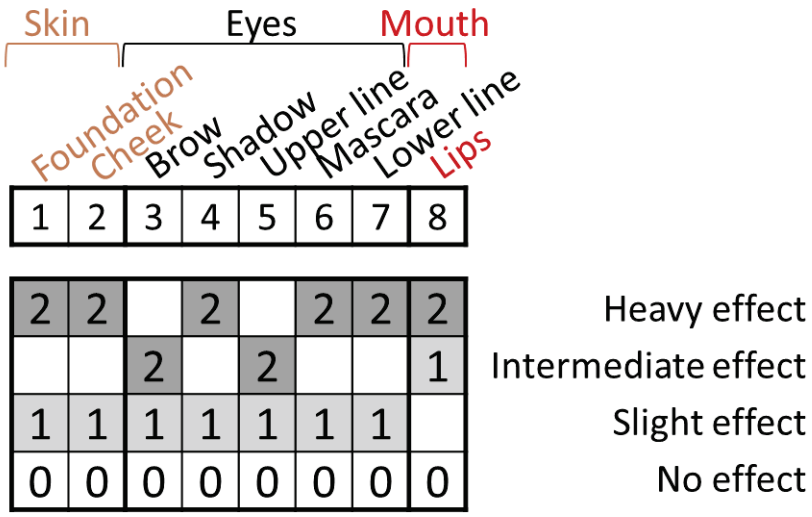

Figure 8.4: Makeup Classification Rules Depending on Steps

8.3 Facial Cosmetics

In this section, commonly used facial cosmetics, also called makeup, are specified. The specification results from the observation of numerous makeup tutorials. To evaluate facial cosmetics in detail, they must be classified into categories. In this chapter, a classification approach, based on the effect and exact location of applied cosmetics, is proposed.

8.3.1 Specification of Facial Cosmetics

Facial cosmetics are mainly applied on female faces to increase their attractiveness. Attractiveness is affected by youthfulness, symmetry [106] and averageness [115]. Youthfulness is composed of healthy, lively and also childlike characteristics [92] (e.g. soft skin, large eyes and small nose). All three attributes can be influenced by facial cosmetics. Their positive effects on attractiveness is shown in [30].

The application of facial cosmetics can be split up into eight main steps. Those steps are defined based on the observation of numerous makeup tutorials used for constructing the database in Section 8.2. Those tutorials are provided by ordinary women as well as professional makeup artists. They present different ways to apply makeup ranging from every-day to more exclusive makeup. Table 8.1 summarizes the eight main makeup steps including associated used products and their impacts. Those makeup steps form an 8-digit makeup code. Each makeup step can be applied with a slight or heavy amount, which is indicated in the makeup code by the digit 1 or 2. No application of makeup is indicated by the digit 0.

Table 8.1: Eight Makeup Steps

Step	Products	Effect
Foundation (skin)	Foundation, concealer, powder.	Coverage of skin flaws and natural shadows; change of skin color, face and nose shape; reduction of shininess.
Cheek	Bronzer, blush.	Emphasis and change of perceived position of cheekbones; lively and youthful appearance.
Brow (eyebrow)	Eyebrow pencil.	Accentuation, shaping and change of perceived position of eyebrows; increase of contrast.
Shadow (upper eyelid, eyebrow bone)	Eyeshadow.	Emphasis of lid crease; increase of depth; change of perceived size and color of eyes.
Upper line (upper eyelid)	Eyeliner, kajal.	Enhancement of contours; change of perceived size of eyes; thickening of lashline.
Mascara (lashes)	Mascara, false lashes.	Increase of density, swing and length of lashes; illusion of bigger eyes.
Lower line (lower eyelid)	Eyeliner, kajal.	Enhancement of contours; change of perceived size of eyes.
Lips	Lip liner, lipstick, lip gloss.	Enhancement of contours; change of perceived size, color and contrast; shininess.

8.3.2 Classification of Applied Facial Cosmetics

The application of facial cosmetics is classified by its application area and its effect on human perception.

8.3.2.1 Classification by facial subareas

The face is divided into its most significant subareas as skin, eyes and mouth. The makeup steps foundation and cheek belong to skin, whereas lips belong to mouth. Most steps belong to the eye area, which are namely brow, shadow, upper line, mascara and lower line makeup.

Each subarea is considered separately. This gives insight concerning its sensitiveness

to facial cosmetics and its contribution to the overall results. For each subarea, the applied cosmetics are classified by their altering effect as described in the following.

8.3.2.2 Classification by impact on facial appearance

The effect of facial cosmetics depends on how much and in which way the perceived size and color of facial features are changed. Three main categories (see Table 8.2) were established after examining numerous makeup tutorials used in Section 8.2.

Figure 8.4 describes the classification of the applied cosmetics per facial subarea. This allows the automated deduction of the categories based on the makeup code. The highest makeup category of all steps belonging to a certain subarea defines the makeup category of this given subarea.

The classification of the eye area is performed as follows: If shadow, mascara or lower line are applied heavily, it leads to a classification of the eye area into the category 'heavy', since those steps have a mask-alike or artificial effect. Heavy application of brow or upper line indicate the category 'intermediate', since the shape of eyes is enhanced. If any makeup step in the eye area is applied slightly, it leads to a classification into the category 'slight'.

If the foundation or cheek makeup step is applied heavily, the skin area is classified into the category 'heavy'. Foundation uniforms, evens and flats the facial shape. Natural shadows and marks are covered. Properly placed highlights change the apparent shape and size of facial features, e.g. nose. The cheek makeup step changes the perceived position, color and size of cheekbones. This leads to a distinction from the personal characteristics and therefore has an artificial or mask-alike effect. There is no skin makeup category 'intermediate'.

The slight application of lipstick, lip liner or lip gloss enhances the contours and contrast of the mouth area and therefore leads to a classification into the category 'intermediate'. Heavy application of lip makeup however causes changes in size and shape and therefore leads to the category 'heavy'. There is no mouth makeup category 'slight'.

Table 8.2: Categories of the Impact of Facial Cosmetics

Category	**Description**
No	No makeup applied, no effect
Slight	Slight changes in color and perceived shape
Intermediate	Strong enhancement of contours and characteristic features
Heavy	Estrangement from personal characteristics, mask-alike and artificial

The makeup category of the face as a whole is equal to the highest category of the subareas. However, there is one special case, since the subareas' categories contribute unequally to the face makeup category, mouth makeup has little impact on the overall perceived amount of makeup. Intermediate mouth makeup leads only to a makeup category 'slight' for the face as a whole.

8.4 Evaluation and Results

In this section, the impact of facial cosmetics on automatic face recognition is evaluated. Initially, the test setup is described and then the results are presented in the next part.

8.4.1 Test Setup

The makeup serie images are presented to the face recognition system for identification. Each identity is defined by a reference image. The accuracy of the face recognition system is here measured by the identification rate (IDR). The face recognition is conducted by applying Local Binary Patterns (LBP) with a block size of 10×10 pixels and a neighborhood with $(P, R) = (8, 2)$. P denotes the number of considered sampling points within radius R.

As it is explained in Section 8.3.2, the application of facial cosmetics can be categorized by application area and impact of makeup. The face as a whole and skin, eye and mouth subareas are examined separately. For each of them, makeup images from the category 'no', 'slight', 'intermediate' and 'heavy' are evaluated. To evaluate skin makeup, only images where solely skin makeup has been applied are considered. Skin makeup is usually applied before other steps. The database currently contains 55 images with solely skin makeup. Since 53 of them are classified into the makeup category 'slight', the number of heavy skin makeup images is not large enough in current database to represent the category 'heavy' correctly. To evaluate it as well, the size of the database would have been more important. Hence, only slight skin makeup is evaluated here. For evaluating eye and mouth makeup, the cropped images of the eye and mouth area are tested.

8.4.2 Evaluation Results

In this section, the identification rates resulting from the tests are presented. In the first test, no makeup images are used as the reference images. In the second test, the reference images are replaced by a subset of intermediate makeup images.

8.4.2.1 Test with No Makeup Images as References

The database currently contains 50 reference images with no makeup. Each of them are taken in an other setting than the makeup serie images.

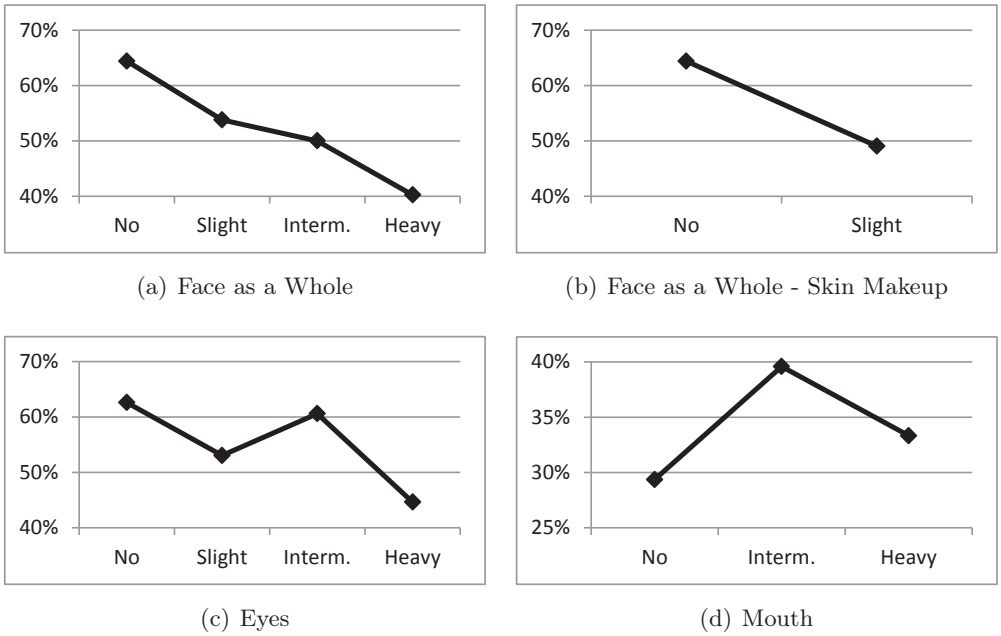

(a) Face as a Whole

(b) Face as a Whole - Skin Makeup

(c) Eyes

(d) Mouth

Figure 8.5: IDR when Reference Images are selected from No Makeup Images

As it is shown in Figure 11.10(a), the ability to identify a person's face decreases with increasing amount of makeup. The IDRs for the categories 'no', 'slight' and 'heavy' decrease almost linearly, while the one for the makeup category 'intermediate' shows a small increase (i.e. does not decrease linearly) but is still lower than the one obtained for the 'slight' category in the graph. The statement from [29], which claims that facial cosmetics degrade the accuracy of face recognition systems, is hereby confirmed. The results are in line with the expectations. Slight makeup test images achieve a little lower IDR than no makeup images. Slight makeup has little effect on human perception and maintains a natural look as defined in Table 8.2. Intermediate makeup in contrast is clearly visible and therefore provides a lower IDR. Heavy makeup has a strong impact on persons' characteristic appearance hence is perceived as mask-alike. The IDR for faces with heavy makeup reach only two third of the IDR for faces with no makeup. To gain detailed insights into the results, the face is divided into its three most significant makeup application areas, namely skin, eyes and mouth.

As it is shown in Figure 11.10(b), skin makeup causes a decrease in the face recognition ability. Skin makeup uniforms the face and changes the perceived position, color, shape and size of facial features. This leads to a distinction from the personal characteristics and therefore prevents face recognition.

Figure 11.10(c) shows the IDR for eye recognition. It follows the same scheme in

Figure 11.10(a) in terms that the IDRs for the categories 'no', 'slight' and 'heavy' decrease almost linearly, while the one for the makeup category 'intermediate' results in a local peak. The peak is higher than the one in Figure 11.10(a). Compared to the categories 'slight' and 'heavy', intermediate makeup images provide the highest IDR, which is almost as high as the IDR computed for images where no makeup is applied. Apparently, intermediate makeup in the eye area has no negative impact on face recognition. It enhances characteristic features and contours, which leads to better distinguishable eye shapes. Heavy eye makeup however influences eye recognition adversely. The eye area is dominated by large applications of unnaturally colored makeup which have an estranging and unifying effect. Shape, size and contours of the eyes get less distinctive. Slight eye makeup has only a slight negative impact on eye recognition. Some makeup steps as brow and upper line enhance the contours of facial characteristics, while others as eye shadow, mascara and lower line do not.

The IDRs for the mouth area are shown in Figure 11.10(d). The overall IDR curve is lower than the ones obtained for all other facial parts. This leads to the conclusion, that the mouth area contributes less to face recognition compared to the contributions of other areas. The low IDRs are caused by facial expression which affects predominantly the mouth area. Nevertheless, it is shown that application of facial cosmetics in the mouth area leads to better identification results. This is explained by its contour enhancing and contrast increasing effect. Again, intermediate makeup leads to the best results. Heavy makeup also includes changes of size which leads to a lower IDR compared to intermediate makeup. There is no makeup category 'slight' for the mouth area as explained in Section 8.3.2.2.

The IDR curve of the face as a whole is most similar to the one corresponding to the eye area, although the IDR curve for the eye area is overall little higher. This implies that the eye area is the most important facial subarea in face recognition, which is also stated in [96]. The eyes are the most distinctive facial part. The reduced peak at the face IDR curve is explained as follows. Intermediate makeup enhances characteristic features and contours, which leads to a better recognition of eyes and mouth. Skin makeup decreases the recognition ability because of its uniforming effect and changes in perceived size and shape of facial features. Slight and heavy makeup have a negative impact on face, skin and eye recognition. Images of the makeup category 'no' result generally in the best recognition rates. Mouth makeup steps are out of line because they have a positive effect on recognition. However, the mouth area has little impact on the face recognition.

The aim of evaluating the impact of facial cosmetics is to improve face recognition in reality. The previous results state that intermediate makeup plays an extraordinary role in face recognition. The question arises if intermediate makeup images are used as reference images, we will have a positive effect on face recognition or not.

8.4.2.2 Test with Intermediate Makeup Images as References

In this section, images with intermediate makeup are used as reference images. The database provides makeup series for 23 persons with intermediate makeup images. The remaining makeup series provide only images belonging to the makeup categories 'no', 'slight' or 'heavy'. Therefore, the evaluation is conducted with 23 reference images originating from makeup series. They consequently do not underlie other conditions than the test images but rather possess the same camera settings, skin and illumination conditions. Since the reference images are from the same session, it is less realistic compared to the test for which no makeup images are used as reference images and this is why we obtain almost perfect result (100%) in Figure 8.6 when intermediate makeup images are used as references. 175 test images are available for the specified 23 persons. 51 of them are classified into the makeup category 'no', 54 into 'slight', 30 into 'intermediate' and 40 into 'heavy'.

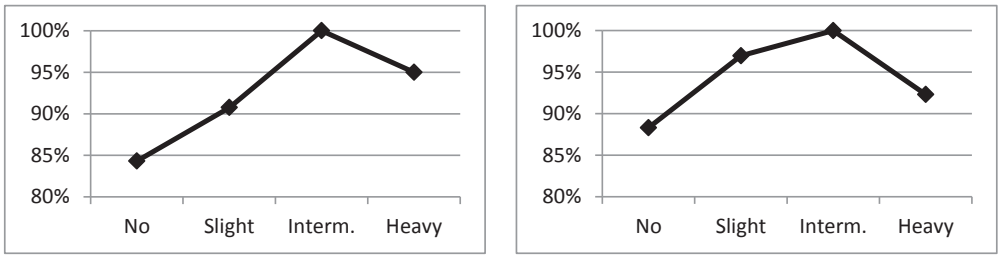

(a) Face as a Whole (b) Eyes

Figure 8.6: IDR when Reference Images are selected from Intermediate Makeup Images

The IDR curve for face recognition with intermediate makeup reference images is higher compared to the one resulting from no makeup images used as references. This is caused by the feature enhancing effect in the reference images due to intermediate makeup and the similarity of the reference images to the test images based on the same makeup series as origin. Here, increasing makeup does not lead to decreasing IDRs. The IDRs for the categories 'no', 'slight' and 'heavy' are almost linearly increasing, while the one for the makeup category 'intermediate' results again in a high peak as shown in Figure 8.6(a). Facial images with intermediate makeup have the highest IDR, namely 100%. Images where no makeup is applied result in the lowest IDR.

The IDRs for the eye area show a similar structure, which reinforces the statement, that the eye area dominates the face recognition. Eyes with intermediate makeup are recognized the best while eyes with no makeup provide the lowest IDR.

8.5 Conclusion

Facial cosmetics are commonly and daily used in many cultures and may alter the perception of facial features.

In order to propose a study on the impact of facial cosmetics on face recognition, a database is built, which is publicly available. Also, the categorization of the most common facial cosmetics and an objective classification approach are developed.

This database is used for preliminary evaluation of the impact of facial cosmetics on face recognition. If the reference images do not include any make-up, facial cosmetics do have a negative impact on face recognition. Surprisingly, the application of facial cosmetics in the reference images can help to obtain better identification rate. Facial cosmetics create intraclass variations. If they are only applied at one of the image sets, they obviously lead to a decrease of the accuracy of face recognition systems. In [121], it is underlined that intraclass variations between reference and test images greatly affect the accuracy of face recognition systems. In both cases, the eye subarea plays a major role in face recognition while the mouth area is not pivotal.

Both the makeup categorization approach and the established database are suitable for face recognition and related application areas, e.g. beauty evaluation, computer-suggested makeup or automated makeup detection. Based on the provided images and detailed information about the application area and amount of applied makeup, algorithms can be trained to recognize different kinds of makeup. If makeup is detected, facial subareas can be weighted differently to improve face recognition results as similarly performed in [96] for facial occlusions. To obtain more stable and detailed results, the size of the database can be increased. The definition of the makeup category 'slight' requires further refinement.

Chapter 9

Kinect Face Database and Impact Analysis on Face Recognition

The recent success of emerging RGB-D cameras such as the Kinect sensor depicts a broad prospect of 3-dimensional data based computer applications. However, due to the lack of standard testing database, it is difficult to evaluate how much the face recognition technology may benefit from this up-to-date imaging method. In order to establish the connections between the Kinect sensor and face recognition, in this chapter, we present the first publicly available face database (KinectFaceDB) based on the Kinect sensor for face recognition. The database consists of different data modalities (well-aligned and processed 2D, 2.5D, 3D and video based face data) and multiple facial variations. We conduct benchmark evaluations on the proposed database using standard face recognition methods, and demonstrate the performance gain by integrating the depth data with the RGB data via score-level fusion. We also compare the Kinect images (of the KinectFaceDB) with the traditional high quality 3D scans (of the FRGC database) in the context of face biometrics, which demonstrates the imperative needs of the proposed database for face recognition.

9.1 Introduction

Recently, the emerging RGB-D cameras such as the Kinect sensor [68] have been successfully applied to many 3D based applications. Thanks to its efficiency, low-cost, ease of RGB-D mapping and multiple-modalities, the Kinect sensor has received vast amounts of attentions from different research communities [141] not only in computer vision [1], but also in computer graphics [55, 59], augmented reality (AR) [38], human-computer-interaction (HCI) [62], instrument measurement [65] and robotics [43]. For the biometrics community, directly inheriting from the power of body parts segmentation and tracking using the Kinect [123], a number of works has been presented for gait recognition [47, 109, 130] and body anthropometric analysis [11, 100, 137]. However, the adoption of this powerful new sensor for face recognition has been mostly overlooked. The reason is due to the lack of standard testing dataset that limits the deployment of new algorithms and applications in this very dynamic research domain. Therefore, it is of great importance to provide a standard database for researchers to design and experiment 3D and multi-modal (i.e. 2D+3D) based face recognition using the Kinect data, so as to establish the connection between the Kinect and face recognition research.

In this chapter, a standard database (i.e., the KinectFaceDB) is presented to evaluate face recognition algorithms based on the Kinect. The proposed database consists of 936 shots of well-aligned 2D, 2.5D and 3D face data and 104 video sequences from 52 individuals taken by the Kinect sensor. It contains 9 different facial variations (including different facial expressions, illuminations, occlusions, and poses) within 2 different sessions. We conduct benchmark evaluations on the proposed database using a number of baseline face recognition methods. Specifically, we report the results (of identification/verification) of Eigenface [12], LBP [4], SIFT [85], and LGBP [140] for the 2D and 2.5D based face recognition, and conduct both the rigid method (i.e., ICP) [93] and the non-rigid method (i.e., TPS) [39] for 3D based face recognition. Score-level fusion of the RGB and depth data is also conducted, which demonstrates significantly improved results. The proposed KinectFaceDB are compared with a widely used high quality 3D face database (i.e., the FRGC database), in order to show the effects of 3D data quality in the context of face biometrics. In addition to its applications in face recognition, we also show in this chapter that the proposed database can be applied to many other tasks (e.g., facial demographic analysis and 3D face modelling). The main contributions of this chapter can be summarized as follows:

- A complete multi-modal (i.e., well-aligned and processed 2D, 2.5D, 3D, and video based face data) face database based on the Kinect is built and thoroughly described.
- Extensive experiments are conducted for the benchmark evaluations of 2D, 2.5D, and 3D based recognition using standard face recognition methods.
- Face recognition results on both the KinectFaceDB and the FRGC are compared following the same protocol, which demonstrate the data quality differences between the Kinect sensor and the laser scanner in the context of face biometrics.
- State-of-the-arts of existing 3D face databases are reviewed and discussed.

The rest of this chapter is structured as follows. In Section 9.2, we review the 3D face databases in the literature. Details of the proposed database are described in Section 9.3. In Section 9.4, experiments for benchmark evaluations and fusion are explained. The comparative results of experiments on KinectFaceDB and FRGC are reported in Section 9.5. Finally the conclusion is given in Section 9.6.

9.2 Review of 3D Face Databases

This section provides a review of publicly available 3D face databases. (A list of more generic face databases can be found at [114].) In biometrics research, face databases serve as the standard platform for comparative evaluations of face recognition algorithms [49], and therefore are important for the development of robust and reliable face recognition systems. Toward this goal, a large number of face databases have

been proposed for mainly two reasons: (1) to test face recognition algorithms robust to one or more specific facial variations (e.g. the Yale face database B [48] includes faces with 9 poses and 64 illumination conditions); (2) to help in the development of face recognition algorithms using a specific data modality (e.g. Honda/UCSD Video Database for video based face recognition [79, 80].). Some face databases provide various facial variations and multi-modality data, which allows various evaluation tasks (such as FRGC [107]). Some of the commonly used face databases include FERET [108], AR [91], PIE [50], ORL [117] and FRGC etc.

Table 9.1: Summary of Off-the-Shelf 3D Face Databases.

Database	Year of Publication	DB Size	No. of Subjects	3D Sensor	2D Texture	Expression	Illumination	Occlusion	Pose	Video
FRGC (Ver. 2.0) [107]	2005	121589	466	Minolta Vivid 900/910 [122]	✓	✓	✓			
ND-2006 [44]	2006	13450	888	Minolta Vivid 910	✓	✓				
GavabDB [97]	2004	549	61	Minolta VI-700 digitizer	✓	✓			✓	
3D-RMA [32]	1998	360	120	Structured Light					✓	
XM2VTSDB [94]	1999	1180	295	Stereo Camera	✓					✓
U-York [101]	n.a.	5250	350	n.a.	✓	✓	✓		✓	
BU-3DFE [139]	2006	2500	100	3DMD digitizer [2]	✓	✓			✓	
BJUT-3D [99]	2005	n.a.	500	CyberWare 3030RGB/PS [28]	✓	✓				
Texas 3DFRD [53]	2010	1149	118	MU-2 stereo imaging system [103]	✓	✓				
UMB-DB [27]	2011	1473	143	Minolta Vivid 900	✓	✓		✓		

In comparison to the large number of published 2D face databases, the number of available 3D face databases is relatively small. Table 9.1 gives an overview of off-the-shelf 3D face databases with statistics of different properties. In the table, it is clear that most of existing databases (FRGC, ND-2006, GavabDB, BJUT-3D and UMD-DB) adopts high quality laser scanners for face data acquisition. The 3D face acquisitions of BU-3DFE, XM2VTSDB and Texas 3DFRD are achieved by high quality stereo imaging systems, which can yield similar data accuracy in comparison to the data obtained by laser scanners. Although those high quality scanning systems can provide accurate facial details (e.g. the wrinkles and eyelids) for analysis, the capturing procedure is rather long and requires user cooperation. On the other hand, only 3D-RMA is captured by relatively low-quality 3D inference scheme, where 4000 points of each identity is obtained by structured light. This scanning scheme is similar to the one proposed by Freedman et al. [10] that is used in the Kinect, however its quality is rather low and no texture mapping is provided. Description of the sensor used in U-York face database is not available.

A face database should include enough variations in order to test the robustness of

face recognition algorithms. Facial variations such as facial expressions, illuminations, partial occlusions and pose variations are normally considered in typical face databases (e.g. [91, 107]). However, because 3D structures are the complementary information with respect to 2D textures, 2D and 3D face recognition techniques have different capabilities in treating different facial variations. For example, 2D face recognition methods [4, 12] are usually more robust to facial expression variations than 3D face recognition methods; on the other hand, 3D face recognition algorithms [18, 93] are known to be invariant to illumination changes. Therefore, the variations in a 3D face database shall be carefully selected. Because facial expression is a major challenge in 3D face recognition, almost all 3D face databases include this variation (except 3D-RMA). The second commonly used variation in 3D face databases are different poses. The pose variation can demonstrate how 3D face recognition algorithms can address a difficult problem in 2D recognition via the alignment of two 3D surfaces by rigid transformation usually performed by Iterative Closest Points method (ICP) [13,24]). In FRGC and U-York, different illumination conditions are also considered, even if illumination usually does not affect 3D face recognition. In addition to the commonly considered variations, partial occlusion is a very challenging problem for both 2D and 3D face recognition but only few databases contain occluded faces [27, 91, 118]. Recently, the UMB-DB [27] is proposed for the evaluation of 3D face recognition under occluded conditions.

Almost all 3D face databases are also multi-modal in the sense that 2D texture images are also provided (except for 3D-RMA). For the databases using stereo vision technologies (BU-3DFE, XM2VTSDB and Texas 3DFRD), 3D structure is inferred from two or more RGB cameras, thus the 2D/3D texture mapping is straightforward. However, for the databases based on laser scanners, the 2D texture images are usually taken by an external RGB camera. Therefore the 2D texture and 3D data are by default not aligned. The alignment can be achieved using additional facial landmarks and warping algorithms such as Thin Plate Spline (TPS) method [36]. It should be noted that only one database (XM2VTSDB) in our review provides also video data, and the video sequence is only for 2D texture sequences. This is because the off-the-shelf 3D scanners are not able to provide 2.5D depth map or 3D point cloud in real time. For this reason, almost all 3D face recognition studies are restricted to still 3D faces.

9.3 The Kinect Face Database

The Kinect Face Database is a multi-modal face database (with well aligned 2D, 2.5D, 3D and video data) based on the Kinect sensor. In this section, the database structure and the acquisition environment are described in part 9.3.1 and part 9.3.2, respectively; then the details of how to obtain the multi-modal data and how to achieve the alignment of different data modalities are presented in part 9.3.3; post-processing including noise removal and facial landmarking are then introduced in

part 9.3.4; finally the potential usage of this database is discussed in part 9.3.5.

9.3.1 Database Structure

The proposed KinectFaceDB contains sets of processed face data in a comprehensible structure. In order to exploit all possible face representations based on the Kinect's imaging capability, we captured and then processed the face data into four different formats: RGB image, depth map, 3D point cloud and RGB-D video sequences. There are totally 52 volunteers in the database, including 38 males and 14 females. Those participants are born between 1974 and 1987, come from different countries and thus belong to different ethnicities. We classify their ethnicities into the following categories (with the number of participants in the parentheses): Caucasian (21), Middle East/Maghreb (11), East Asian (10), Indian (4), African American (3) and Hispanic (3). The participants are asked to attend two sessions for the database recording. There are 5 to 14 days interval between the two sessions, for which the same recording protocol is applied. A meta-data file including the information of gender / year of born / ethnicity / with or without glasses / capturing time for session 1&2 is associated with each identity. The demographic classification of the proposed database is shown in Figure 9.1.

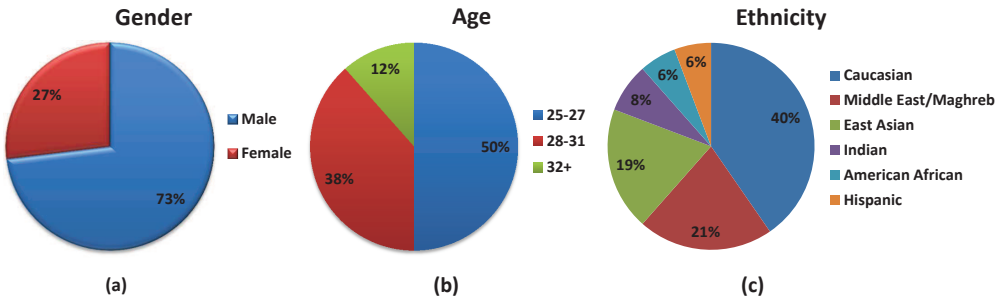

Figure 9.1: Demographics of KinectFaceDB validation partition by: (a) gender, (b) age, and (c) ethnicity.

In each session, four types of face data are captured: (1) 2D RGB image, (2) 2.5D depth map, (3) 3D point cloud and (4) 2D/2.5D video sequences. We carefully selected 9 types of facial variations in both sessions: neutral face, smiling, mouth open, strong illumination, occlusion by sunglasses, occlusion by hand, occlusion by paper, right face profile and left face profile. Examples with above variations are illustrated in Figure 9.2. The images were taken under controlled conditions but no restraints on wearing (clothes, glasses, etc.), make-up, hair style etc. were imposed to participants.

We also devised a protocol to record RGB-D face data in video sequences. The protocol consists of a slow head movement in both horizontal (yaw) and vertical (pitch) directions. Figure 9.3 demonstrates the procedure of one participant to record such

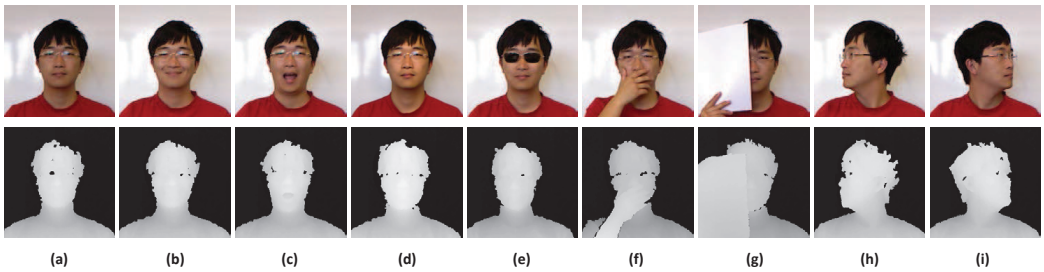

Figure 9.2: Illustration of different facial variations acquired in our database: (a) neutral face; (b) smiling; (c) mouth open; (d) strong illumination; (e) occlusion by sunglasses; (f) occlusion by hand; (g) occlusion by paper; (h) right face profile and (i) left face profile. (Upper: the RGB images. Lower: the depth maps aligned with above RGB images.)

a video sequence. The video sequences allow the extraction of multiple frames with different poses (in addition to the left/right profile recorded with the still images) so as to test 2D/3D face recognition algorithms robust to poses. Also, video based face recognition [79] can be studied on this dataset. Moreover, with increasing interest from the computer graphics community, accurate 3D face models can be extracted from such video data [56].

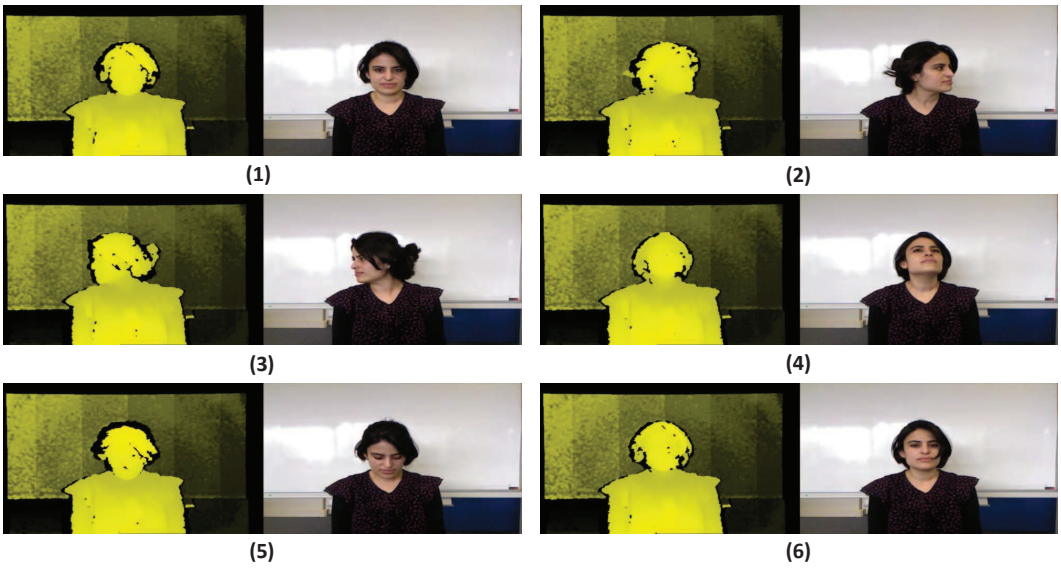

Figure 9.3: Procedure to record the video sequence: the head movement of a participant follows the path ($1 \rightarrow 2 \rightarrow 3 \rightarrow 4 \rightarrow 5 \rightarrow 6$). The head yaw is first performed which follows the procedure (approximately): $0^\circ \rightarrow +90^\circ \rightarrow -90^\circ \rightarrow 0^\circ$; then the head pitch is performed as: $0^\circ \rightarrow +45^\circ \rightarrow -45^\circ \rightarrow 0^\circ$.

9.3.2 Acquisition Environment

A controlled indoor environment (nature light source at daytime, with normal indoor LED diffusions) is set up for the database capturing. A Kinect is mounted and stabilized (where its lens are in parallel to ground floor by adjusting its tilt) on top of a laptop. The participants were asked to sit in front of the Kinect sensor at a distance (ranging from $0.7m - 0.9m$) and to follow the pre-defined acquisition protocol (in compliance with the database structure described in Section 9.3.1). A white board is placed behind the participants with the distance to the Kinect at $1.25m$, so as to produce a simple and easily filtered background. A LED lamp is set in front of the participants to produce strong illumination variation. Three pairs of sunglasses and a white paper are used to produce the occlusion variations. A human operator is required to sit in front of the laptop (in the opposite position of the participants) to monitor and control the acquisition process.

We developed a tool (based on OpenNI [51]) to facilitate the database capturing. The tool automatically captures, processes and organizes faces of participants according to the pre-defined database structure. Since we focus on the face region, we crop the captured RGB image and depth map into a pre-defined ROI (with resolution of 256×256). The pre-cropping scheme ensures the captured faces have a simple/uniform background (the white board only, and therefore easy to segment); also, it minimizes the differences between the RGB image and Depth map after the alignment (see Section 9.3.3.3). The details of the acquisition process are presented in the next section.

9.3.3 Acquisition Process

Microsoft Kinect was primarily designed for multimedia entertainment purposes, where it requires an integration of different sensing/display/processing functionalities (for the data source ranging from video/audio to depth) for the targeted ambient intelligence. Since our goal focuses on the building of a face database consisting of RGB-D and 3D face data, in this section, we summarize the imaging procedure of the Kinect, how we can obtain the 3D data, as well as the alignment of RGB and depth images so as to obtain the final output (still RGB-D image, 3D point cloud and video face data) in our database.

9.3.3.1 RGB and Depth Imaging from the Kinect

The Kinect sensor includes 3 main components for RGB-D data capturing: an infrared (IR) laser emitter, a RGB camera and an IR camera. The RGB camera captures RGB images I_{RGB} directly, whereas the laser emitter and IR camera act together as an active depth sensor to retrieve the distance information from the scene.

Freedman et al. introduced the triangulation process of the Kinect for the depth measurement based on the IR laser emitter and the IR camera in [10]. In the system, a pattern of spots (created by transillumination through a raster) are projected to the world scene by the IR laser emitter and the reflection of such pattern is captured by the IR camera. The captured pattern is then compared with a reference pattern (a pre-captured plane at a known distance) so as to produce a disparity map $I_{Disparity}$ of the spots displacement d. From the obtained disparity map $I_{Disparity}$, it is straightforward to deduce a depth map via simple triangulation process. A simplified model to describe such triangulation is suggested in [65]:

$$z_{world}^{-1} = (\frac{m}{f \times b}) \times d^{'} + (Z_0^{-1} + \frac{n}{f \times b}) \tag{9.1}$$

where z_{world} is the distance between the Kinect and the real-world location (namely the depth, in the unit of mm); d' is the normalized disparity value by normalizing the raw disparity value d between 0 and 2047, thus $d = m * d' + n$ where m and n are the de-normalization parameters; b and f are the base length and focal length, respectively; and Z_0 is the distance between the Kinect and the pre-defined reference pattern. The calibration parameters including b, f and Z_0 are estimated and provided by the device vendor (Microsoft).

With above procedures, the Kinect outputs a RGB image (where $I_{RGB}(x, y) = \{v_R, v_G, v_B\}$, and v_R, v_G, v_B refer to the values of R, G, B channels at image location (x, y)) and a depth map (where $I_{Depth}(x, y) = z_{world}$ and z_{world} indicates the depth value at image location (x, y)) simultaneously, with the resolution of 640×480. On top of the obtained RGB and depth images, the 3D face data and aligned RGB-D face data can be generated with later processes.

9.3.3.2 Converting to 3D Face Data

For the use of 3D face recognition, world 3D coordinates (according to a reference origin) of a given face are required. Thanks to the embodiment of the Kinect, the calculation of 3D points representing the surface of a face is straightforward. Knowing the depth map $I_{Depth}(x, y) = z_{world}$, the 3D coordinates of each point $(x_{world},\ y_{world},\ z_{world})$ (in the unit of $\{mm,\ mm,\ mm\}$) can be calculated from its image coordinates (x, y) as below:

$$x_{world} = -\frac{z_{world}}{f}(x - x_0 + \delta x) \tag{9.2}$$

and

$$y_{world} = -\frac{z_{world}}{f}(y - y_0 + \delta y) \tag{9.3}$$

where x_0 and y_0 are the principal point of the image coordinates, and δx and δy represent the corrections for lens distortions. Those parameters are easily accessible

from the device outputs.

Based on above projections, the 3D coordinates (a 3D point cloud) of each pre-cropped face depth image are computed and stored as '.obj' files in our database. Those files can be used for general 3D face recognition purposes and also be used to evaluate the 3D data quality of the Kinect in the context of biometrics in later experiments.

9.3.3.3 Alignment of RGB and Depth for Face Data

For face recognition based on both the RGB and depth images, establishing the correspondences between the RGB values and the depth/3D values at the same location on a face is an essential step. For example, designing a RGB-D descriptor which can summarize features from both the RGB and depth values jointly for each pixel might potentially reveal important facial characteristics. However, due to the intrinsic architecture of the Kinect sensor (where the RGB and depth images are sampled separately from two different cameras with a displacement between them), the RGB image and the depth map captured by the Kinect are not well aligned. Therefore, we further project the depth value from the IR camera plane to the RGB camera plane. From the depth map, we have already estimated the corresponding 3D coordinate ($x_{world},\ y_{world},\ z_{world}$) of each pixel using the method presented in Section 9.3.3.2, then the projection from the 3D coordinates to the 2D RGB camera plane can be achieved by using the traditional Tsai's camera model [135]. First, the 3D coordinates based on the IR camera is transformed to the 3D coordinate system defined by the RGB camera using affine transformation:

$$\begin{bmatrix} x_{world\prime} \\ y_{world\prime} \\ z_{world\prime} \\ 1 \end{bmatrix} = \begin{bmatrix} & R & & T \\ 0 & 0 & 0 & 1 \end{bmatrix} \begin{bmatrix} x_{world} \\ y_{world} \\ z_{world} \\ 1 \end{bmatrix} \tag{9.4}$$

where $R \in \mathbb{R}^{3\times3}$ is the rotation matrix and $T \in \mathbb{R}^{3\times1}$ is the translation vector. Then the 3D coordinates based on the RGB camera can be mapped to the ideally undistorted RGB camera plane as:

$$\begin{bmatrix} x_{RGB} \\ y_{RGB} \\ 1 \end{bmatrix} = f_{RGB}/z_{world\prime} \begin{bmatrix} x_{world\prime} \\ y_{world\prime} \\ z_{world\prime} \end{bmatrix} \tag{9.5}$$

based on the focal length f_{RGB} of the RGB camera. Finally, the true location $(x_{RGB\prime}, y_{RGB\prime})$ of a 3D point in the RGB camera plane is recovered by correcting the distortions and mapping to the RGB image origin:

$$\begin{bmatrix} x_{RGB\prime} \\ y_{RGB\prime} \\ 1 \end{bmatrix} = VD \begin{bmatrix} x_{RGB} \\ y_{RGB} \\ 1 \end{bmatrix} \tag{9.6}$$

where $D \in \mathbb{R}^{3\times3}$ and $V \in \mathbb{R}^{3\times3}$ are estimated to correct the uncertainties due to imperfections in hardware timing and digitisation, as well as the lens distortions. Some previous works made additional efforts to calibrate the intrinsic and extrinsic parameters of the RGB camera based on an extra RGB camera [21] or the embedded IR camera [20]. In our method, we directly adopt the Kinect factory calibration parameters which can also produce satisfactory alignment results. Illustration of the RGB-D alignment is shown in Figure 9.4. In the figure, one can observe the geometrical distortions (in addition to the translation at the image boundary) when re-mapping the depth map to the RGB image.

Figure 9.4: Illustration of the RGB-D alignment: the depth map (left) is aligned with the RGB image (right) captured by the Kinect at the same time.

Because we apply a pre-cropping scheme (as described in Section 9.3.2) to the mapped depth image, the large information loss and distortions at the image boundary are not included in our final output. We then store the RGB image and the aligned depth map (using the original scale in mm), respectively. Once we found the correspondences between the RGB image and the depth image, it is straightforward to map the RGB color to the 3D points. The 3D point cloud with corresponding color mappings are then recorded. Visualization of a 3D face after color mapping is displayed in Figure 9.5 (with background removal using a threshold τ). Finally, we store the video sequences of the aligned RGB and depth frames from both the RGB camera and the IR camera using the protocol described in Section 9.3.1. The video based face data can then be used for multiple purposes ranging from the video based face recognition using either 2D [79] or 3D [95] to the dense face model reconstruction [56] from 3D frames.

9.3.4 Post-Processing

We take into account two post-processing steps: noise removal and facial landmarking to finalize the database construction.

9.3.4.1 Noise Removal

Unlike the RGB images, depth images sensed by the Kinect is known to be noisy and inaccurate. A notable problem is the depth values on some pixels (that can be

Figure 9.5: Illustration of color mapping on 3D points cloud of a given face: from left to right views.

randomly distributed) are sensed as 0 mm whereas their true values are not zero. This may occur by the following reasons: (1) the points are too far (and the depth values cannot be computed accurately), (2) they are too close (there is a blind region due to limited fields of view for the projector and the camera); (3) they are in the cast shadow of the projector (there are no IR dots); (4) surfaces reflect poor IR lights (such as hairs or specular surfaces) [141]. Thanks to our setting (faces at sensible distances, uniform background), the sensing noises due to (1) (2) are automatically eliminated. The sensing noises caused by (3) (4) could be easily removed by setting a non-negative threshold and the existing holes can be filled in various manners (median/mean filters, morphological operations, Markov random fields etc., the approach we applied in our evaluation is described in Section 9.4.2).

Another noteworthy issue is the resolution of the captured depth. In comparison with the traditional 3D scanners (such as the KONICA Minolta scanner, with depth resolution of 0.1 mm within the sensing range, which has been used to capture the FRGC database [107]), the depth resolution of the Kinect is much lower (about 2 mm for the points spacing at 1 m [65]). Therefore, details of a face (for example, the wrinkles and eyelids) cannot be recorded using the Kinect. Those details can be regarded as soft biometric characteristics [61] [31] and could be useful information for identity discrimination. Although existing 3D face recognition studies claim that the salient region of depth (i.e. the nose region, which is not affected too much by the resolution problem) is the most important information for face recognition, it is important to understand how much the results can be dependent of different resolutions of the sensors (e.g. Kinect vs. Minolta) in the context of biometrics (i.e. identification and verification). For this reason, we evaluate the resolution impacts using the same protocol of 3D and depth based face recognition algorithms on both FRGC and our database, and report the comparative results in Section 9.5. Figure 9.6 gives a visual example of different depth resolutions of the same person from the Kinect and Minolta sensors.

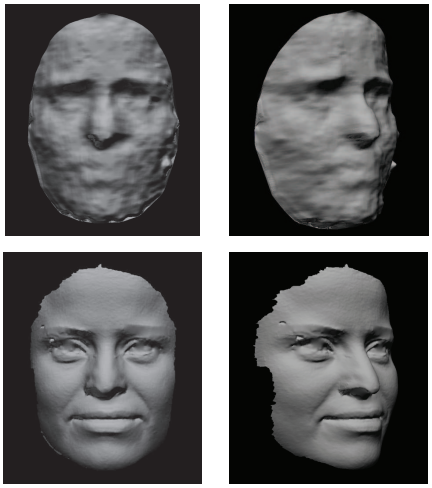

Figure 9.6: Cropped and smoothed 3D face captured by the Kinect (upper row) and Minolta (lower row) of the same person, frontal view (left column) and side view (right column). The 3D face from Minolta keeps more details (wrinkles, eyelids etc.).

9.3.4.2 Facial Landmarking

To facilitate the facial region extraction and normalization in face recognition, we defined 6 anchor points on a face (namely left eye center, right eye center, nose-tip, left mouth corner, right mouth corner and chin, see Figure 9.7.). Those anchor points are manually annotated for the RGB images. Then the corresponding locations in the depth images and 3D points clouds are also mapped. Note that the two face profiles are not annotated because only one side of the face is available. Even though the anchor points of occluded faces (faces occluded by sunglasses, hand and paper respectively) are not all visible, we estimated their positions so as to provide the full annotations on those occluded faces (similar to the annotations one can find in AR face database [91]).

Figure 9.7: The 6 facial anchor points: 1. left eye center, 2. right eye center, 3. nose-tip, 4. left mouth corner, 5. right mouth corner and 6. chin.

9.3.5 Potential database usages in addition to face recognition

The principal application of the proposed Kinect database is for face recognition. However, it may be of interest to some other research tasks. In this section, we suggest the usage of our database for two potential applications which have recently received much attention from the research community.

9.3.5.1 Facial Demographic Analysis

One potential application could be facial demographic analysis, including gender recognition, age estimation, and ethnicity identification from face images. Thanks to the population diversity in the proposed database (see Figure 9.1), it can promote the studies of demography on the novel Kinect sensor. According to a recent survey [45], most state-of-the-art methods for gender recognition and ethnicity identification are based on FERET face database and 2D pixel intensities. Nevertheless, Lu et al. [86] suggested that 3D shape of the human face provides competitive discriminative power on demographic classification to the intensity modalities. As a device integrates both intensity and 3D functionalities, the Kinect can act as an ideal sensor for above tasks.

9.3.5.2 3D Face Modelling

Since the emergence of the Kinect, dense 3D modelling based on this new sensor has attracted large attentions from computer vision and graphics researchers. Pioneering works [55, 59] have demonstrated how to build a dense 3D map of indoor scene/object by camera tracking using sparse features (e.g. SIFT [85], FAST [116]) and optimization of 3D points aggregations, taking advantage of the properties of real-time, low-cost and RGB-D mapping from the Kinect. More recently, 3D face modelling using the Kinect is introduced [56,145] to generate 3D avatar for applications such as video conference and MMOGs (massive multiplayer online games). We record our video data in KinectFaceDB following a similar procedure as described in [56], an example of the 3D model generated from such video is shown in Figure 9.8.

It can be observed in Figure 9.8 that the generated 3D face model from a video sequence has a much higher data quality than the 3D face model from a single depth image of the Kinect sensor (an example is given in Figure 9.6). The video based face modelling as shown in the figure aggregates and averages the data points from multiple single depth frames in a cylindrical coordinates system, so as to capture the complementary information brought by the given video sequence. Then a bilateral smoothing is applied to remove noises whie keeping edges. The generated 3D faces from the Kinect based video sequences have demonstrated comparable accuracy w.r.t. laser scanner based 3D faces [134]. Nevertheless, the averaging strategy used here might not be the optimal solution for 3D face modelling; more advanced techniques can be applied so as to yield potentially more accurate results. The videos recorded in our database can therefore serve as a standard dataset to evaluate the

quality of 3D face models generated by different algorithms.

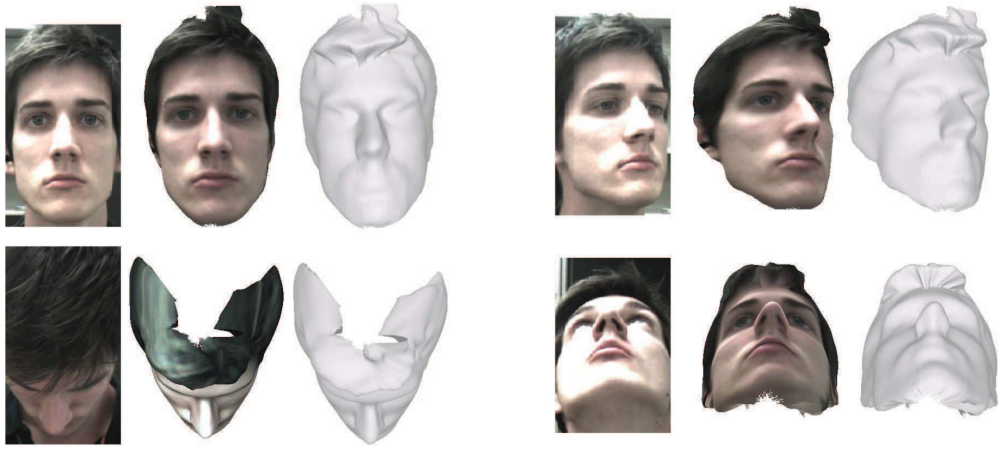

Figure 9.8: An example of a 3D face model generated using a video of cooperative head movement (images taken from [56]).

In addition to above discussed applications, other possible usages include but not limited to: head pose estimation, facial expression analysis, face registration, RGB-D feature extraction, occlusion detection and plastic surgery.

9.4 Benchmark Evaluations

In this section, we provide the benchmark evaluation results on the proposed Kinect-FaceDB using standard face recognition methods. The benchmark evaluation is conducted for 2D, 2.5D, and 3D based face recognition. For 2D and 2.5D based face recognition, PCA [12], LBP [4] , SIFT [85], and LGBP [140] based methods are tested. For 3D based face recognition, both the rigid method based on ICP [93] and the non-rigid method based on TPS [39] are evaluated. In order to show that the integration of the RGB data and the depth data can improve the recognition results, we also provide the fusion results from both the RGB and depth images using score-level fusion. Details and results of the benchmark evaluation are provided in the following sections.

9.4.1 Baseline Techniques and Settings

PCA (i.e., the Eigenface method), LBP, SIFT, and LGBP based methods are selected as the baseline techniques for the 2D and 2.5D based face recognition. For 2D face recognition, the methods are applied to the RGB images; whereas in 2.5D face recognition, the depth images are used. In PCA based method, the training data are used to build a low dimensional face subspace, in which the face recognition is performed. For LBP based method, the operator $LBP^{u2}_{8,2}$ is used to summarize

features on 8×8 blocks. SIFT based method extracts the key points from all training and testing images, for which the similarity measure is achieved by key points matching. In LGBP based method, the Gabor features are firstly computed, and then the LBP operator is applied to extract features on the Gabor filtered images. The fusion of RGB and depth images are achieved by directly extending the baseline techniques to use multiple modalities via score-level fusion.

Two representative 3D face alignment techniques (i.e., the ICP based rigid registration [13], [24] and the TPS based non-rigid registration [36]) are used in 3D face recognition. In the ICP based method [93] , the volume difference based on Euclidean distance between two 3D meshes are computed as the dissimilarity measure in face recognition after the rigid alignment by ICP. For TPS based method, we tested the method proposed in [39] (which is the baseline method in the European project Tabula Rasa (EU FP7) [111]), that computes the warping parameters (WPs) based on the non-rigid TPS alignment after the rigid ICP-registration. The final face representation of the TPS based method thus can be regarded as the deviations of a 3D face from a common geometric structure. Distances between the WPs of the probe face and the pre-calculated WPs of the gallery faces are computed for identification/verification by taking the mean cosine distance.

9.4.2 Pre-processing

Because the RGB data and the depth data in our KinectFaceDB are already aligned, given the facial landmarks, face cropping and normalization can be easily accomplished. Using the eye coordinates, we cropped, normalized, and down-sampled the 2D and 2.5D faces into 96×96 dimensions.

The 3D face cropping is achieved by preserving the vertices in a sphere with the radius of $100mm$, which are centred at $20mm$ away from the nose tip in the +z direction. Afterwards, spikes are removed by thresholding and a hole filling procedure is applied (the holes and spikes are interpolated linearly to form a complete mesh, the values to fill holes and spikes are estimated by taking the mean of valid pixels in the neighbourhood of a 5×5 patch). Finally, a bilateral smoothing filter is employed to remove the white noises while preserving the edges (the example of pre-processed 3D face from the Kinect can be found in Figure 9.6).

9.4.3 Evaluation Protocol

We consider both the identification and verification modes in the benchmark evaluation. In both modes, we use the neutral faces from session 1 as the gallery face. Recognition results of each variation (except for the left/right profiles, since sophisticated face alignment is needed in both the 2D and 2.5D based recognition under large pose variations) from both session 1 and session 2 are calculated. Then the overall identification/verification rates are reported for all tested facial variations in

both sessions. In our evaluation, the rank-1 identification rate and the verification rate where the false acceptance rate (FAR) equals to 0.001 are reported.

The ROC (receiver operating characteristic) curves of PCA based method for both 2D and 2.5D based face recognition are shown in Figure 9.9. In the figure, it is clear that different facial variations lead to different verification results, and the time-elapsing between the two sessions also significantly affect the recognition performance.

9.4.4 Evaluation Results

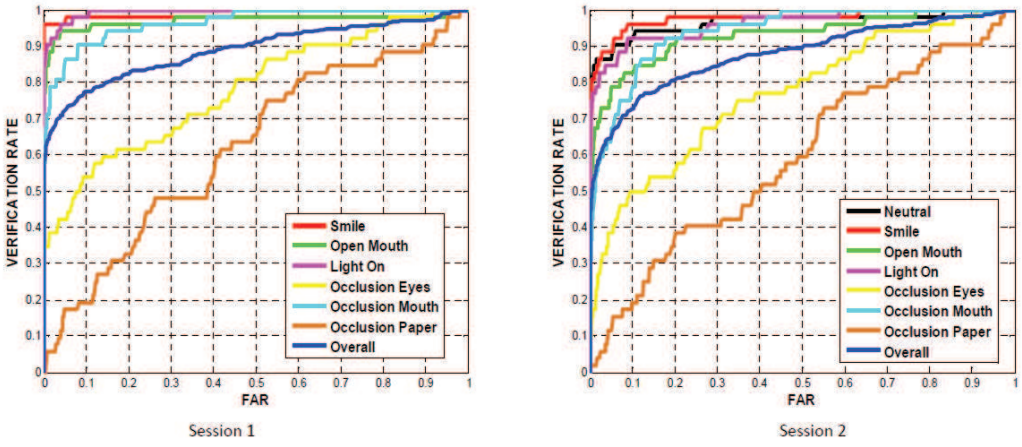

(a) ROC curves of 2D Face Verification using PCA

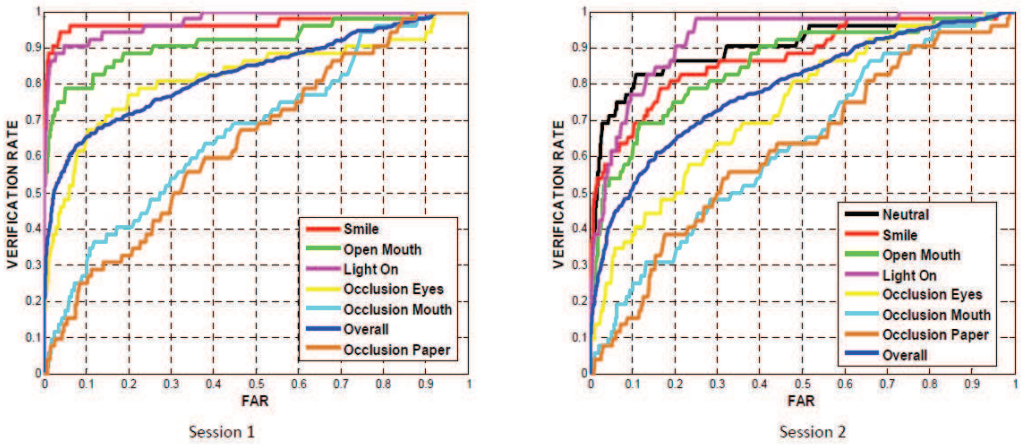

(b) ROC curves of 2.5 D Face Verification using PCA

Figure 9.9: The ROC curves of 2D and 2.5D based face recognition using PCA for different facial variations.

9.4.4.1 Results of 2D Face Recognition

Table 9.2 and 9.3 show the identification rates and the verification rates of 2D face recognition results using PCA, LBP, SIFT, and LGBP under different facial variations for the two sessions. As can be observed in the table, PCA is not robust to large local distortions (such as the extreme facial expressions and the partial occlusions), since the local distortions can alter the entire face representation in the PCA space. In the contrary, because LBP, SIFT, and LGBP are local based methods, they are more robust to such local distortions.

In the table, it can be observed that the partial occlusions (i.e., sunglasses, hand on face, and paper on face) are very challenging to all tested methods, especially in the verification mode. Nevertheless, LGBP based method is more robust to partial occlusions in comparison to the other methods, and gives the best overall performances. This result conforms to the findings in [140], where the authors suggested that the multi-resolution/multi-orientation based Gabor decomposition and the local patch based representation of LGBP can enhance the robustness in presence of partial occlusions.

Table 9.2: Rank-1 Identification Rate for 2D Face Recognition.

Session	Method	Neutral	Smile	Open mouth	Illu-mination	Sun-glasses	Hand on face	Paper on face	Overall
Session 1	PCA	N/A	96.15%	78.85%	90.38%	38.46%	73.08%	7.69%	64.10%
	LBP	N/A	**100%**	96.15%	**100%**	90.38%	**100%**	67.31%	92.31%
	SIFT	N/A	**100%**	96.15%	88.46%	84.62%	94.23%	57.69%	86.86%
	LGBP	N/A	**100%**	**98.08%**	98.08%	**92.31%**	98.08%	**78.85%**	**94.23%**
Session 2	PCA	82.69%	78.85%	67.31%	73.08%	19.23%	51.92%	1.92%	53.57%
	LBP	**100%**	98.08%	**94.23%**	**100%**	**92.31%**	94.23%	57.69%	90.93%
	SIFT	98.08%	98.08%	86.54%	78.85%	57.69%	82.69%	17.31%	74.18%
	LGBP	**100%**	**100%**	92.31%	**100%**	88.46%	**100%**	**84.62%**	**95.05%**

Table 9.3: Verification Rate ($FAR = 0.001$) for 2D Face Recognition.

Session	Method	Neutral	Smile	Open mouth	Illu-mination	Sun-glasses	Hand on face	Paper on face	Overall
Session 1	PCA	N/A	96.15%	76.92%	84.62%	34.62%	51.92%	0%	58.01%
	LBP	N/A	96.15%	90.38%	96.15%	**88.46%**	92.31%	40.38%	**75.96%**
	SIFT	N/A	**100%**	88.46%	73.08%	61.54%	78.85%	5.77%	43.59%
	LGBP	N/A	**100%**	**92.31%**	**98.08%**	80.77%	**94.23%**	**57.69%**	71.79%
Session 2	PCA	73.08%	61.54%	51.92%	55.77%	7.69%	26.92%	1.92%	40.11%
	LBP	92.31%	82.69%	73.08%	88.46%	65.38%	67.31%	17.31%	59.34%
	SIFT	90.38%	84.62%	48.08%	57.69%	30.77%	59.62%	0%	38.74%
	LGBP	**96.15%**	**94.23%**	**84.62%**	**96.15%**	**67.31%**	**82.69%**	**42.31%**	**61.26%**

9.4.4.2 Results of 2.5D Face Recognition

Table 9.4 and 9.5 illustrate the evaluation results on 2.5D face data. Although previous studies (according to [18]) suggested to directly apply PCA on the 2.5D range images, results of PCA based method in our experiment is not as good as the ones obtained with LBP and LGBP, especially for large facial variations. On the other hand, LBP yields the best overall identification/verification results on the depth images in both sessions (even if LBP was primarily designed as a texture description). Unlike the results for 2D face recognition, the Gabor features used in LGBP cannot improve the recognition results based on LBP. It should be noted that the SIFT based method cannot yield meaningful results on the depth images. This is because the SIFT algorithm identifies key points at the salient gradient locations of an image. Since the depth map is highly smooth, the SIFT based method is inappropriate for 2.5D based face recognition.

From the experiment, our results suggest that the LBP based method (as well as its depth-specific variants such as [57, 58]) are more appropriate to represent and discriminate depth face patterns. It should be noted that the use of 2.5D depth maps give worse results than the use of 2D intensity images (for all tested methods). This is because the depth scanning quality by the Kinect is relatively low. Nevertheless, the depth map can supply complementary information in addition to the intensity image, and therefore can be integrated with the 2D based method as a multi-modal face recognition system, which generates higher recognition rates. We demonstrate the combination of 2D and 2.5D information in Section 9.4.5 based on score-level fusions.

Table 9.4: Rank-1 Identification Rate for 2.5D Face Recognition.

Session	Method	Neutral	Smile	Open mouth	Illumination	Sunglasses	Hand on face	Paper on face	Overall
Session 1	PCA	N/A	84.62%	57.69%	76.92%	36.54%	7.69%	5.77%	44.87%
	LBP	N/A	**94.23%**	**84.62%**	**96.15%**	**84.62%**	65.38%	19.23%	**74.04%**
	SIFT	N/A	7.84%	3.92%	7.84%	0%	1.96%	1.96%	1.63%
	LGBP	N/A	90.38%	82.69%	94.23%	59.62%	**69.23%**	**44.23%**	73.40%
Session 2	PCA	46.15%	42.31%	36.54%	30.77%	13.46%	5.77%	0%	25%
	LBP	**92.31%**	73.08%	**80.77%**	**94.23%**	**73.08%**	**38.46%**	5.77%	**65.38%**
	SIFT	5.88%	1.96%	0%	5.88%	3.92%	0%	3.92%	1.12%
	LGBP	80.77%	**75%**	65.38%	78.85%	34.62%	**38.46%**	**25%**	56.87%

9.4.4.3 Results of 3D Face Recognition

In addition to the direct usage of 2.5D depth maps, the use of 3D surface registration algorithms (such as ICP and TPS) for 3D face is a popular approach for 3D face recognition [3, 18]. In this chapter, we tested two 3D face recognition methods based on ICP and TPS on the proposed KinectFaceDB, respectively. Table 9.6 and 9.7 show the face identification and verification results. In the table, we can observe

Table 9.5: Verification Rate ($FAR = 0.001$) for 2.5D Face Recognition.

Session	Method	Neutral	Smile	Open mouth	Illu-mination	Sun-glasses	Hand on face	Paper on face	Overall
Session 1	PCA	N/A	67.31%	38.46%	48.08%	15.38%	0%	0%	17.95%
	LBP	N/A	75%	**75%**	**78.85%**	**34.62%**	19.23%	1.92%	**41.03%**
	SIFT	N/A	1.96%	0%	0%	0%	0%	0%	0.33%
	LGBP	N/A	**76.92%**	69.23%	57.69%	28.85%	**36.54%**	**3.85%**	36.86%
Session 2	PCA	21.15%	15.38%	15.38%	17.31%	7.69%	0%	0%	8.52%
	LBP	**55.77%**	34.62%	15.38%	**34.62%**	**23.08%**	**11.54%**	**5.77%**	**26.92%**
	SIFT	0%	0%	0%	0%	0%	0%	0%	0%
	LGBP	46.15%	**50%**	**23.08%**	**34.62%**	7.69%	**11.54%**	1.92%	26.37%

that face recognition based on the 3D points cloud is more robust to certain type of variations (e.g., the time-elapsing for neutral faces) than the 2.5D depth based methods. However, it generates inferior results for facial expression and occlusion variations. The results indicate that although 3D registration methods can better align different faces in the recognition, it is difficult to handle large local facial distortions. Therefore, high-order local patch based features (such as LBP, LGBP, or curvature descriptors) are preferred to achieve more robust 3D/2.5D face recognition results for the Kinect data.

In the table, the TPS based method generates better recognition results in most cases than the ICP based method. This is because the non-linear alignment acted by TPS can partially handle the facial expression problem to some extent (which conforms to the results in [39]). Nevertheless, none of the methods can handle the partial occlusion problem. For faces occluded by hand and paper, the large surface distortions completely mislead the face registration (thus we do not report the results for paper on face, which are meaningless for 3D face recognition). In addition, as shown in our experiment, the tested methods cannot yield reliable results for the verification task using low quality Kinect data.

Table 9.6: Rank-1 Identification Rate for 3D Face Recognition.

Session	Method	Neutral	Smile	Open mouth	Illu-mination	Sunglasses	Overall
Session 1	ICP	N/A	**63.46%**	26.92%	51.92%	**50%**	38.46%
	TPS	N/A	59.62%	**47.06%**	**71.15%**	38.46%	**44.53%**
Session 2	ICP	46.15%	42.31%	23.08%	44.23%	38.46%	32.37%
	TPS	**78.85%**	**46.15%**	**38.46%**	**67.31%**	**53.85%**	**48.70%**

9.4.4.4 General Remarks

In addition to the occlusions used in previous works (e.g., [27,91,118]), we introduce a novel facial occlusion in the KinectFaceDB (namely paper on face). Comparing with

Table 9.7: Verification Rate ($FAR = 0.001$) for 3D Face Recognition.

Session	Method	Neutral	Smile	Open mouth	Illu-mination	Sunglasses	Overall
Session 1	ICP	N/A	**26.92%**	1.92%	26.92%	**13.46%**	**16.92%**
	TPS	N/A	19.23%	**23.53%**	**28.85%**	7.69%	12.11%
Session 2	ICP	23.08%	**25%**	1.92%	15.38%	**17.31%**	14.42%
	TPS	**32.69%**	17.31%	**15.38%**	**28.85%**	**17.31%**	**19.81%**

the traditional partial occlusions (e.g., sunglasses and hand on face), the occlusion of paper on face is very challenging in face recognition according to the results we obtained. In this variation, only the left half of a face is visible. Although previous studies suggest that only half of a face [54] can provide sufficient information for face recognition (due to the face symmetry), the paper occlusion introduces large, non-uniform noise so that it needs to be deliberately handled. This controlled occlusion is similar to many occlusion cases encountered in crowded scenes. In addition, the facial asymmetry is also lost in this occlusion, which can also provide useful clues for face recognition [84]. For a possible solution, as suggested in [96], explicit occlusion analysis could be useful to remove the features extracted from the occluded part (i.e., the paper), so as to improve the recognition results by only taking into account the non-occluded facial part.

9.4.5 Fusion of RGB and Depth Face Data

To justify that the Kinect is more helpful than sole RGB based cameras for face recognition, we conduct an additional fusion step to combine both the RGB (2D) and the depth (2.5D) face information from the Kinect in face recognition. The weighted sum fusion strategy is thus adopted for this purpose, where the z-score normalization is first applied to the dissimilarity scores of both matchers (of RGB and depth). In our experiment, the weights are determined by grid search on all the gallery and probe faces.

Table 9.8 and 9.9 illustrate the fusion results from both the RGB and depth using PCA, LBP and LGBP (SIFT is not used because it cannot capture the correct information from depth images as shown in Section 9.4.4.2). From the results, it is clear that the fusion process significantly improve the results from sole RGB based face recognition. For example, the overall rank-1 identification rate of Session 1 is increased from 64.10% to 76.92%, 92.32% to 97.12%, and 94.23% to 96.79% for the PCA, LBP and LGBP based methods, respectively. This experiment demonstrates that 3D information provided by the Kinect can greatly reinforce the recognition performance from its 2D images.

Table 9.8: Fusion of RGB and Depth for Face Recognition Rank-1 Identification Rate.

Session	Method	Neutral	Smile	Open mouth	Illu-mination	Sun-glasses	Hand on face	Paper on face	Overall
Session 1	PCA	N/A	96.15%	88.46%	**100%**	59.62%	78.85%	38.46%	76.92%
	LBP	N/A	**100%**	98.08%	**100%**	**92.31%**	**98.08%**	**94.23%**	**97.12%**
	LGBP	N/A	**100%**	**100%**	**100%**	90.38%	**98.08%**	92.31%	96.79%
Session 2	PCA	82.69%	82.69%	71.15%	90.38%	46.15%	57.69%	30.77%	65.93%
	LBP	**100%**	**100%**	**98.08%**	98.08%	**94.23%**	94.23%	69.23%	93.41%
	LGBP	**100%**	**100%**	96.15%	**100%**	88.46%	**98.08%**	**76.92%**	**94.23%**

Table 9.9: Fusion of RGB and Depth for Face Recognition Verification Rate ($FAR = 0.001$).

Session	Method	Neutral	Smile	Open mouth	Illu-mination	Sun-glasses	Hand on face	Paper on face	Overall
Session 1	PCA	N/A	96.15%	84.62%	90.38%	30.77%	51.92%	0%	58.65%
	LBP	N/A	**100%**	92.31%	98.08%	**90.38%**	92.31%	15.38%	83.65%
	LGBP	N/A	**100%**	**94.23%**	**98.08%**	76.92%	**98.08%**	**55.77%**	**86.22%**
Session 2	PCA	75%	71.15%	46.15%	71.15%	5.77%	19.23%	1.92%	41.48%
	LBP	**96.15%**	80.77%	71.15%	92.31%	**63.46%**	69.23%	19.23%	73.63%
	LGBP	94.23%	**90.38%**	**88.46%**	**96.15%**	61.54%	**78.85%**	**46.15%**	**78.57%**

9.5 Data Quality Assessment of KinectFaceDB and FRGC

It is straightforward to visually observe the 3D data quality differences between the Kinect and a high quality laser scanner (e.g., the Minolta, see Figure 9.6). The scanner parameters such as the depth accuracy and depth resolution also indicate the significant data quality difference between the two sensors. Recently, additional efforts have been made to better understand the Kinect's accuracy [65]. However, it is not obvious to quantify the exact data quality differences in the context of face biometrics. Nevertheless, it is an essential issue to evaluate the identification/verification differences of 2.5D/3D faces captured by the Kinect and Minolta, in order to allow the deployment of practical face recognition systems using the Kinect by the state-of-the-art 2.5D/3D face recognition algorithms (whose results were reported based on the data captured by high quality laser scanners (e.g., the Minolta) in the literature (such as the data in the FRGC database).

Following the same protocol as described in section 9.4.3, we tested different 2.5D/3D face recognition algorithms (PCA, LBP, and LGBP based methods using 2.5D depth images; ICP and TPS based methods using 3D point clouds) on both the KinectFaceDB and the FRGC. For KinectFaceDB, we use all neutral faces in session 1 as the gallery faces and the corresponding neutral faces from session 2 as the probe faces. Similarly, we select 2 neutral faces from 2 different sessions of 198 subjects (from FRGC ver.1) to form the gallery and probe set of FRGC re-

spectively. In both databases, the rank-1 identification rates and verification rates (where $FAR = 0.001$) are reported for comparison.

Table 9.10 shows the comparative results on the KinectFaceDB and the FRGC. In the figure, the results of FRGC are significantly better than the results of KinectFaceDB for all tested methods. It should be noted that the result differences in the verification mode are much larger than the ones in the identification mode. This suggests that the Kinect is more appropriate for the non-cooperative face identification, whereas high quality laser scanner is more suitable for the verification mode which demands more user cooperation. For FRGC, the TPS based method using 3D yields better recognition rates than the 2.5D based methods (i.e., PCA, LBP, and LGBP). On the other hand, for KinectFaceDB, 2.5D LBP achieves much better recognition rates than the 3D based methods (i.e., ICP and TPS). This is because the low data quality of Kinect can significantly affect the sophisticated face registration procedures of TPS based method, so as to greatly deteriorate the final recognition results. This phenomena suggests that a simple yet efficient depth descriptors using 2.5D depth images is preferred for the Kinect based face recognition in comparison to the methods using sophisticated surface registration based on 3D points.

Table 9.10: KinectFaceDB vs. FRGC

Mode	DB	2.5D PCA	2.5D LBP	2.5D LGBP	3D ICP	3D TPS
Rank-1	KinectFaceDB	46.15%	**92.31%**	80.77%	46.15%	78.85%
Id. Rate	FRGC	68.18%	93.94%	93.94%	58.08%	**96.97%**
Ver. Rate	KinectFaceDB	21.15%	**55.77%**	46.15%	23.08%	32.69%
($FAR = 0.001$)	FRGC	53.54%	81.82%	83.33%	39.90%	**87.37%**

Although the 2.5D/3D face recognition capability of the Kinect is inferior than the ones of a high quality laser scanner, the intrinsic advantages of the Kinect make it as a competitive sensor in real world applications. We summarize its merits for face recognition as follows: (1) it works in real time, which allows online face enrolment in non-cooperative scenarios; (2) its 3D data provides complementary information to the 2D data, and can be easily integrated in a multi-modal based face recognition; (3) with a short period of video recording (e.g., a few seconds), 3D face recognition in video is feasible and can potentially improve recognition rates in comparison to 3D face recognition based on still images.

Besides its advantages in comparison to the traditional 3D sensors, it should be noted that the Kinect sensor is limited in dealing with long-distance capturing such as in the surveillance scenario. Instead, it is more suitable for face identification/verification tasks in the office/indoor environment for PC operators, or game players. In such circumstances, users are not required to cooperate in the data acquisition

procedure. On the other hand, traditional 3D laser scanners (which cannot handle long-distance capturing too) require the user to cooperate in the capturing procedure for several seconds.

With the increasing interests on the Kinect sensor, we suggest that newly developed 2.5D/3D or 2D+3D face recognition algorithms should not only be tested on databases with high quality scans (such as the FRGC database), but also on the more challenging KinectFaceDB, so as to make their methods more robust and reliable in more practical scenarios.

9.6 Conclusion

In this chapter, we presented a complete multi-modal (including well-aligned 2D, 2.5D, 3D and video based face data) face database based on the Kinect sensor. The database structure and acquisition environment are carefully described. The processes of how to obtain the well aligned and processed 2D, 2.5D, 3D and video face data are thoroughly introduced. We highlight the advantages of the proposed KinectFaceDB (as well as the Kinect based face recognition) via the review of existing 3D face databases and extensive experimental evaluations. In addition, multiple potential applications of the proposed KinectFaceDB are also discussed. Standard face recognition techniques (including PCA, LBP, SIFT, LGBP, ICP, and TPS) are applied on different data modalities (including 2D, 2.5D, and 3D based face data), and score-level fusion is conducted to demonstrate the performance gain from the integration of depth and RGB. Quantitative comparison (in the context of biometrics) of the proposed KinectFaceDB and the state-of-the-art FRGC database is provided, which can guide the deployment of existing algorithms and the development of new face recognition methods toward more practical systems.

To conclude, the proposed KinectFaceDB supplies a standard medium to fill the gap between traditional face recognition and the emerging Kinect technology. As a future work, it is necessary to revisit the literature on 3D and 2D+3D face recognition algorithms (which were mostly elaborated with high quality 3D face data) using the proposed KinectFaceDB for achieving reliable, robust and more practical face recognition system using the Kinect. The design of new algorithms and new facial descriptors for the low-quality 3D data is another important topic to investigate. In addition, 3D face recognition using video data is a new prospect, where more evaluations will be conducted using the video data from the Kinect in the future. Finally, how to efficiently combine (e.g., via fusion, co-training) different data modalities (RGB, depth and 3D) so as to maximize the exploitation of the Kinect for face recognition should also be studied.

Chapter 10

Conclusions and Future Perspectives

10.1 Summary

Although face recognition has been investigated extensively, it still suffers from variations due to various factors in real-world scenarios. Each day, 3D sensing technologies advance and the acquisition devices become more accurate and less expensive. 3D face recognition evades illumination and pose problems, however there are still challenges such as spoofing attacks or disguise variations which affect the performances of both 2D and 3D face recognition.

In this thesis, we have investigated spoofing attacks and disguise variations in face recognition and proposed countermeasure techniques for the protection of face recognition systems against these challenges.

In the first part of the thesis, we have explored the topic of spoofing in face recognition. Spoofing is a very new topic for researchers in face biometrics domain. Therefore studies on this topic are limited.

It has been shown that face recognition systems are vulnerable to photograph and video attacks. This is why, countermeasure techniques are necessary to mitigate the impact of spoofing on face recognition. In Chapter 3, we proposed a countermeasure technique, which is based on texture and contrast analysis, for the detection of photograph attacks.

Compared to 2D spoofing attacks such as photograph and video, 3D mask attacks to face recognition systems is a considerably new subject. The main reason for the delay in mask spoofing studies is due to the unavailability of public mask databases. In Chapter 4, we analyzed the impact of mask attacks on both 2D and 3D face recognition in detail. For our studies, we used the mask database which is prepared by MORPHO [98] within the context of the European Union (EU) research project TABULA RASA [111]. This database includes many high-quality mask samples. In addition to texture images, it includes 3D scans for both real and mask samples. Thanks to the nature of this database, we were able to conduct the benchmark evaluations for both 2D and 3D face recognition. The results show that existing systems are vulnerable to spoofing attacks. Especially the performance of 3D face

recognition systems deteriorate considerably when high quality masks are used for spoofing purposes.

In Chapter 5, we analyzed several characteristics of masks and real faces such as texture, reflectance and smoothness characteristics. We developed four different countermeasure techniques for the detection of mask attacks. All these countermeasures provide significant detection accuracies alone. However we observed that fusion of these countermeasures further improves the results. We obtained 99% classification accuracy for masks and real samples by fusion in this study.

Second challenge for face recognition systems explored in this study is disguise variations. There are several types of disguise variations such as variations due to facial cosmetics, plastic surgery, facial alterations, beard, moustache, hair style, aging and wrinkles. The impact of each of these disguise variations on face recognition systems is different. In this study, we have explored variations due to facial alterations, occlusions and facial cosmetics.

In Chapter 6, we show the impact of facial alterations on face recognition. For this purpose, we prepared a simulated nose alteration database using FRGC v1.0. Then we evaluated the impact of facial alteration on both 2D and 3D face recognition and observed that although the performances of both modalities deteriorate, the performance decrease is more for 3D compared to 2D face recognition.

In Chapter 7, we proposed a new block based face recognition approach which increases the performance significantly in the existence of nose alterations. The advantage of this approach is that it can be used for all types of alterations applied on face. Today, more and more people undergo plastic surgeries not only for medical reasons but also to improve their appearance or even to hide their true identity. In order to increase recognition performance in the existance of plastic surgery operations on face, this proposed block based approach is very beneficial.

Makeup products are within reach of everyone who seeks ways to evade recognition or for beauty purposes. This is why, in Chapter 8, we analyzed the impact of makeup on face recognition. For this purpose, we prepared an extensive makeup database. The impact of makeup on face recognition is analyzed in detail. The results show that existing recognition systems are vulnerable to facial makeup and especially makeup on eye region affects recognition performance significantly.

Finally, in the last chapter, in order to establish the connections between the Kinect sensor and face recognition, the first publicly available face database based on the Kinect sensor for face recognition is presented. The database consists of different data modalities and multiple facial variations such as occlusions, expression, illumination. We conduct benchmark evaluations on the proposed database using standard face recognition methods, and demonstrate the performance gain by inte-

grating the depth data with the RGB data via score-level fusion. We also compare the Kinect images with the traditional high quality 3D scans (of the FRGC database) in the context of face biometrics, which demonstrates the imperative needs of the proposed database for face recognition.

10.2 Future Work

To start with, spoofing is a very new topic in face recognition domain hence the number of studies regarding spoofing (including anti-spoofing) is still very limited. In this thesis, we proposed several countermeasures for the detection of 3D mask attacks and obtained almost perfect classification accuracy of 99%. The limitation of our study is that we were able to test the performances of the proposed countermeasures using the masks made from one type of material, which is polychrome mineral powder. When masks made from different materials are used, we may obtain different performance accuracies. Our future works are initially, to test the performances of the proposed countermeasures using masks made from different materials in order to observe if we can still obtain satisfactory results, and then to propose new countermeasures for more challenging mask databases with higher number of subjects as soon as available.

For our study regarding facial alterations, due to the lack of publicly available 3D plastic surgery databases, we prepared a simulated nose alteration database in order to observe the impact of plastic surgery operations on face recognition. As a future work, our aim is to test the proposed block based face recognition approach, which was tested for nose alteration in Chapter 7, on a real 3D plastic surgery database. Furthermore, in our studies, we were able to test the performance of the block based face recognition approach only in the existance of nose alterations. Our future work is to test the performance of this technique in the existance of other facial alterations in order to demonstrate that our approach is beneficial for all types of plastic surgery operations. Although, the proposed approach is robust and provides significant recognition performances in the existance of facial alterations, as a future work, our aim is to propose more robust techniques against facial alterations.

3D face recognition techniques are robust to facial makeup since makeup does not change the 3D shape. However, our analysis show that facial makeup has a significant impact on 2D face recognition performance. Up to now, there have been studies on the impact analysis of makeup on face recognition, however techniques which mitigate this impact have not been explored. Our future works are to detect facial makeup and investigate robust techniques against facial makeup.

Finally, in the last chapter, benchmark evaluations are conducted on the proposed Kinect face database. As a future work, we want to use this Kinect face database to develop robust techniques against occlusions. We also plan to use this database for

other tests such as gender recognition, the computation of higher quality 3D scans from video data available in this database.

Chapter 11

Résumé Etendu en Français

1. Introduction

Motivation

La reconnaissance des humains est devenue un sujet important puisque les besoins et les investissements pour les applications de sécurité augmentent continuellement. La biométrie permet de définir des systèmes fiable et efficace de gestion de l'identité à l'aide de l'utilisation de caractéristiques physiques et comportementales des sujets qui sont permanents, universels et facile d'accès. C'est pourquoi, le thème de la biométrie attire davantage d'attention de nos jours.

Chaque biométrie a ses propres avantages et inconvénients. Par exemple, la biométrie d'empreintes digitales est la plus répandue, mais elle requiert une collaboration forte de l'utilisateur. De même, la reconnaissance de l'iris est très précise, mais elle dépend fortement de la qualité de l'image et également requiert la participation active des sujets.

La reconnaissance faciale est avantageuse en termes d'accessibilité et de fiabilité. Elle permet l'identification pour les sujets non informés qui n'ont pas à coopérer.

Bien que la reconnaissance faciale a été examinée intensivement, elle souffre encore de variations en raison de divers facteurs dans les scénarios du monde réel.

Dans cette thèse, deux défis en reconnaissance faciale sont analysés à savoir le leurrage et le camouflage. Bien que ces défis affectent les performances des systèmes de la reconnaissance faciale 2D et 3D, les études sur ces sujets sont limitées.

Lors d'une tentative du leurrage, une personne tente de se faire passer pour une autre personne et par ce moyen, tente d'accéder à un système de reconnaissance. Puisque les données de visage peuvent être acquis facilement sans contact, le leurrage est une menace réelle pour les systèmes de reconnaissance faciale. En raison du nombre limité d'études sur ce sujet, de nos jours, le leurrage (y compris l'anti-leurrage) est un sujet très populaire pour les chercheurs dans le domaine de la reconnaissance faciale.

Il a été démontré que les systèmes de reconnaissance faciale sont vulnérables à des attaques de photographie et vidéo. L'objectif est de développer des contremesures

nonintrusives sans dispositifs supplémentaires et sans l'intervention humaine qui peuvent être intégrés dans les systèmes de reconnaissance faciale existants afin de les protéger contre les attaques de leurrage.

Par rapport à des attaques du leurrage 2D comme la photographie et la vidéo, les attaques des systèmes de la reconnaissance faciale à l'aide de masques 3D est un sujet nouveau. La principale raison du retard dans les études du leurrage avec masque est dû à l'indisponibilité des bases de données publiques. La préparation d'une base de donées de masques est beaucoup plus difficile et plus coûteuse que la préparation de bases de données de photographies ou vidéo. Initialement, pour préparer un masque de haute qualité, un scanner 3D est nécessaire pour obtenir le modèle 3D de la personne cible, qui est généralement des dispositifs coûteux. La procédure se poursuit avec la fabrication des masques qui est également une proédure coûteuse.

Dans cette thèse, la motivation principale est de développer des techniques de contre-mesures afin de protéger les systèmes de reconnaissance faciale contre les attaques de leurrage. Pour cette raison, nous avons examiné le leurrage faciale 2D et 3D.

Nous avons d'abord analysé les attaques de leurrage 2D, qui peuvent être réalisées en utilisant des photographies ou des vidéos. Nous avons proposé une nouvelle technique de contre-mesure [72] pour la détection des attaques avec photographies. Cette étude a été notre étude préliminaire dans le domaine du leurrage faciale.

Ensuite, nous avons examiné les attaques avec masque 3D. Nous avons montré les vulnérabilités des systèmes de reconnaissance faciale 3D et 2D à des attaques avec masque. Les résultats de cette étude montrent que les systémes de reconnaissance existants ne sont pas robustes contre les attaques avec masque, et les contre-mesures doivent être développés pour atténuer l'impact de ces attaques.

Pour cette raison, nous avons analysé plusieurs caractéristiques des masques et des échantillons du visage réels comme la texture, la reflectance et la continuité, et nous avons développé plusieurs techniques de contre-mesures. Nous avons également intégré la contre-mesure offrant la meilleure performance dans le système de reconnaissance faciale 3D retenu afin de montrer l'amélioration de la performance avec la contre-mesure.

Les accessoires de camouflage peuvent être utilisés pour modifier l'apparence d'un individu, à se faire passer pour une autre personne, ou à cacher son identité. Bien que la reconnaissance faciale avec des variations de camouflage est un défi majeur, les études sur ce sujet sont limitées. Dans cette thèse, des variations dues à des altérations faciale, à du maquillage et à des accessoires faciale sont examinées.

Depuis que la chirurgie plastique est devenue plus avancée et abordable, elle présente de nouveaux défis pour les systèmes de reconnaissance faciale. Il n'y a pas de base

de données en chirurgie plastique 3D accessible au public. Pour cette raison, nous avons préparé une base de données de modification de nez (2D+3D) simulé, dans lequel le nez de chaque personne est remplacé par un autre choisi au hasard. Dans notre étude, nous avons démontré la chute des performances en reconnaissance pour les deux modalités, en particulier pour la 3D, en présence d'altérations du nez. C'est pourquoi, ensuite, nous avons proposé une approche en reconnaissance faciale, qui réduit l'impact des modifications faciale en reconnaissance faciale.

Le maquillage faciale change l'apparence perçue d'un visage peut donc avoir un impact en reconnaissance faciale. Méme si le maquillage ne change pas les caractéristiques de la forme 3D d'un visage, il a un impact sur la reconnaissance faciale 2D. Afin d'évaluer l'impact en détail, nous présentons une base de données en maquillage, qui comprend de nombreux échantillons annotés comme le non-maquillage, le maquillage léger et le maquillage appuyé.

Enfin, dans cette thèse, nous présentons une base de données Kinect, qui est la premiére base de données du visage publique acquise par le caméra Kinect. Le capteur Kinect est moins chere par rapport aux scanners de haute qualité, et offre des performances en reconnaissance significatifs. L'évaluations de référence ont été menées sur la base de données proposée pour plusieurs variantes comme les occultations, l'expression et l'éclairage.

Contributions Originales

Les contributions originales de cette thèse peuvent être résumées en huit points: l'analyse d'impact du leurrage avec masque sur les systèmes existants en reconnaissance faciale, plusieurs contre-mesures pour détecter les attaques avec masque et photographie, une base de données de modification simulée de nez, une approche robuste de modifications du visage, une vaste base de données du visage des maquillés, une vaste base de données du visage Kinect, et plusieurs évaluations de référence pour montrer les performances des techniques en utilisant les données Kinect.

Plan

Le plan de la thèse est la suivant:

- Dans le chapitre 2, nous donnons une introduction au leurrage et aux variations de camouflage et examinons l'état de l'art pour les travaux pertinents.
- Dans le chapitre 3, notre technique de contre-mesure, qui est utilisée pour protéger les systèmes en reconnaissance faciale contre les attaques avec photographie, est présentée.
- Dans le chapitre 4, l'impact du leurrage avec masque en reconnaissance faciale 2D et 3D est évaluée.

- Dans le chapitre 5, nos techniques de contre-mesures, qui sont utilisées pour protéger les systèmes en reconnaissance faciale contre les attaques avec masque 3D, sont présentées.
- Dans le chapitre 6, l'impact des modifications du visage (altération nez en particulier) en reconnaissance faciale 2D et 3D est analysé.
- Dans le chapitre 7, une approche de la reconnaissance faciale, robuste aux altérations du visage, est proposée.
- Dans le chapitre 8, nous présentons d'abord une base de données lieé au maquillage. Ensuite, nous analysons l'impact de la cosmétique en reconnaissance faciale.
- Dans le chapitre 9, une base de données de visages avec Kinect, qui comprend des modalités différentes et de nombreuses variations, est présentée. Nous effectuons des évaluations en utilisant des méthodes de reconnaissances faciales standards, et démontrons le gain en performance en intégrant les données de profondeur avec les données RGB via la fusion.
- Dans le chapitre 10, les conclusions et des perspectives sont fournis.

2. Leurrage et Camouflage

Dans cette section, nous avons expliqué les systèmes biométrique et avons donné une brève information sur la reconnaissance faciale.

Ensuite, dans cette section, le leurrage en reconnaissance faciale a été analysé en deux groupes : les attaques du leurrage 2D et les contre-mesures, et les attaques du leurrage 3D et les contre-mesures. L'état de l'art est fourni pour les deux groupes.

Enfin, dans cette section, plusieurs types de camouflage ont été décrits et une revue de la littérature sur les variations de camouflage a été présenté. Nous avons étudié principalement trois types des variations de camouflage qui sont des variations dues à des modifications du visage, du maquillage et des occultations (accessoires visage).

3. Contre-mesure Technique contre les Attaques avec Photographie

Dans ce chapitre, une nouvelle approche anti-leurrage, qui est basée sur l'analyse des caractéristiques de contraste et de la texture, est proposée pour détecter leurrage avec photo. Comme l'image de photo est une image acquise deux fois, elle peut montrer des caractéristiques de contraste et de texture trés différentes par rapport à une image réelle. La méthode locale LBPV est choisie dans cette étude pour l'extraction des caractéristiques. L'approche est testée sur la base de données de photo-imposteurs NUAA , qui inclure les changements d'éclairage et lieu. Les résultats montrent que l'approche est en concurrence avec d'autres méthodes existantes.

La technique est robuste aux changements d'éclairage, non-intrusive et simple.

La base de données NUAA [131], qui est l'une des rares bases de données photographiques accessibles au public, est sélectionnée pour cette étude. Elle est construite en utilisant une webcam standard. La Figure 11.1 montre les images originale et de photographie dans différentes sessions. La lieu et l'éclairage de chaque session est différente. Les ensembles de test et d'entrainement sont construits à partir de différentes sessions. La base de données comprend 15 sujets. À chaque séance, les images des deux sujets vivants et leurs photos sont capturées avec un taux de trame de 20 images par seconde. 500 images sont recueillies pour chaque sujet. Les images sont toutes frontale avec une expression neutre. Il n'y a pas de mouvements apparents comme des clignotants des yeux et mouvements de la tête. Par conséquent, les images capturées et les images recapturés ont plus de similitudes, ce qui rend la détection du leurrage plus difficile.

Afin d'évaluer les performances de la contre-mesure proposée sur la base de données NUAA, la contre-mesure proposée est appliquée en utilisant les modéles de LBPV.

Les résultats montrent que l'approche proposée, qui est basée sur l'analyse de la texture et du contraste, donne des résultats très satisfaisants dans la détection du leurrage avec photographie.

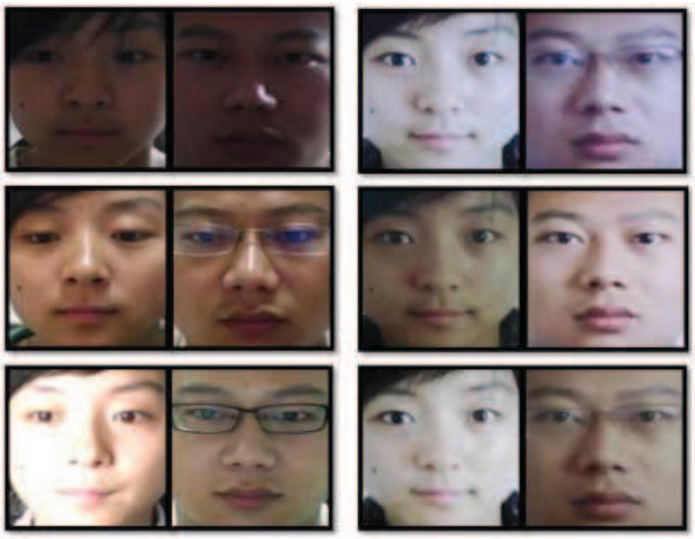

Figure 11.1: Chaque colonne contient des échantillons de la session 1, session 2 et session 3 de la base de données NUAA [131]. Dans chaque rangée, la paire gauche est d'un humain vivant et la paire droite d'une photo. Il contient diverses modifications (par exemple, le genre, l'éclairage, avec/sans lunettes). Illustration extraite de [131].

Il y a eu plusieurs études sur les techniques de contre-mesures pour la détection

des attaques avec photographie. Par rapport à des attaques en leurrage 2D comme la photographie et la vidéo, les attaques avec masque 3D est un sujet nouveau. L'impact des attaques avec masque 3D sur des systèmes de la reconnaissance existants a été d'abord analysé dans notre étude [74].

Dans le prochain chapitre de la thèse, nous montrons les vulnérabilités des systèmes de reconnaissance faciale à des attaques avec masque.

4. L'impact de Leurrage Masque sur la Reconnaissance Faciale

Il existe plusieurs types d'attaques en leurrage comme la photographie, vidéo ou masque. Au meilleur de nos connaissances, l'impact du leurrage masque sur la reconnaissance faciale a été analysée pour la toute premiére fois dans notre étude [74]. La raison de ce retard est principalement dû à l'absence de bases de données publiques avec masque. Dans cette étude, nous utilisons une base de données de masques 2D+3D qui a été préparé pour le projet de recherche Tabula Rasa [111]. Ce chapitre fournit de nouveaux résultats en démontrant l'impact des attaques avec masque sur les systèmes en reconnaissance faciale 2D et 3D. Les résultats montrent que les systèmes de reconnaissance faciale sont vulnérables aux attaques avec masque, donc les contre-mesures doivent être développées pour réduire l'impact des attaques avec masque en reconnaissance faciale. Les résultats montrent également que l'analyse de la texture 2D fournit plus d'informations que l'analyse de la forme du visage en 3D afin de développer des techniques de contre-mesures contre les attaques avec des masques de haute qualité.

Dans la base de données avec masque utilisée dans nos études, initialement, les scans des sujets dans la base de données ont été prises par un scanner 3D qui utilise une technologie de lumiére structurée. Le modèle 3D de chaque sujet a été envoyé à une imprimante 3D et les masques ont été fabriqués par impression 3D Sculpteo [110]. Le matérial utilisé pour les masques est polychromes poudre minérale, qui est de façon standard utilisée pour l'impression 3D.

Dans la base de données du masque, 20 sujets apparaissent au total. Les masques ont été fabriqués pour 16 de ces sujets. Pour les échantillons réels dans la base de données, une moyenne de 10 scans de chaque sujet a été acquis. Pour les échantillons de masque dans la base de données, une moyenne de 10 scans de chaque sujet portant soit son propre masque ou le masque du autres personnes qui apparaissent dans la même base de données ont été acquises. Enfin, 200 acquisitions réelles du visage à partir de 20 sujets et 198 acquisitions du masque de 16 masques sont utilisés pour les évaluations. La Figure 11.2 montre un exemple de cette base de données pour un accés vrai visage et l'accés d'attaque avec masque correspondant.

Afin d'analyser l'impact des attaques avec masque sur la reconnaissance faciale, la technique de WP [39] et la technique de LBP [4] sont sélectionnés pour la reconnais-

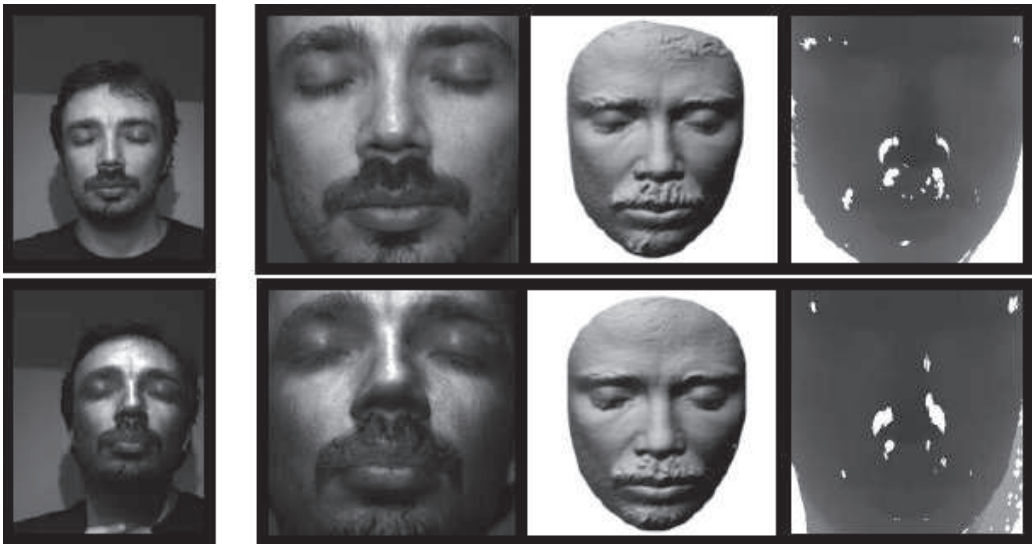

Figure 11.2: L'exemple de la base de données masque qui est créé par MORPHO. De gauche à droite (rangée du haut) Le vrai visage, l'image de texture recadrée, l'acquisition 3D aprés prétraitement, la carte centrée de profondeur estimée à partir de l'acquisition brute 3D (rangée du bas) les mêmes images avec l'attaque du masque correspondante.

sance faciale 3D et 2D, respectivement. L'analyse d'impact en notre étude montre que:

- Bien que les attaques avec masque ont réussi à leurrer les systémes de reconnaissance faciale 2D et 3D, le systéme de la reconnaissance faciale 3D est plus vulnérable à cette attaque par rapport au systéme de reconnaissance faciale 2D.
- Les taux d'erreur égal (EER) du mode de base augmente de 1.8% à 25.1% pour le systéme de la reconnaissance faciale 3D et de 4.7% à 9.9% pour le systéme de reconnaissance faciale 2D sous les attaques.
- Les caractéristiques de forme 3D d'un visage réel et l'attaque avec masque correspondant sont plus similaires par rapport à leurs caractéristiques de texture. Par conséquent, l'analyse de la texture peut révéler plus d'informations pour détecter les attaques avec masque par rapport à l'analyse de caractéristiques de forme 3D.
- La robustesse contre leurrage avec masque est observée pour dépendu à la fois de la méthode et de la modalité.
- Les systémes en reconnaissance faciale sont vulnérables aux attaques de leurrage avec masque donc, les contre-mesures sont nécessaires pour réduire leur impact sur la reconnaissance faciale.

Dans le prochain chapitre de la thèse, initialement, nos techniques de contre-mesures, qui sont proposées pour détecter les attaques avec masque 3D, sont expliquées. Ensuite, la contre-mesure, qui offre les meilleures performances en matiére de détection de masque, est intégrée au système de reconnaissance faciale 3D sélectionné afin d'observer l'impact positif de la contre-mesure sur les performances de reconnaissance.

5. Les Techniques de Contre-mesures contre les Attaques avec Masque

Il existe plusieurs types d'attaques de leurrage comme la photographie, vidéo ou masque. Des études récentes montrent que les systèmes de la reconnaissance faciale sont vulnérables à ces attaques. Dans ce chapitre, les nouvelles techniques de contre-mesures, qui sont basées sur l'analyse des différentes formes, de la texture et de la réflectance caractéristiques des vrais visages et des masques, sont expliquées pour à détecter le leurrage par masque. Dans ce chapitre, les contre-mesures sont élaborées à l'aide de l'utilisation de données 2D (images de texture) et de données 3D (scans 3D) disponibles dans la base de données avec masque. Les résultats montrent que chacune des contre-mesures proposées ont réussis à détecter le leurrage. En raison de l'absence de base de données avec masque, des études sur leurrage d'identité sont limitées. Ce chapitre fournit les résultats en proposant de nouvelles contre-mesures pour protéger les systèmes de la reconnaissance contre ces attaques.

Quatre contre-mesures sont proposées dans cette étude pour discriminate les masques et les échantillons réels. Trois d'entre elles utilisent les données 2D (images de texture), et la derniére utilise les données 3D (cartes de profondeur estimées à partir des scans 3D premiéres) disponibles dans la base de données du masque.

L'organigramme des contre-mesures proposées dans ce chapitre sont présentées à la Figure 11.3. Dans cette figure, l'analyse micro-texture appliquée sur les images de texture est appelé CM1, appliquée sur les images de réflectance est appelé CM2, appliquée sur les cartes de profondeur est appelé CM4, et enfin la contre-mesure pour lesquelles les valeurs d'intensité de pixels sur une image de réflectance sont utilisées directement par le classificateur est appelée CM3 (CM signifie la contre-mesure).

L'image acquise du masque peut visuellement être très similaire à l'image acquise du visage réel (par exemple, les images de texture dans la deuxième colonne de la Figure 11.2). Un regard attentif sur les différences entre les vrais visages et les visages des masques révèle que leurs propriétés de surface sont différentes. Pour la fabrication de masque, des imprimantes 3D été ont utilisées, par conséquent, ils peuvent contenir des défauts de qualité d'impression qui peuvent être détectées avec des motifs de micro-texture. Pour CM1, l'analyse micro-texture est appliquée sur les images de texture, et la fonction histogramme de longueur 833 est obtenue. Enfin, le SVM classificateur linéaire est utilisé pour détecter les masques et vrais visages.

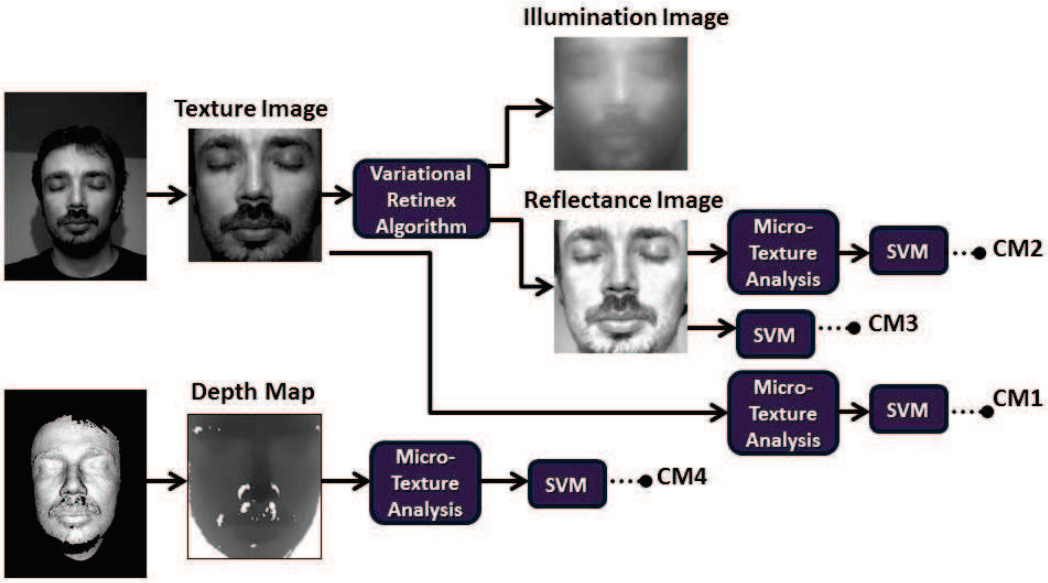

Figure 11.3: L'organigramme des contre-mesures proposées.

Pour CM2, initialement, les composantes d'illumination et de réflectance (Figure 11.3) des images de texture sont obtenues en utilisant l'algorithme de Retinex variationnelle. Ensuite, l'analyse micro-texture est appliquée sur les composants de réflectance des images plutôt que des images de texture. La raison de cette analyse sur les images de réflectance est qu'une étude attentive des différences entre les images de la réflectance des visage réelles et visage masque révèle que les caractéristiques de texture sur leurs éléments de réflexion sont également différents. Les vecteurs de caractéristiques de longueur 833, qui sont obtenus en appliquant l'analyse de micro-texture sur les images de réflectance, sont utilisés par le SVM classificateur linéaire.

Nos observations sur les éléments de réflexion du masque et de vrais visages révèlent que les caractéristiques de réflectance du masque et des échantillons des visages réelles sont différentes, en particulier dans certaines régions spécifiques du visage (les cils, sourcils et moustache). Sur la base de ces observations, dans cette étude, par CM3, nous utilisons les valeurs d'intensité de la composante de réflexion de chaque image pour le SVM classificateur linéaire.

La forme 3D du masque de haute qualité est également très similaire à la forme 3D du visage réel correspondant. Notre analyse montre que le scan du masque est plus lisse que le scan du visage réel. En particulier, les parties du visage avec les poils du visage sont très différentes. Puisqu'il n'y a pas de vrai poils de visage (par exemple, moustache, sourcils) sur les masques, le scan 3D du masque est plus lisse dans ces régions par rapport au scan du vrai visage. Lorsque les scanners de haute qualité sont utilisés pour l'acquisition, bien qu'il y ait une diminution du nombre de trous,

il est encore possible d'observer quelques trous sur le scan en particulier les parties du visage avec les poils du visage. Ainsi, dans notre étude, par CM4, l'analyse micro-texture est également appliquée sur les cartes de profondeur qui sont estimés à partir des scans 3D brutes, et l'autre histogramme des caractéristiques de longueur 833 est obtenu. Enfin, le SVM classificateur linéaire est utilisé pour détecter des visages réels et des masques.

Ces contre-mesures peuvent être utilisées pour protéger les systèmes de reconnaissance faciale 2D et 3D contre les attaques avec masque. La Figure 11.4 montre les performances de classification des quatre contre-mesures. Les résultats de cette étude montrent que l'analyse sur des images de réflectance fournit de meilleurs résultats par rapport à l'analyse de la texture et de la profondeur des images. Tous les 4 contre-mesures fournissent des informations satisfaisantes donc peuvent être utilisées comme sources indépendantes de discriminer des masques et visages réels. Mais, avec la fusion de ces contre-mesures, on observe une amélioration significative des performances. Par exemple, dans cette étude, une précision de classification de 99% (précision presque parfaite) est atteinte pour vrai visage vs. masque par fusion.

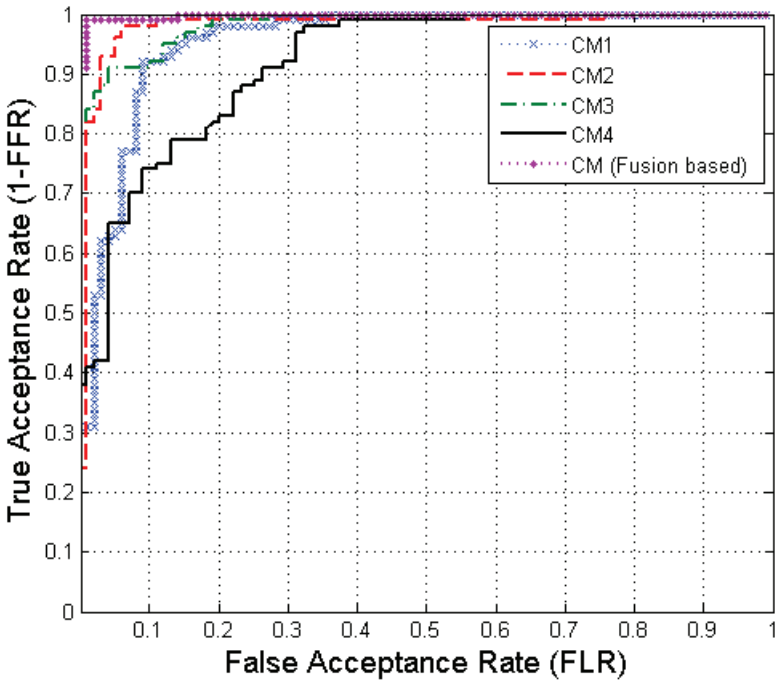

Figure 11.4: Les performances de classification des contre-mesures.

Dans cette étude, nous avons également intégré la contre-mesure offrant la meilleure performance du système de reconnaissance faciale 3D sélectionné. Nous avons observé que l'inclusion de la contre-mesure améliore les résultats du système 3D sous

attaques, alors qu'il dégrade les performances de base du système lorsqu'il n'est pas confronté à une attaque.

6. L'impact des Retouches sur le Nez en Reconnaissance Faciale

Des nombreux défis majeurs en reconnaissance faciale, comme la pose, l'éclairage, l'expression et le vieillissement, ont été étudiés intensivement. Toutes ces variations modifient la texture et/ou la forme du visage d'une manière similaire pour les différents individus. Mais, les études sur les modifications appliquées sur le visage par la chirurgie plastique ou maquillage important dans diverses quantités et dans diverses formes, sont encore très limitées. Dans cette thèse, nous analysons comment ces changements sur la région du nez affectent les performances en reconnaissance faciale de plusieurs techniques clés. À cet effet, une base de données simulée est préparée en utilisant FRGC v1.0 dans lequel le nez de chaque personne est remplacé par un autre choisi au hasard. Puisque c'est une base de données 3D, l'analyse de l'impact ne se limite pas seulement avec 2D, qui est l'une des originalités de la présente étude. Les comparaisons des performances de trois algorithmes 2D et de quatre algorithmes 3D sont fournis. En outre, différemment des travaux précédents, des résultats de référence pour la base de données d'origine sont également évaluées. Par conséquent, l'impact qui est uniquement lié aux altérations du nez peut être mesurée. Les résultats expérimentaux indiquent qú avec l'introduction de modifications, les deux modalités perdent de précision, en particulier 3D.

Pour les tests de vérification, le Receiver Operating Characteristic (ROC) des courbes qui représentent les taux de vérification (VR) en fonction des taux de fauses acceptations (FAR) sont présentés avec les taux de vérification à 0.001 FAR.

Pour les tests d'identification, le premier échantillon de chaque individu dans l'ensemble de test est utilisé comme galerie et le reste en tant que test. Les taux de reconnaissance rang-1 sont évaluées.

Expérience 1 - Performance sur la base de données originale : Il est important de calculer les performances sur les ensembles de données originales pour avoir une base de référence. Par ce moyen, l'impact des modifications appliquées peut être mesuré avec précision. À cet effet, les algorithmes 2D et 3D sont évalués sur DB-o ou les similitudes sont calculées entre chaque paire d'image d'origine.

Expérience 2 - Performance sur la base de données simulé : Dans ce scénario, les scores de similarité entre chaque paire DB-o et DB-s sont calculés et utilisés pour évaluer les performances de la reconnaissance. Pour l'ensemble d'entrainment, pour chaque sujet sélectionné, la moitié des images correspondantes sont prises à partir de DB-o et le reste de DB-s. Cette expérience est identique à l'expérience 1, sauf les images de test sont maintenant remplacées par leurs versions modifiées.

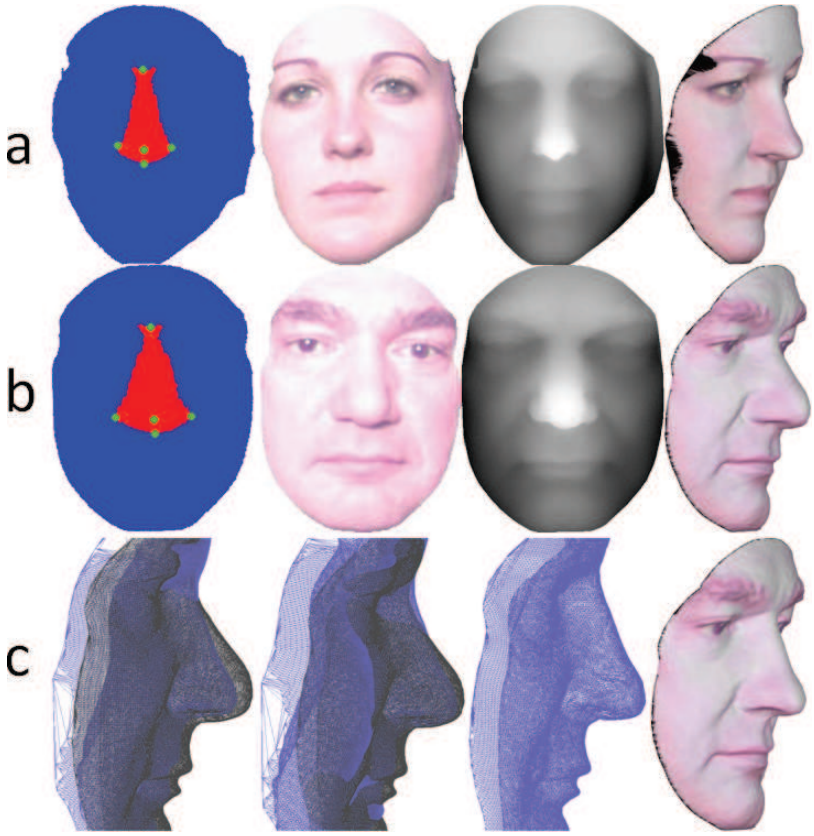

Figure 11.5: De gauche à droite: (a) la région du nez avec des points de repére, carte des couleurs, carte de profondeur et de profil pour le modéle cible (b) Les mêmes images pour le modéle de source (c) Deux modèles superposés avant et après l'alignement, le maillage résultant après déformation et vue de profil pour le modèle synthétisé.

Impact sur la reconnaissance faciale 2D :

Trois méthodes principales sont choisies pour être évaluées pour la reconnaissance faciale 2D : Analyse en composants principales (PCA), l'analyse discriminante linéaire (LDA) [12] et motif binaire local (LBP) [4]. PCA et LDA sont des approches basées sur l'apparence, qui sont largement utilisées pour la réduction de dimensions et l'extraction de caractéristiques. D'autre part, LBP est un algorithme basé texture pour la description de structures locales.

Les taux de vérification à 0.001 FAR et les courbes ROC pour les trois algorithmes sont donnés sur la Figure 11.6.

Sur la Figure 11.6, la meilleure performance est obtenue en utilisant la méthode LBP avec une différence marquée. Cela montre qú d'une méthode de texture comme LBP est beaucoup plus appropriée que les approches basées sur l'apparence (PCA

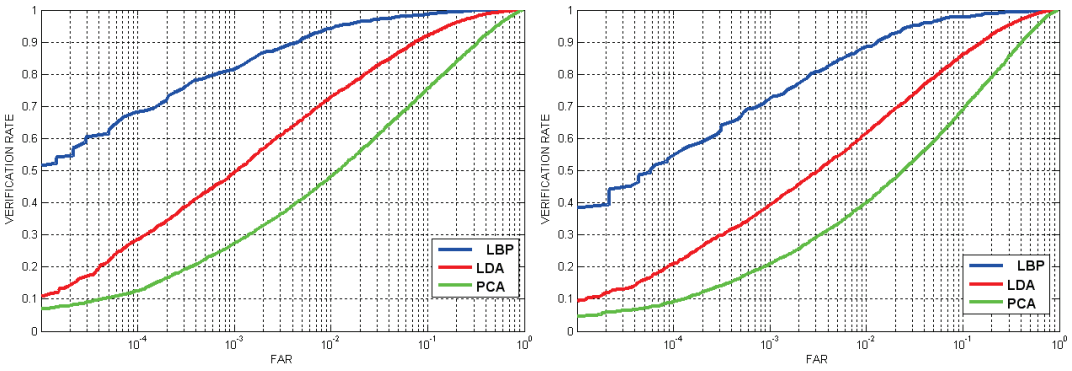

Figure 11.6: Les taux de vérification pour tous les algorithmes 2D pour l'expérience 1 (à gauche) et l'expérience 2 (à droite).

et LDA) en cas de modification de nez. Avec ces trois techniques, la différence relative entre les résultats de l'expérience 1 et 2 indique une diminution significative des performances en présence d'altérations du nez.

Impact sur la reconnaissance faciale 3D :

Pour l'évaluation de systèmes en reconnaissance faciale 3D, quatre algorithmes sont choisis ou les surfaces faciales sont représentées comme des cartes de profondeur ou des nuages de points.

La plupart des techniques 2D peut être appliqué sur les cartes de profondeur. Dans cette section, similaire aux sections seul'evaluation 2D, PCA et LDA sont sélectionnés pour être évalués sur les cartes de profondeur.

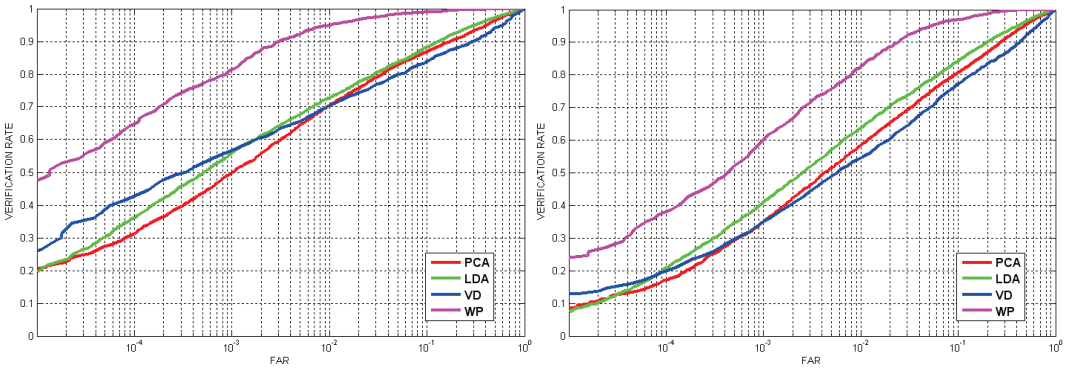

Figure 11.7: Les taux de vérification pour tous les algorithmes 3D pour l'expérience 1 (à gauche) et l'expérience 2 (à droite).

En outre, deux approches différentes sont mises en oeuvre pour la reconnaissance faciale 3D à l'aide de l'utilisation de nuages de points. Dans cette représentation, les visages sont tenus d'être aligués avant du mesure des similarité.

Pour cette raison, dans la première technique, les visages sont alignés avec un modèle de visage générique à l'aide de l'utilisation trois points caractéristiques (deux coins des yeux extérieurs et la pointe du nez) et ensuite les valeurs de profondeur sont régulièrement échantillonnées. La similarité entre les deux visages est obtenu en calculant la moyenne des distances z de tous les sommets. De cette façon, la différence de volume (VD) est approximée entre les deux surfaces faciales.

Pour la deuxième approche (WP), nous avons implanté la méthode présentée dans [39] et expliqué dans le chapitre 4, qui utilise les paramètres de déformation TPS.

La Figure 11.7 montre que avec les quatre techniques, la différence relative entre les résultats de l'expérience 1 et 2 indique une diminution significative des performances en présence d'altérations du nez. Les meilleures performances sont obtenues avec la technique de WP.

La nouveauté de cette étude est que les analyses ne sont pas limités à des images 2D. L'effet des modifications apportées peut également être déterminé en 3D. Et en outre, puisqu'il est possible de mesurer les performances initiales sur FRGC v1.0, une comparaison authentique entre les pré- et post-altération des performances peuvent être fournit, ce qui est un avantage significatif de cette étude par rapport aux précédentes.

Les résultats révèlent que les algorithmes évalués ne sont pas robustes aux variations causées par des altérations au niveau du nez. En outre, la comparaison des performances de vérification des algorithmes 2D et 3D montrent que le 3D est beaucoup plus vulnérable contre les variations du nez par rapport à 2D.

Des algorithmes de reconnaissance faciale robustes sont nécessaire pour atténuer les effets de modifications faciales. Dans le prochain chapitre, nous proposons une approche de reconnaissance faciale robuste à des modifications du nez.

7. Reconnaissance Faciale Robuste à Nez Altération

La reconnaissance faciale robuste aux modifications appliquées sur le visage par la chirurgie plastique ou le maquillage peut encore être considéré comme un sujet nouveau. Dans cette étude, une approche est proposée qui prévoit une assez bonne performance de la reconnaissance, avec l'avantage de la robustesse à ce genre de retouches. Pour cette étude, une base de données de visages avec modification du nez est simulée est préparée en utilisant FRGC v1.0. C'est une base de données 3D, donc l'approche peut être testée à la fois en 2D et en 3D, qui est l'une des contributions de cette étude. En outre, différemment des précédents travaux, des résultats de référence pour la base de données d'origine sont donnés. L'impact qui est purement lié aux modifications du nez est mesuré en utilisant les deux l'approches proposées

et les techniques classiques qui sont basés sur la description globale à des fins de comparaison. Les résultats indiquent que, bien que modalités2D et 3D en perdent précision en raison des modifications, l'approche proposée est supérieure en termes des performances de la reconnaissance et de la robustesse aux modifications par rapport aux techniques classiques.

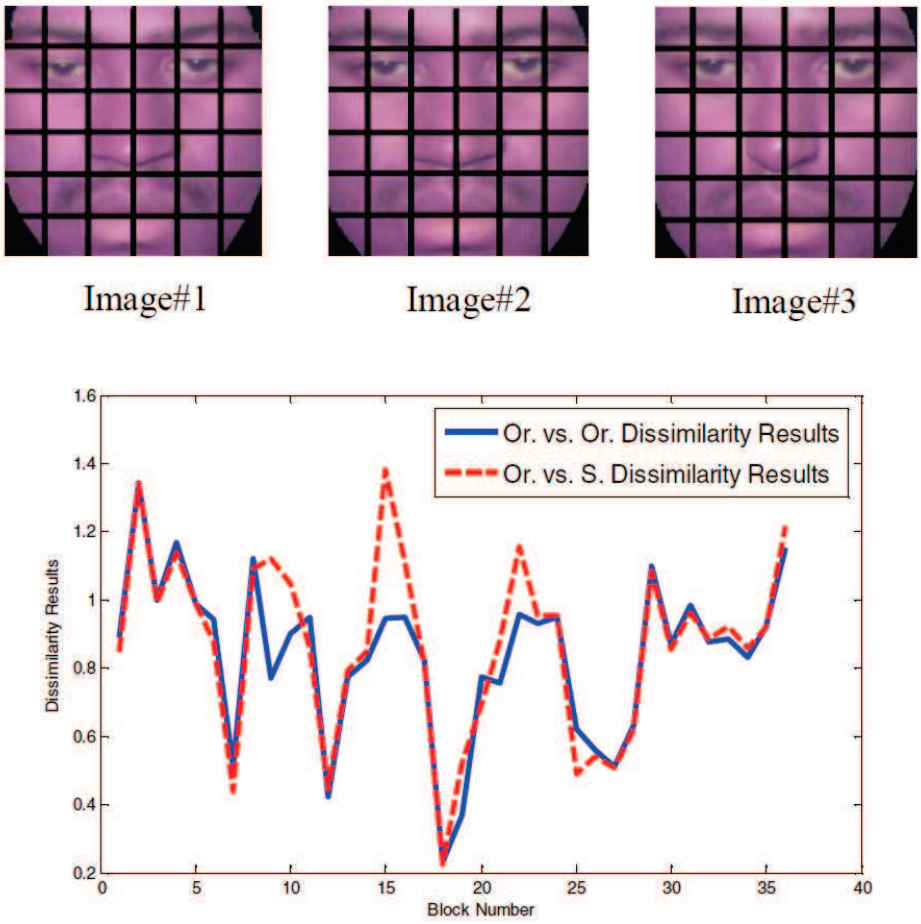

Figure 11.8: Les résultats de dissemblances obtenus par comparaison originale vs. originale entre Image 1 et Image 2, et par comparaison originale vs. synthétique entre Image 1 et Image 3.

La Figure 11.8 montre un exemple de notre analyse en utilisant l'image d'origine dans la galerie (Image 1), une autre image de la même personne pour la comparaison l'originale vs. l'originale (Image 2) et une image synthétique qui est en fait Image 2 après une modification du nez pour la comparaison l'originale vs. le synthétique (Image 3). La figure montre les résultats de dissemblances calculés pour chacun des 36 blocs. PCA est utilisé pour extraire des caractéristiques de bloc. Les résultats de dissemblances entre les blocs de Image 1 et Image 2 sont calculées pour comparer l'originale vs. l'originale. Les résultats de dissimilarités entre les blocs de Image 1

et Image 3 sont calculées pour comparer l'originale vs. la synthétique. De la Figure 11.8, il est clair que les résultats de la dissemblances pour les deux comparaisons sont semblables pour la plupart des numéros de blocs, sauf ceux qui ont subi une altération du nez.

Les résultats de [40, 126, 127] montrent que les méthodes de reconnaissance standards ne sont pas robustes aux variations causées par altérations du nez, en particulier pour en mode vérification. Des algorithmes robustes sont nécessaires pour atténuer les effets de retouches faciales. Par conséquent, dans cette étude, une nouvelle approche est proposée, qui fournit des résultats plus robustes par rapport aux méthodes classiques. Il s'agit simplement d'une méthode d'analyse pour le visage, pour laquelle seuls les blocs d'images qui optimisent les performances de la reconnaissance sont utilisées dans le calcul de dissemblance entre des paires d'images par l'application d'une technique spéciale.

Dans le prochain chapitre de la thèse, nous analysons une autre variante de camouflage dans la reconnaissance faciale, qui est le maquillage faciale. Dans cette étude, nous avons présenté une vaste base de données de visages maquillés et a analysé en détails l'impact du maquillage sur la reconnaissance faciale.

8. Base de Données du Visage des Cosmétiques et Analyse de L'impact sur la Reconnaissance Faciale

Le maquillage change l'apparence perçue d'un visage et peut donc avoir un impact sur la reconnaissance automatique des visages. Dans cette étude, evaluer leur impact en détails, le visage dans son ensemble et ses sous-ensembles d'application du maquillage les plus importants comme la peau, les yeux et la bouche sont étudiés séparément. Après avoir spécifié les étapes du maquillage, une approche de catégorisation de maquillage est développé pour classer les produits appliqués en fonction de leurs effets sur la perception humaine. Pour évaluer l'impact de cosmétiques pour le visage, une base de données de plusieurs images avec et sans maquillage pour chaque personne est construit.

Figure 11.9: L'exemple de la base de données de visage maquillés pour une image de référence et de série d'images dans leur forme originale.

Cette base de données de visages maquillés est utilisé pour l'évaluation préliminaire de l'impact des cosmétiques faciale en la reconnaissance faciale. Si les images de

référence ne comprennent pas le maquillage, le maquillage a un impact négatif sur la reconnaissance faciale. Étonnamment, l'application de cosmétiques sur le visage dans les images de référence peut aider à obtenir un meilleur taux d'identification. Le maquillage peut créer des variations intra-classe. Si elles ne sont appliquées qu'à l'une des séries d'images, elles conduisent manifestement à une diminution de la précision des systèmes de reconnaissance faciale. La sous-zone des yeux joue un rôle majeur dans la reconnaissance faciale tandis que la zone de la bouche n'est pas essentielle.

La base de données contient actuellement 389 images. 50 d'entre elles sont des images de référence et 339 d'entre elles appartiennent à une série d'images de maquillage. 109 des images de maquillage sont classés dans la catégorie de 'non' maquillage, 147 en 'léger', 54 en 'intermédiaire' et 79 en 'chargé'. Chaque image est disponible dans sa version originale (Figure 11.9) et forme détourée.

Les tailles du visage, des yeux et de la bouche sont des images de 150×140 pixels, 60×140 pixels et 40×70 pixels, respectivement. Pour chaque forme originale d'une image, les coordonnées des centres des yeux et coins de la bouche sont annotés manuellement et reportées dans un fichier texte.

La base de données contient actuellement 50 images de référence sans maquillage. Chacune d'entre elles sont prises dans une autre séquence que les images de la série de maquillage.

Comme il est montré sur la Figure 11.10 (a), la capacité d'identifier le visage d'une personne diminue avec l'augmentation de la quantité de maquillage. Les taux d'identification pour les catégories 'non', 'légère' et 'chargée' diminuent presque linéairement, tandis que l' autre pour la catégorie de maquillage 'intermédiaire' montre une légère augmentation (c'est à dire ne diminue pas de façon linéaire) mais est encore inférieur à celle obtenue pour la catégorie 'légère' dans le graphique. L'affirmation dans [29], qui prétend que les cosmétiques pour le visage dégradent la précision des systèmes de la reconnaissance faciale, est confirmée. Les résultats sont en ligne avec les attentes. Le maquillage léger atteint un taux d'identification un peu plus bas que les images sans maquillage. Le maquillage léger a peu d'effet sur la perception humaine et maintient un aspect naturel. Le maquillage intermédiaire est clairement visible et offre un taux d'identification faible donc. Le maquillage chargé a un fort impact sur l'apparence caractéristique des personnes donc est perçu comme masque presque. Le taux d'identification des visages avec le maquillage chargé atteint seulement deux tiers du taux d'identification des visages sans maquillage. Pour avoir un aperçu détaillé des résultats, le visage est divisé en trois parties importantes, que sont la peau, les yeux et la bouche.

Comme il est montré sur la Figure 11.10 (b), le maquillage de la peau provoque une diminution de la capacité de la reconnaissance faciale. Le maquillage de la peau

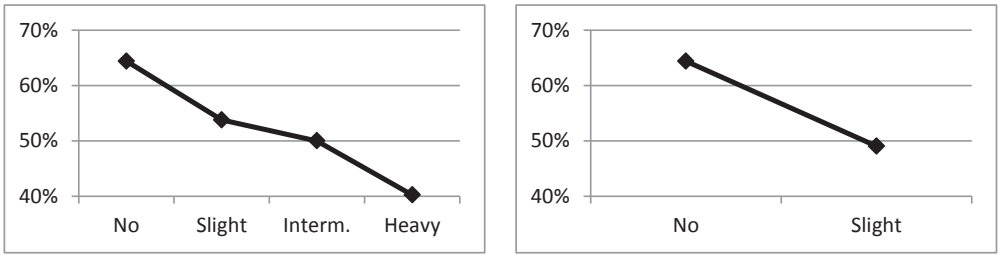

(a) Face as a Whole

(b) Face as a Whole - Skin Makeup

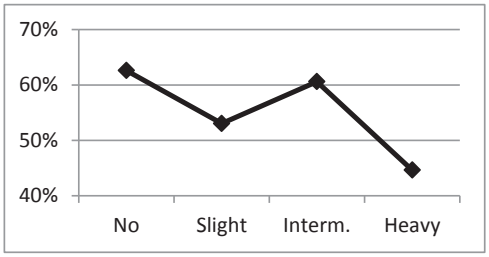

(c) Eyes

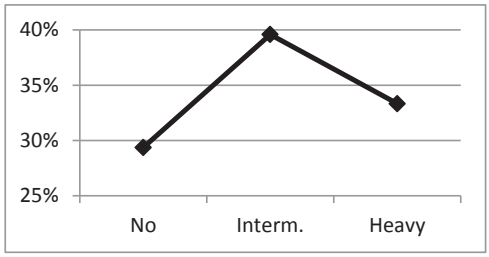

(d) Mouth

Figure 11.10: Les taux d'identification (Les images de référence sont choisies parmi les images sans maquillage).

lisse le visage et modifie la position apparente, la couleur, la forme et la taille des traits du visage. Cela conduit à une distinction des caractéristiques personnelles et empêche par conséquent la reconnaissance faciale.

La Figure 11.10 (c) montre les taux d'identification pour la reconnaissance de l'oeil. Il suit le même schéma qu'en Figure 11.10 (a). Les taux d'identification pour les catégories 'non', 'légère' et 'chargée' diminuent presque linéairement, tandis que pour l'autre catégorie de maquillage 'intermédiaire' les résultats sont localement faibles. Apparemment, le maquillage intermédiaire dans la zone des yeux n'a pas d'impact négatif sur la reconnaissance faciale. Il améliore les caractéristiques et les contours, ce qui conduit à des formes occlulaires plus contratées. Mais, le maquillage chargé des yeux influence la reconnaissance de l'oeil défavorablement. La forme, la taille et les contours des yeux deviennent moins distinctifs.

Les taux d'identification de la zone de la bouche sont représentées sur la Figure 11.10 (d). La courbe globale de taux d'identification est inférieure à celles obtenues pour toutes les autres parties du visage. Cela conduit à la conclusion, que la zone de la bouche contribue moins à la reconnaissance faciale par rapport aux contributions d'autres parties du visage. Il est également indiqué que l'application de cosmétiques pour le visage dans la zone de la bouche conduit à de meilleurs résultats en identification. Cela s'explique par l'effet de l'amélioration du contour. Encore une fois, le maquillage intermédiaire conduit à de meilleurs résultats. Le maquillage chargé

comprend également des modifications de taille ce qui conduit à un taux plus faible d'identification par rapport à maquillage intermédiaire.

Dans cette étude, nous utilisons ensuite des images avec le maquillage intermédiaire comme images de référence. La base de données fournit des séries de maquillage pour 23 personnes avec des images de maquillage intermédiaires. Les séries de maquillage restants fournissent des images appartenant aux catégories de maquillage 'non', 'légère' ou 'chargée'. Par conséquent, l'évaluation est réalisée avec 23 images de référence provenant des vidéo de maquillage. Ils possèdent les mêmes réglages du matériel d'acquisition, de la peau et des conditions d'éclairage avec les images de test. Puisque les images de référence sont issues d'une même session, il est peu réaliste par rapport à l'essai pour lequel les images sans maquillage sont utilisées comme images de référence. C'est pourquoi nous obtenons résultat presque parfait (100%) lorsque des images de maquillage intermédiaires sont utilisés comme références.

9. Base Kinect de Données de Visage et Analyse de L'impact en Reconnaissance Faciale

Le succès récent de nouvelles caméras RGB-D comme le capteur Kinect représente une large perspective des applications informatiques. Toutefois, en raison de l'absence de base de données de test standard, il est difficile d'évaluer l'apport de la technologie en reconnaissance faciale. Afin d'établir les connexions entre le capteur Kinect et la reconnaissance de visage, dans cette étude, nous présentons la première base de données accessible au public de visage (KinectFaceDB) basée sur le capteur Kinect pour la reconnaissance faciale. La base de données se compose de différentes modalités de données (données de visage 2D, 2.5D, 3D et vidéo bien alignées et transformées) et de multiples variations du visage. Nous effectuons des évaluations de référence sur la base de données proposée en utilisant des méthodes de reconnaissance faciale standards, et démontrons le gain de performance en intégrant les données de profondeur avec les données RGB via la fusion. Nous comparons également les images Kinect (du KinectFaceDB) avec les scans 3D de haute qualité traditionnels (de la base de données FRGC) dans le contexte de la biométrie du visage, ce qui démontre que le besoin impératif d'une telle base de données en la reconnaissance faciale.

10. Conclusions et Perspectives d'Avenir

Résumé

Dans cette thèse, nous avons étudié les attaques de leurrage et de camouflage en reconnaissance faciale et proposé des techniques de contre-mesures pour la protection des systèmes en reconnaissance faciale contre ces défis.

Il a été démontré que les systèmes de reconnaissance faciale sont vulnérables à des at-

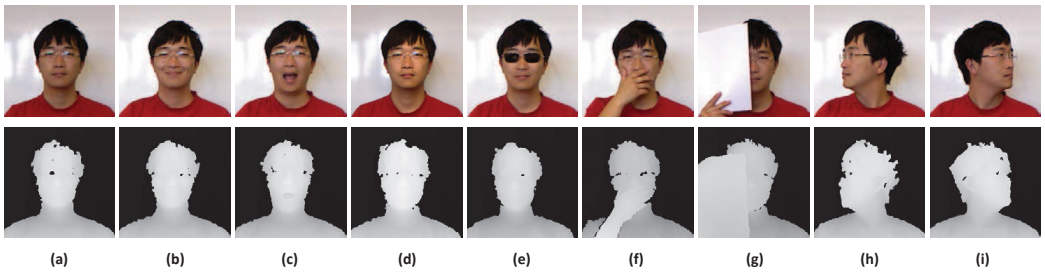

Figure 11.11: L'illustration des différentes variations du visage incluses dans notre base de données: (a) le visage neutre; (b) le sourire; (c) la bouche ouverte; (d) un fort éclairage; (e) l'occultations par des lunettes de soleil; (f) l'occultations à la main; (g) l'occultations par papier; (h) le profil de la face droite et (i) le profil de la face gauche. (Supérieur: les images RGB. Inférieures: Des cartes de profondeur alignés avec des images RGB ci-dessus))

taques avec photographie et vidéo. C'est pourquoi, les techniques de contre-mesures sont nécessaires pour atténuer l'impact du leurrage d'identité sur la reconnaissance faciale. Dans le chapitre 3, nous avons proposé une technique de contre-mesure, qui est basé sur l'analyse de la texture et le contraste, pour la détection des attaques avec photographie.

Dans le chapitre 4, nous avons analysé l'impact des attaques avec masque en reconnaissance faciale aussi bien 2D que 3D en détails. Pour nos études, nous avons utilisé la base de données avec masques qui a été préparée par MORPHO [98] dans le cadre du projet de l'Union européenne (UE) de recherche Tabula Rasa [111]. Les résultats montrent que les systèmes existants sont vulnŕrables aux attaques de leurrage. En particulier, la performance des systèmes de reconnaissance faciale 3D se détériore considérablement quand des masques de haute qualité sont utilisés à des fins du leurrage.

Dans le chapitre 5, nous avons analysé plusieurs caractéristiques des masques et vrais visages comme les caractéristiques de texture, de réflectance et de régularité. Nous avons développé quatre techniques de contre-mesure différents pour la détection des attaques avec masque. Toutes ces contre-mesures seules fournissent des précisions de détection importants. Mais, nous avons observé que la fusion de ces contre-mesures améliore encore les résultats. Nous avons obtenu 99% de précision de classification pour les masques et les échantillons réels par fusion dans cette étude.

Dans le chapitre 6, nous montrons l'impact des modifications du visage sur la reconnaissance faciale. Á cette fin, nous avons préparé une base de données avec des modifications simulé du nez à partir de FRGC v1.0. Ensuite, nous avons évalué l'impact de la modification du visage en reconnaissance faciale 2D et 3D et observé que, bien que les performances des deux modalités se détériorent, la baisse des per-

formances est plus pour la 3D que la 2D.

Dans le chapitre 7, nous avons proposé une nouvelle approche de reconnaissance faciale qui augmente les performances de manière significative en présence d'altérations du nez. L'avantage de cette approche est qu'elle peut être utilisée pour tous les types d'altérations appliquées sur le visage.

Dans le chapitre 8, nous avons analysé l'impact du maquillage en reconnaissance faciale. Á cette fin, nous avons préparé une base de données riche en maquillage. L'impact du maquillage sur la reconnaissance faciale est analysé en détail. Les résultats montrent que les systémes de reconnaissance existants sont vulnérables au maquillage facial et en particulier le maquillage au viveau de la région des yeux affecte de maniére significative les performances de reconnaissance.

Enfin, dans le dernier chapitre, la premiére base de données, accessible au public, de visages basée sur le capteur Kinect est présenté. La base de données se compose de différentes modalités et de multiples variations du visage comme les occultations, expression, éclairage. Nous effectuons des évaluations de référence sur la base de données proposée en utilisant des méthodes standards en reconnaissance du visage , et de démontrons le gain de performance en intégrant les données de profondeur avec les données RGB via la fusion. Nous comparons également les images Kinect avec les scans 3D de haute qualité traditionnels (de la base de données FRGC) dans le contexte de la biométrie du visage, ce qui démontre le besoin impératifs de le base du données proposée pour la reconnaissance faciale.

Perspectives d'Avenir

Nos futurs travaux sur le leurrage consisteront à tester les performances des contre-mesures proposées en utilisant des masques fabriqués à partir de différents matériaux afin d'observer si nous pouvons encore obtenir des résultats satisfaisants, et de proposer de nouvelles contre-mesures pour les bases de données avec masque plus difficiles dès que disponible.

Pour notre étude sur les modifications du visage, notre objectif est de tester les performances de la technique proposée pour les modifications du nez à l'existence d'autres altérations du visage afin de démontrer que notre approche est bénéfique pour tous les types d'opérations de chirurgie plastique.

Pour notre étude sur le maquillage facial, nos futurs travaux consisteront à détecter le maquillage facial et à étudier des techniques robustes contre le maquillage facial.

Enfin, comme un travail futur, nous voulons utiliser la base de données de visage Kinect pour développer des techniques robustes contre les occultations. Nous prévoyons également d'utiliser cette base de données pour d'autres tests comme la

reconnaissance du genre, construction de modéle 3D de qualité à partir des données vidéo disponibles dans cette base de données.

Bibliography

[1] Special issue on computer vision for rgb-d sensors: Kinect and its applications. *IEEE Transactions on Systems, Man, and Cybernetics, Part B: Cybernetics*, 42(4):1295 –1296, 2012. 97

[2] 3dMD. *http : //www.3dmd.com/*. 99

[3] A. F. Abate, M. Nappi, D. Riccio, and G. Sabatino. 2d and 3d face recognition: A survey. *Pattern Recogn. Lett.*, 28(14):1885–1906, 2007. 1, 9, 114

[4] T. Ahonen, A. Hadid, and M. Pietikainen. Face description with local binary patterns: Application to face recognition. *IEEE Transactions on Pattern Analysis and Machine Intelligence*, 28(12):2037 –2041, 2006. 9, 19, 38, 66, 74, 80, 86, 98, 100, 110

[5] J. Alexander and J. Smith. Engineering privacy in public: Confounding face recognition, privacy enhancing technologies. *International Workshop on Privacy Enhancing Technologies*, pages 88–106, 2003. 18, 19

[6] N. Almoussa. Variational retinex and shadow removal. *Technical Report, The Mathematics Department, UCLA*, 2008. 46, 47, 48

[7] M. Angeloglou. *A History of Make-up*. Macmillan, 1970. 17, 85

[8] J. Bai, T.-T. Ng, X. Gao, and Y.-Q. Shi. Is physics-based liveness detection truly possible with a single image? *IEEE International Symposium on Circuits and Systems*, pages 3425–3428, 2010. 12

[9] W. Bao, H. Li, N. Li, and et al. A liveness detection method for face recognition based on optical flow field. *Int. Conf. on Image Analysis and Signal Processing (IASP)*, pages 233–236, 2009. 11

[10] F. Barak, S. Alexander, M. Meir, and A. Yoel. Depth mapping using projected patterns. *US Patent : 20100118123*, 2010. 99, 104

[11] I. B. Barbosa, M. Cristani, A. D. Bue, L. Bazzani, and V. Murino. Re-identification with rgb-d sensors. *ECCV Workshops (1)*, 7583:433–442, 2012. 97

[12] P. N. Bellhumer, J. Hespanha, and D. Kriegman. Eigenfaces vs. fisherfaces: Recognition using class specific linear projection. *IEEE Transactions on Pattern Analysis and Machine Intelligence*, 17(7):711–720, 1997. 9, 19, 66, 74, 98, 100, 110

[13] P. J. Besl and N. D. McKay. A method for registration of 3-d shapes. *IEEE Trans. Pattern Anal. Mach. Intell.*, 14(2):239–256, 1992. 9, 37, 100, 111

[14] J. R. Beveridge, G. H. Givens, P. J. Phillips, B. A. Draper, D. S. Bolme, and Y. M. Lui. Frvt 2006: Quo vadis face quality. *Image Vision Comput.*, 28(5):732–743, 2010. 9

[15] H. S. Bhatt, S. Bharadwaj, R. Singh, M. Vatsa, and A. Noore. Evolutionary granular approach for recognizing faces altered due to plastic surgery. *IEEE International Conference on Automatic Face & Gesture Recognition and Workshops*, pages 720–725, 2011. 17, 73

[16] F. L. Bookstein. Principal warps: Thin-plate splines and decomposition of deformations. *IEEE Trans. Pattern Analysis and Machine Intelligence*, pages 567–585, 1989. 38, 64

[17] A. Bottino, M. De Simone, and A. Laurentini. A computer-aided technique for planning plastic surgery based on 3d face scans: preliminary results. *Proceedings of Int. Conf. on 3D Body Scanning Technologies*, 2010. 64

[18] K. W. Bowyer, K. Chang, and P. Flynn. A survey of approaches and challenges in 3d and multi-modal 3d+2d face recognition. *Comput. Vis. Image Underst.*, 101(1):1–15, 2006. 9, 100, 114

[19] Smile by Webshots. $http://good-times.webshots.com$. xii, 62

[20] C. Herrera C., J. Kannala, and J. Heikkilä. Accurate and practical calibration of a depth and color camera pair. 6855:437–445, 2011. 106

[21] D. Herrera C., J. Kannala, and J. Heikkilä. Joint depth and color camera calibration with distortion correction. *IEEE Transactions on Pattern Analysis and Machine Intelligence*, 34(10):2058 –2064, 2012. 106

[22] M.-M. Chakka, A. Anjos, S. Marcel, and et al. Competition on counter measures to 2-d facial spoofing attacks. *IEEE IAPR Int. Joint Conference on Biometrics (IJCB)*, pages 1–6, 2011. 12

[23] C.-C. Chang and C.-J. Lin. Libsvm : a library for support vector machines. *ACM Transactions on Intelligent Systems and Technology*, pages 2:27:1–27:27, 2011. 14, 29, 50

[24] Y. Chen and G. Medioni. Object modelling by registration of multiple range images. *Image Vision Comput.*, 10(3):145–155, 1992. 9, 100, 111

[25] G. Chetty and M. Wagner. Multi-level liveness verification for face-voice biometric authentication. *Biometrics Symposium: Special Session on Research at the Biometric Consortium Conference*, pages 1–6, 2006. 12

[26] T. Choudhury, B. Clarkson, T. Jebara, and A. Pentland. Multimodal person recognition using unconstrained audio and video. *Proc. of International Conference on Audio-Visual Biometric Person Authentication*, pages 176–181, 1999. 11

[27] A. Colombo, C. Cusano, and R. Schettini. Umb-db: A database of partially occluded 3d faces. pages 2113–2119, 2011. 99, 100, 115

[28] Cyberware. *http* : *//www.cyberware.com/*. 99

[29] A. Dantcheva, C. Chen, and A. Ross. Can facial cosmetics affect the matching accuracy of face recognition systems? *IEEE International Conference on Biometrics: Theory, Applications and System (BTAS)*, 2012. 18, 86, 93

[30] A. Dantcheva and J.-L. Dugelay. Female facial aesthetics based on soft biometrics and photo-quality. *IEEE International Conference for Multimedia and Expo (ICME)*, 2011. 89

[31] A. Dantcheva, C. Velardo, A. D'Angelo, and J.-L.Dugelay. Bag of soft biometrics for person identification. *Multimedia Tools Appl.*, 51(2):739–777, 2011. 107

[32] 3D RMA Database. *http* : *//www.sic.rma.ac.be/* ∼ *beumier/DB/*3d_r*ma.html*. 99

[33] NUAA Photograph Impostor Database. *http* : *//parnec.nuaa.edu.cn/xtan/data/NuaaImposterdb.html*. 12, 23, 39

[34] Print Attack Database. *http* : *//www.idiap.ch/dataset/printattack*, 2011. 12

[35] J. Daugman. How iris recognition works. *IEEE Transactions on Circuits and Systems for Video Technology*, 14(1):21–30, 2004. 8

[36] J. Duchon. Splines minimizing rotation-invariant semi-norms in sobolev spaces. In *Constructive Theory of Functions of Several Variables*, volume 571 of *Lecture Notes in Mathematics*, pages 85–100. 1977. 100, 111

[37] M.-L. Eckert, N. Kose, and J.-L. Dugelay. Facial cosmetics database and impact analysis on automatic face recognition. *IEEE International Workshop on Multimedia Signal Processing (MMSP)*, pages 434–439, 2013. 18

[38] Mark Elendt, editor. *International Conference on Computer Graphics and Interactive Techniques, SIGGRAPH 2011, Vancouver, BC, Canada, August 7-11, 2011, Talks Proceedings*. ACM, 2011. 97

[39] N. Erdogmus and J.-L. Dugelay. On discriminative properties of tps warping parameters for 3d face recognition. *IEEE Int. Conf. on Informatics, Electronics and Vision (ICIEV)*, pages 225–230, 2012. xi, 20, 37, 38, 98, 110, 111, 115

[40] N. Erdogmus, N. Kose, and J.-L. Dugelay. Impact analysis of nose alterations on 2d and 3d face recognition. *IEEE Int. Workshop on Multimedia Signal Processing 2012 (MMSP)*, pages 354–359, 2012. 17, 74, 78, 79, 80, 83

[41] N. Erdogmus and S. Marcel. Spoofing in 2d face recognition with 3d masks and anti-spoofing with kinect. *International Conference on Biometrics: Theory, Applications and Systems (BTAS)*, pages 1–6, 2013. xi, 13, 14, 15

[42] Face-Place. *http : //tarrlab.cnbc.cmu.edu/face − place*. 18, 85

[43] M. F. Fallon, H. Johannsson, and J. J. Leonard. Efficient scene simulation for robust monte carlo localization using an rgb-d camera. pages 1663–1670, 2012. 97

[44] T. C. Faltemier, K. W. Bowyer, and P. J. Flynn. Using a multi-instance enrollment representation to improve 3d face recognition. *IEEE International Conference on Biometrics: Theory, Applications, and Systems (BTAS)*, pages 1–6, 2007. 99

[45] G. Farinella and J.-L. Dugelay. Demographic classification: Do gender and ethnicity affect each other? *IEEE/IAPR International Conference on Informatics, Electronics & Vision (ICIEV)*, 2012. 109

[46] The American Society for Aesthetic Plastic Surgery. *http : //www.surgery.org/sites/default/files/Stats*2010.*pdf*, 2010. 61, 70

[47] M. Gabel, E. Renshaw, A. Schuster, and R. Gilad-Bachrach. Full body gait analysis with kinect. *Annual International Conference of the IEEE Engineering in Medicine and Biology Society (EMBC)*, 2012. 97

[48] A. S. Georghiades, P. N. Belhumeur, and D. J. Kriegman. From few to many: Illumination cone models for face recognition under variable lighting and pose. *IEEE Trans. Pattern Anal. Mach. Intelligence*, 23(6):643–660, 2001. 19, 99

[49] R. Gross. Face databases. In *Handbook of Face Recognition*. Springer, New York, 2005. 98

[50] R. Gross, I. Matthews, J. Cohn, T. Kanade, and S. Baker. Multi-pie. *IEEE International Conference on Automatic Face Gesture Recognition (FG)*, pages 1–8, 2008. 99

[51] OpenNI User Guide. *http : //www.openni.org/documentation*, 2010. 103

[52] Z. Guo, L. Zhang, and D. Zhang. Rotation invariant texture classification using lbp variance (lbpv) with global matching. *Elsevier Pattern Recognition*, pages 706–719, 2010. xi, 21, 24, 25, 27, 39

[53] S. Gupta, K. R. Castleman, M. K. Markey, and A. C. Bovik. Texas 3d face recognition database. *IEEE Southwest Symposium on Image Analysis Interpretation (SSIAI)*, pages 97 –100, 2010. 66, 99

[54] J. Harguess and J. K. Aggarwal. A case for the average-half-face in 2d and 3d for face recognition. *IEEE Computer Society Conference on Computer Vision and Pattern Recognition Workshops (CVPR Workshops)*, pages 7 –12, 2009. 116

[55] P. Henry, M. Krainin, E. Herbst, X. Ren, and D. Fox. Rgb-d mapping: Using kinect-style depth cameras for dense 3d modeling of indoor environments. *I. J. Robotic Res.*, 31(5):647–663, 2012. 97, 109

[56] M. Hernandez, J. Choi, and G. Medioni. Laser scan quality 3-d face modeling using a low-cost depth camera. *Proceedings of the European Signal Processing Conference*, pages 1995–1999, 2012. xiii, 102, 106, 109, 110

[57] Y. Huang, Y. Wang, and T. Tan. Combining statistics of geometrical and correlative features for 3d face recognition. *Proc. of BMVC*, pages 90.1–90.10, 2006. 114

[58] T. Huynh, R. Min, and J.-L. Dugelay. An efficient LBP-based descriptor for facial depth images applied to gender recognition using RGB-D face data. *ACCV Workshop on Computer Vision with Local Binary Pattern Variants*, 2012. 114

[59] S. Izadi, D. Kim, O. Hilliges, D. Molyneaux, R. A. Newcombe, P. Kohli, J. Shotton, S. Hodges, D. Freeman, A. J. Davison, and A. W. Fitzgibbon. Kinectfusion: real-time 3d reconstruction and interaction using a moving depth camera. pages 559–568, 2011. 97, 109

[60] A. Jain, H. Lin, and R. Bolle. On-line fingerprint verification. *IEEE Transactions on Pattern Analysis and Machine Intelligence*, 19(4):302 –314, 1997. 8

[61] A. K. Jain, S. C. Dass, and K. Nandakumar. Soft biometric traits for personal recognition systems. In *Biometric Authentication*, volume 3072 of *Lecture Notes in Computer Science*, pages 731–738. 2004. 107

[62] R. Johnson, K. O'Hara, A. Sellen, C. Cousins, and A. Criminisi. Exploring the potential for touchless interaction in image-guided interventional radiology. *Proceedings of the SIGCHI Conference on Human Factors in Computing Systems*, pages 3323–3332, 2011. 97

[63] I. A. Kakadiaris, G. Passalis, G. Toderici, M. N. Murtuza, L. Yunliang, N. Karampatziakis, and T. T. Theoharis. Three-dimensional face recognition in the presence of facial expressions: An annotated deformable model approach. *IEEE Trans. on Pattern Analysis and Machine Intelligence*, pages 640–649, 2007. 64

[64] KeyLemon. $https://www.keylemon.com/keylemonfacesdk-liveliness-detection/$, 2013. xi, 11

[65] K. Khoshelham and S. O. Elberink. Accuracy and resolution of kinect depth data for indoor mapping applications. *Sensors*, 12(2):1437–1454, 2012. 97, 104, 107, 117

[66] Y. Kim, J. Na, S. Yoon, and J. Yi. Masked fake face detection using radiance measurements. *Journal of the Optical Society of America A*, pages 760–766, 2009. 14, 15, 44

[67] R. Kimmel, M. Elad, D. Shaked, R. Keshet, and I. Sobel. A variational framework for retinex. *International Journal of Computer Vision*, pages 7–23, 2003. 46, 47, 48

[68] Microsoft Kinect. $http://www.xbox.com/en-US/KINECT$. 97

[69] N. G. Kingsbury. Rotation-invariant local feature matching with complex wavelets. *Proc. of European Signal Processing Conference (EUSIPCO)*, pages 4–8, 2006. 27

[70] K. Kollreider, H. Fronthaler, and J. Bigun. Evaluating liveness by face images and the structure tensor. *IEEE Workshop on Automatic Identification Advanced Technologies*, pages 75–80, 2005. 11

[71] K. Kollreider, H. Fronthaler, and J. Bigun. Verifying liveness by multiple experts in face biometrics. *IEEE Computer Society Conference on Computer Vision and Pattern Recognition Workshops*, pages 1–6, 2008. 11, 12, 13, 43

[72] N. Kose and J.-L. Dugelay. Classification of captured and recaptured images to detect photograph spoofing. *IEEE Int. Conf. on Informatics, Electronics and Vision (ICIEV)*, pages 1027–1032, 2012. 2, 21, 30

[73] N. Kose and J.-L. Dugelay. Countermeasure for the protection of face recognition systems against mask attacks. *IEEE Automatic Face and Gesture Recognition (FG)*, pages 1–6, 2013. 4, 15, 34, 44, 45, 51

[74] N. Kose and J.-L. Dugelay. On the vulnerability of face recognition systems to spoofing mask attacks. *IEEE Int. Conf. on Acoustics, Speech, and Signal Processing (ICASSP)*, pages 2357–2361, 2013. 4, 13, 31, 33, 34, 40, 44

[75] N. Kose and J.-L. Dugelay. Reflectance analysis based countermeasure technique to detect face mask attacks. *Int. Conf. on Digital Signal Processing (DSP)*, pages 1–6, 2013. 15, 34, 44, 45, 51

[76] N. Kose and J.-L. Dugelay. Shape and texture based countermeasure to protect face recognition systems against mask attacks. *IEEE Computer Vision and Pattern Recognition Workshop, on Biometrics (CVPRW)*, pages 111–116, 2013. 15, 34, 44, 45

[77] N. Kose and J.-L. Dugelay. Mask spoofing on face recognition and countermeasures. *Elsevier - Image and Vision Computing Journal, under review*, 2014. 15, 34, 44, 45, 46, 51

[78] N. Kose, N. Erdogmus, and J.-L. Dugelay. Block based face recognition approach robust to nose alterations. *IEEE International Conference on Biometrics: Theory, Applications and Systems (BTAS)*, pages 121–126, 2012. 17

[79] K.-C. Lee, J. Ho, M.-H. Yang, and D. Kriegman. Video-based face recognition using probabilistic appearance manifolds. *Proceedings of the IEEE computer society conference on Computer vision and pattern recognition*, pages 313–320, 2003. 99, 102, 106

[80] K.-C. Lee, J. Ho, M.-H. Yang, and D. Kriegman. Visual tracking and recognition using probabilistic appearance manifolds. *Comput. Vis. Image Underst.*, 99(3):303–331, 2005. 99

[81] T.-Y. Lee, Y.-N. Sun, Y.-C. Lin, L. Lin, and C. Lee. Three-dimensional facial model reconstruction and plastic surgery simulation. *IEEE Transactions on Information Technology in Biomedicine*, pages 214–220, 1999. 63

[82] J. Li, Y. Wang, T. Tan, and et al. Live face detection based on the analysis of fourier spectra. *Proceedings of the SPIE*, pages 296–303, 2004. 12, 23

[83] J. Liu, J. Chen, and J. Ye. Large-scale sparse logistic regression. *ACM SIGKDD International Conference On Knowledge Discovery and Data Mining*, 2009. 29

[84] Y. Liu, R. L. Weaver, K. Schmidt, N. Serban, and J. Cohn. Facial asymmetry: A new biometric. 2001. 116

[85] D. G. Lowe. Distinctive image features from scale-invariant keypoints. *Int. J. Comput. Vision*, 60(2):91–110, 2004. 19, 98, 109, 110

[86] X. Lu, H. Chen, and A. K. Jain. Multimodal facial gender and ethnicity identification. pages 554–561, 2006. 109

[87] J. Määttа, A. Hadid, and M. Pietikainen. Face spoofing detection from single images using micro-texture analysis. *Proc. of IEEE Int. Joint Conf. on Biometrics (IJCB)*, pages 1–7, 2011. 10, 12, 30, 49, 50

[88] J. Määttа, A. Hadid, and M. Pietikainen. Face spoofing detection from single images using texture and local shape analysis. *IET Biometrics*, pages 3–10, 2012. 12, 30

[89] M. De Marsico, M. Nappi, D. Riccio, and J.-L. Dugelay. Moving face spoofing detection via 3d projective invariants. *IAPR Int. Conf. on Biometrics*, pages 73–78, 2012. 11

[90] M. De Marsico, M. Nappi, D. Riccio, and H. Wechsler. Robust face recognition after plastic surgery using local region analysis. *Lecture Notes in Computer Science - Image Analysis and Recognition*, pages 191–200, 2011. 17, 73

[91] A. M. Martinez and R. Benavente. The ar face database. *CVC Technical Report*, (24), 1998. xi, 18, 19, 99, 100, 108, 115

[92] L. Z. McArthur and K. Apatow. Impressions of baby-faced adults. *Social Cognition*, 2(4):315–342, 1984. 89

[93] G. Medioni and R. Waupotitsch. Face modeling and recognition in 3-d. pages 232–, 2003. 20, 98, 100, 110, 111

[94] K. Messer, J. Matas, J. Kittler, and K. Jonsson. Xm2vtsdb: The extended m2vts database. *International Conference on Audio and Video-based Biometric Person Authentication*, pages 72–77, 1999. 99

[95] R. Min, J. Choi, G. Medioni, and J.-L. Dugelay. Real-time 3D face identification from a depth camera. *International Conference on Pattern Recognition (ICPR)*, pages 1739–1742, 2012. 9, 106

[96] R. Min, A. Hadid, and J.-L. Dugelay. Improving the recognition of faces occluded by facial accessories. *IEEE Conference on Automatic Face and Gesture Recognition (FG)*, pages 442–447, 2011. 94, 96, 116

[97] A. B. Moreno and A. Sánchez. Gavabdb: a 3d face database. *Workshop on Biometrics on the Internet*, pages 77–85, 2004. 99

[98] MORPHO. $http://www.morpho.com/$, 2010. xii, 34, 44, 49, 121

[99] Multimedia and Intelligent Software Technology Beijing Municipal Key Laboratory. The bjut-3d large-scale chinese face database. *Technical Report*. 99

[100] B. C. Munsell, A. Temlyakov, C. Qu, and S. Wang. Person identification using full-body motion and anthropometric biometrics from kinect videos. *ECCV Workshops (3)*, 7585:91–100, 2012. 97

[101] University of York Database. $http://www-users.cs.york.ac.uk/\sim nep/research/3Dface/tomh/3DFaceDatabase.html$. 99

[102] T. Ojala, M. Pietikainen, and T. Maenpaa. Multiresolution gray-scale and rotation invariant texture classification with local binary patterns. *IEEE Transactions on Pattern Analysis and Machine Intelligence*, pages 971–987, 2002. 24, 26

[103] G. P. Otto and T. K. W. Chau. 'region-growing' algorithm for matching of terrain images. *Image Vision Comput.*, 7(2):83–94, 1989. 99

[104] S. Pamudurthy, E. Guan, K. Mueller, and M. Rafailovich. Dynamic approach for face recognition using digital image skin correlation. *Audio and Video based Biometric Person Authentication*, pages 1010–1018, 2005. 19

[105] G. Pan, L. Sun, Z. Wu, and S. Lao. Eyeblink-based antispoofing in face recognition from a generic webcamera. *IEEE Int. Conf. on Computer Vision (ICCV)*, pages 1–8, 2007. 12

[106] D. I. Perrett, D. M. Burt, I. S. P. Voak, K. J. Lee, D. A. Rowland, and R. Edwards. Symmetry and human facial attractiveness. *Evolution and Human Behavior*, 20:295–307, 1999. 89

[107] P. J. Phillips, P. J. Flynn, T. Scruggs, K. W. Bowyer, J. Chang, K. Hoffman, J. Marques, J. Min, and W. Worek. Overview of the face recognition grand challenge. *IEEE Computer Society Conference on Computer Vision and Pattern Recognition (CVPR)*, 1:947–954, 2005. 9, 17, 41, 63, 99, 100, 107

[108] P. J. Phillips, H. Moon, P. Rauss, and S. A. Rizvi. The feret evaluation methodology for face-recognition algorithms. *Proceedings of Conference on Computer Vision and Pattern Recognition (CVPR)*, pages 137–143, 1997. 9, 99

[109] J. Preis, M. Kessel, M. Werner, and C. Linnhoff-Popien. Gait recognition with kinect. *Proceedings of the First Workshop on Kinect in Pervasive Computing*, 2012. 97

[110] Sculpteo 3D Printing. *http* : *//www.sculpteo.com/en/*, 2009. 34

[111] TABULA RASA Project. *http* : *//www.tabularasa* − *euproject.org/*, 2010. 13, 33, 34, 37, 44, 111, 121

[112] S. A. Rabi and P. Aarabi. Face fusion: An automatic method for virtual plastic surgery. *International Conference on Information Fusion*, pages 1–7, 2006. 63

[113] N. Ramanathan, A. Chowdhury, and R. Chellappa. Facial similarity across age, disguise, illumination and pose. *International Conference on Image Processing*, pages 1999–2002, 2004. 18

[114] Face recognition homepage. *http* : *//www.face* − *rec.org/databases*. 18, 85, 98

[115] G. Rhodes, A. Sumich, and G. Byatt. Are average facial configurations attractive only because of their symmetry? *Psychological Science*, 10:52–58, 1999. 89

[116] E. Rosten and T. Drummond. Machine learning for high-speed corner detection. pages 430–443, 2006. 109

[117] F. S. Samaria and A. C. Harter. Parameterisation of a stochastic model for human face identification. *Proceedings of the IEEE Workshop on Applications of Computer Vision*, pages 138 –142, 1994. 99

[118] A. Savran, N. Alyüz, H. Dibeklioğlu, O. Çeliktutan, B. Gökberk, B. Sankur, and L. Akarun. Biometrics and identity management. *Bosphorus Database for 3D Face Analysis*, pages 47–56, 2008. 100, 115

[119] K. Scherbaum, T. Ritschel, M. Hullin, T. Thormählen, V. Blanz, and H.-P. Seidel. Computer-suggested facial makeup. *Comp. Graph. Forum (Proc. of Eurographics 2011)*, 30(2), 2011. 17, 85

[120] Cinema Secrets. *http* : *//www.cinemasecrets.com*. xii, 62

[121] H. Sellahewa and S. A. Jassim. Image-quality-based adaptive face recognition. *IEEE Transactions on Instrumentation and Measurement*, 59(4):805–813, 2010. 96

[122] Minolta Sensor. *http* : *//www.konicaminolta.com/*. 9, 99

[123] J. Shotton, A. Fitzgibbon, M. Cook, T. Sharp, M. Finocchio, R. Moore, A. Kipman, and A. Blake. Real-time human pose recognition in parts from single depth images. *Proceedings of the IEEE Conference on Computer Vision and Pattern Recognition*, pages 1297–1304, 2011. 97

[124] P. Silva and A.-S. Rosa. Face recognition based on eigeneyes. *Pattern Recognition and Image Analysis*, pages 335–338, 2003. 18

[125] K. R. Singh, R. S. Khedgaonkar, and S. P. Gawande. A new approach to local plastic surgery face recognition using near sets. *International Journal of Engineering Science and Technology, NCICT Special Issue*, pages 71–75, 2011. 17, 73

[126] R. Singh and M. Vatsa. Effect of plastic surgery on face recognition: A preliminary study. *IEEE Computer Society Conference on Computer Vision and Pattern Recognition Workshops*, pages 72–77, 2009. 15, 16, 62, 73, 74, 78, 80, 83

[127] R. Singh, M. Vatsa, H. S. Bhatt, S. Bharadwaj, A. Noore, and S. S. Nooreyezdan. Plastic surgery: A new dimension to face recognition. *IEEE Transactions on Information Forensics and Security*, pages 441–448, 2010. xi, 16, 62, 65, 66, 67, 73, 74, 78, 79, 80, 83

[128] R. Singh, M. Vatsa, and A. Noore. Face recognition with disguise and single gallery images. *Image and Vision Computing*, pages 245–257, 2008. 18, 19

[129] R. Singh, M. Vatsa, and A. Noore. Recognizing face images with disguise variations. *Recent Advances in Face Recognition*, pages 149–160, 2008. 18

[130] E. Stone and M. Skubic. Evaluation of an inexpensive depth camera for in-home gait assessment. *J. Ambient Intell. Smart Environ.*, 3(4):349–361, 2011. 97

[131] X. Tan, Y. Li, J. Liu, and L. Jiang. Face liveness detection from a single image with sparse low rank bilinear discriminative model. *Proc. of the European conference on Computer vision*, pages 504–517, 2010. xi, xiii, 12, 22, 23, 26, 28, 29, 31, 129

[132] ThatsMyFace. $http://www.thatsmyface.com/Products/products.html$. xi, 13, 34, 35

[133] Behind the Knife: A Guide to Plastic Surgery. $http://behind-the-knife-cosmetic-surgery.blogspot.com$. xii, 62

[134] C. Tomasi and R. Manduchi. Bilateral filtering for gray and color images. *International Conference on Computer Vision*, pages 839–846, 1998. 109

[135] R. Tsai. An efficient and accurate camera calibration technique for 3d machine vision. *Computer Vision and Pattern Recognition*, 1986. 105

[136] S. Ueda and T. Koyama. Influence of make-up on facial recognition. *Perception*, 39(2):260–264, 2010. 86

[137] C. Velardo and J.-L. Dugelay. Real time extraction of body soft biometric from 3d videos. *Proceedings of the ACM international conference on Multimedia*, pages 781–782, 2011. 97

[138] videoyoutube. $http://www.youtube.com/watch?v=rNQ2oDEyVNw$. xii, 86

[139] L. Yin, X. Wei, Y. Sun, J. Wang, and M. J. Rosato. A 3d facial expression database for facial behavior research. *IEEE International Conference on Automatic Face and Gesture Recognition*, pages 211–216, 2006. 99

[140] W. Zhang, S. Shan, W. Gao, X. Chen, and H. Zhang. Local gabor binary pattern histogram sequence (lgbphs): a novel non-statistical model for face representation and recognition. *IEEE International Conference on Computer Vision (ICCV)*, 1:786–791, 2005. 19, 20, 98, 110, 113

[141] Z. Zhang. Microsoft kinect sensor and its effect. *IEEE MultiMedia*, 19(2):4 –10, 2012. 97, 107

[142] Z. Zhang, D. Yi, and et.al. Face liveness detection by learning multispectral reflectance distributions. *IEEE Automatic Face and Gesture Recognition (FG)*, pages 436–441, 2011. 14, 15, 44

[143] J. Zhao, H. Wang, H. Ren, and S.-C. Kee. Lbp discriminant analysis for face verification. *Proc. of IEEE Computer Society Conference on Computer Vision and Pattern Recognition (CVPRW)*, pages 167–173, 2005. 39

[144] W. Zhao, R. Chellappa, P. J. Phillips, and A. Rosenfeld. Face recognition: A literature survey. *ACM Comput. Surv.*, 35(4):399–458, 2003. 8

[145] M. Zollhöfer, M. Martinek, G. Greiner, M. Stamminger, and J. Sübmuth. Automatic reconstruction of personalized avatars from 3d face scans. *Comput. Animat. Virtual Worlds*, 22(2-3):195–202, 2011. 109